Pre-Clinical Assessment and Optimization of the IGF-Trap for the Treatment of High-Grade Gliomas.

Yin-Hsuan Michely Chen

McGill University
Department of Medicine, Division of Experimental Medicine
Montreal, Quebec, Canada

December 2021

A thesis submitted to McGill University in partial fulfillment of the requirement of the degree of Master of Science

TABLE OF CONTENTS

Abstract:

Glioblastoma is a deadly brain cancer with a dismal five-year survival rate of less than one year. In children, glioblastoma is the leading cause of cancer-related death. To date, no external or environmental risk factors have been identified for this disease. However, emerging research identifying genetic factors that increase cancer incidence have contributed to new classification of brain tumor subtypes and potential therapeutic targets. The type 1 insulin-like growth factor receptor (IGF-IR) was shown to be highly amplified in malignant brain tumors and was shown to be a molecular target for high-grade gliomas in children and adults. The Brodt lab had developed an IGF-IR decoy, the IGF-Trap, and demonstrated growth inhibition of several aggressive tumors including triple negative breast cancer, and colon/lung carcinomas cells *in vivo*. We aimed to evaluate the effect of the IGF-Trap on glioblastoma growth *in vitro* and *in vivo* and further optimize intracerebral delivery of this biological agent for the treatment of high-grade gliomas *in situ*.

In this study, we have identified the canonical MEK/ERK and PI3K/Akt signaling pathways and nuclear translocation of the IGF-IR as two parallel mechanisms downstream of IGF-IR activation and showed that both pathways were inhibited by the IGF-Trap in pediatric high-grade glioma (pHGG) (Chapter III) thereby, validating IGF-IR as a potential target for the treatment of pHGG. Additionally, we carried out in a stepwise manner a therapeutic assessment of the IGF-Trap as an inhibitor of glioma growth *in vivo* using a murine and human adult glioma model (Chapter IV). We showed that the IGF-Trap could inhibit the intracerebral growth of both gliomas and significantly extend survival of tumor-bearing mice. In addition, we confirmed improved intracerebral IGF-Trap delivery when it was encapsulated in trimethyl chitosan-based nanoparticles. Finally, a pilot study was performed to assess the efficacy of transcranial magnetic stimulation as a method for delivering the IGF-Trap through the blood brain barrier (Chapter IV). The present work provides insights into the role of the IGF-axis in

pediatric and adult high-grade glioma and introduces two novel strategies for the delivery of large molecule biologics to the brain for the treatment of brain malignancies.

Résumé:

Le glioblastome est un cancer du cerveau mortel avec un taux de survie à cinq ans étant de seulement un an. Chez les enfants, le glioblastome est la principale cause de décès dû au cancer. A ce jour, aucun facteur de risque externe ou environnemental n'a été identifié pour cette maladie. Cependant, les recherches émergentes identifiant les facteurs génétiques qui augmentent l'incidence du cancer ont contribué à une nouvelle classification des sous-types de tumeurs cérébrales et des cibles thérapeutiques potentielles. Le récepteur du facteur de croissance analogue à l'insuline de type 1 (Insulin-like growth factor 1 receptor, IGF-IR) s'est avéré fortement amplifié dans les tumeurs cérébrales malignes et a été identifié comme cible moléculaire pour les gliomes de haut grade chez les enfants et les adultes. Le laboratoire Brodt a développé un piège à molécule de IGF-IR, *l'IGF-Trap*, et a démontré l'inhibition de la croissance de plusieurs tumeurs agressives, notamment le cancer du sein triple négatif et les cellules de carcinomes du côlon/poumon in vivo. Notre objectif a été d'évaluer l'effet de *l'IGF-Trap* sur la croissance des glioblastomes in vitro et in vivo et d'optimiser davantage l'administration intracérébrale de cet agent biologique pour le traitement des gliomes de haut grade in situ.

Dans cette étude, nous avons identifié les voies de signalisation canoniques MEK/ERK et PI3K/Akt et la translocation nucléaire de l'IGF-IR comme deux mécanismes parallèles en aval de l'activation de l'IGF-IR et avons montré que les deux voies étaient inhibées par *l'IGF-Trap* dans le gliome pédiatrique de haut grade (pediatric high-grade glioma, pHGG) (chapitre III), validant ainsi l'IGF-IR comme cible potentielle pour le traitement du pHGG. De plus, nous avons effectué de manière progressive une évaluation thérapeutique de *l'IGF-Trap* en tant qu'inhibiteur de la croissance des gliomes in vivo en utilisant un modèle de gliome murin et

humain adulte (chapitre IV). Nous avons montré que *l'IGF-Trap* pouvait inhiber la croissance intracérébrale des deux gliomes et prolonger considérablement la survie des souris porteuses de tumeurs. En outre, nous avons confirmé l'amélioration de l'administration intracérébrale *d'IGF-Trap* lorsqu'elle était encapsulée dans des nanoparticules à base de triméthyl chitosane. Enfin, une étude pilote a été réalisée pour évaluer l'efficacité de la stimulation magnétique transcrânienne comme méthode d'administration de *l'IGF-Trap* à travers la barrière hémato-encéphalique (chapitre IV). Le présent travail donne un aperçu du rôle de l'axe IGF dans le gliome de haut grade pédiatrique et adulte et présente deux nouvelles stratégies pour l'administration de produits biologiques à grandes molécules au cerveau pour le traitement des malignités cérébrales.

Preface:

This thesis is presented in a manuscript style, and I have included the following documents

- Chen YM, Leibovitch M., Zeinieh M., Jabado N., and Brodt P. Targeting the IGF-axis in pediatric high-grade glioma inhibits cell cycle progression and cell survival. *submitted*.

- Chen YM., Hashimoto M., Qi S., Perrino S., Meehan B., Jabado N., and Brodt P. Evaluation and optimization of the delivery of IGF-Trap for the treatment of glioblastoma. *In preparation*.

Contribution of authors:

Contribution of authors for each manuscript in Chapters III and IV are as follows:

Chen YM: Chapter III Figures 3, 4, 6, Chapter IV Figures 4, 5, 6, 7

Leibovitch M: Chapter III Figures 1, 2, 5

Hashimito M; Chapter IV. Figures 2, 3, 4

Qi S: Chapter IV Figures 1, 2, 5

Acknowledgements:

First, I would like to express my sincere appreciation to my primary supervisor Dr. Pnina Brodt for her mentorship and support throughout my degree program. Dr. Brodt has encouraged me to participate in conferences, has provided me opportunities to publish, has revised numerous documents including this thesis for me, and has done so much more to help me achieve my fullest potential as a student and as a young researcher.

I would also like to thank my co-supervisor Dr. Nada Jabado for her guidance and expert advising. I was truly inspired by the work ethics, the knowledge, and passion she has for research.

I am immensely grateful of Dr. Matthew Leibovitch who carried on and contributed greatly to Chapter III of my thesis and preparing it for publication. I also would like to thank Dr. Masa Hashimoto, Shu Qi, and Julien Chambon for their work on GL261, U87, and nanoparticle encapsulation, respectively. I have received generous help from Michele Zienieh, Stephanie Perrino, and Brian Meehan with setting up *in vivo* experiments. I have had the privilege to collaborate with all Brodt lab members as well as Michele, and Brian on this project and I learned greatly from each and one of them. Special thanks to Yasmine Benslimane, Charles Essagian and everyone mentioned above for the friendship and support.

Finally, I would like to dedicate this thesis to my parents and my brother, William, who were always there for me through all the ups and downs.

List of abbreviations:

ACVR1	Activin receptor type 1
ADAM3A	ADAM metallopeptidase domain 3A
AKT	Protein kinase B (PKB)
ALS	Acid-labile subunit
ATRX	ATRX chromatin remodeler
BBB	Blood brain barrier
BRET	Bioluminescence resonance energy transfer
c-SRC	Proto-oncogene tyrosine protein kinase Src
CDH	E-cadherin
CDKN2A	Cyclin dependent kinase inhibitor 2A
CNS	Central nervous system
CRK	Crk adaptor protein
CSC	Cancer stem cell
DIPG	Diffused intrinsic pontine glioma
EGF	Epidermal growth factor
EGFR	Epidermal growth factor receptor
EMT	Epithelial to mesenchymal transition
ER	Estrogen receptor
ERK	Extracellular signal regulated protein kinase
FAK	Focal adhesion kinase
FGF	Fibroblast growth factor
FGFR-1	Fibroblast growth factor receptor 1
GAB	Grb associated binder
GBM	Glioblastoma multiforme

GH	Growth hormone
GHRH-R	Growth hormone release hormone receptor
GSK3β	Glycogen synthase kinase 3β
GTR	Gross total resection
HDAC	Histone deacetylase
HER2	Human epidermal growth factor receptor 2
IDH1	Isocitrate dehydrogenase 1
IGF	Insulin-like growth factor
IGF-IR	Type 1 Insulin-like growth factor receptor
IGFBP	Insulin-like growth factor binding proteins
IR	Insulin receptor
IRS	Insulin receptor substrate
JAK	Janus kinase
LFS	Li Fraumeni syndrome
LGG	Low-grade gliomas
LID	Liver specific IGF-1 gene deleted
MAPK	Mitogen-activated protein kinase
MDH1	Malate dehydrogenase 1
MLH1	MutL homolog 1
MMP	metalloproteinase
MMSE	Mini-mental state examination
MRI	Magnetic resonance imaging
MSH2	MutS homolog 2
MSH6	MutS homolog 6
mTOR	Mechanistic target of rapamycin

NBS-HGG	Non-brainstem HGG
NF-1	Neurofibromatosis type 1
NF-κB	κlight chain enhancer of activated B
NMDA	N-methyl-D -aspartate
NP	Nanoparticle
NTRK	Neurotrophin receptor tyrosine kinase gene
PD-1	Programmed cell death-1
PDGFR	Platelet-derived growth factor receptor
PDX	Patient derived xenograft
PFS	Progression free survival
pHGG	Pediatric high-grade glioma
PI3K	Phosphoinositide -3-kinase
PLCγ1	Phospholipase C γ1
PMS2	Postmeiotic segregation increased 2
POU5F1	POU class 5 homeobox1
PSA	Prostate-specific antigen
PTEN	Tensin homolog
PXA	Pleomorphic xanthoastrocytoma
RTK	Receptor tyrosine kinases
SEGA	Subependymal giant cell astrocytoma
SH2	Src homology
SHC	SHC adaptor protein 1
SHH	Sonic hedgehog homolog
SMO	Smoothened

SNAI	Snail family transcriptional repressor
SOC	Standard of care
SOS	Grb2-son-of sevenless
SOX2	Sex determining region Y-box-2
STAT	Signal transducer and transcription
SUMO	Small ubiquitin-like modifier protein
TIMP	Tissue inhibitor of metalloproteinase
TKI	Tyrosine kinase inhibitors
TMS	Transcranial magnetic stimulation
TRAMP	Transgenic adenocarcinoma of mouse prostate
TRK	Tropomyosin receptor kinase
VEGF	Vascular endothelial growth factor
VEGF	Vascular endothelial growth factor
WHO	World Health Organization
WNT	Wingless-related integration site
ZEB	Zinc finger e-box binding homeobox

List of Figures and Tables:

Chapter 4

Chapter 1. Overview of Pediatric Brain Cancer

1.1 Brain Tumor Classification

Brain tumors are the most common solid cancer and the leading cause of cancer-related death in children. Every year approximately 4000 children around the globe are diagnosed with brain tumors. Brain tumors are classified by histological features of the tissue of origin. The neuroepithelial type includes astrocytic tumors, ependymoma, choroid plexus papilloma, oligodendroglioma, mixed glioma and medulloblastoma. Non-neuroepithelial tumors include craniopharyngioma, meningioma, schwannoma, and lymphoma (1). The most common pediatric brain tumors belong to the neuroepithelial type and include the astrocytoma, medulloblastoma, ependymoma, and gliomas. Classic histological typing by morphological criteria is generally based on the predominant tumor cell type. However, tumors may arise from mixed cell types or the lineage may be unidentifiable based on the features exhibited by the tumor cells (2).

Recent advances in genomic analyses have resulted in new classifications based on molecular features. For example, medulloblastoma was classified into 5 histological subtypes namely, the classic, large cell, anaplastic, desmoplastic nodular, and medulloblastoma with extensive nodularity. Recent stratification using gene signatures subcategorized medulloblastoma into wingless-related integration site (WNT), sonic hedgehog homolog (SHH), Group 3 and Group 4. Subgroups with shared characteristics are often associated with clinical outcomes. For medulloblastoma, the histological subgroups desmoplastic nodular and medulloblastoma with extensive nodularity were associated with better prognosis while the large cell and anaplastic subgroups were associated with worse prognosis. In the molecular subgroups the WNT group was associated with the best prognosis while Group 3 had the worst prognosis. Therefore, one can expect that Group 3 tumors often showed large cell and

anaplastic features. Because histological and molecular features are not mutually exclusive, identification of both is required for better diagnosis and treatment (3).

The survival rate for Medulloblastoma has significantly improved in the past two decades. The standard treatment of medulloblastoma in the 1960s to mid-1980, has been surgery followed by craniospinal and primary site radiation therapy. Due to improved surgical technique and cyclophosphamide-based chemotherapy, survival at 5 years has improved from 60-65% to 80-85% (4-6). Additionally, quality of life has improved due to the reduction in dose intensity of craniospinal radiation therapy- a major cause of neurocognitive side effects (7). Molecular genetics have, to date, not yet contributed to improvement in brain tumor treatment. However, potential therapeutic targets are under investigation in multiple clinical trials such as (7). For example, the two inhibitors of Smoothened (SMO), negative regulator of hedgehog signaling, in medulloblastoma were sonidegib (LDE225) and vismodegib (GDC-0449). These two inhibitors have undergone phase I or II clinical trials, but the response in medulloblastoma was still inconclusive (8, 9). Subgroups of molecular alteration provide insight into molecular drivers that could be targeted for more effective and personalized treatment for Medulloblastoma.

In addition to histological and molecular stratification, tumors are also graded based on World Health Organization (WHO) grading system of central nervous system (CNS) tumors, with specific schemes for different types such as the St. Anne classification criteria for gliomas. The scheme divides tumors into four grades using features such as anaplasia, cell density, mitotic activity, vascular proliferation, and necrosis. Tumor grades range from I to IV with I being benign with expected post-operative survival of at least 5 years and IV being malignant with expected survival of 6-15 months (2). Grade I and II tumors are also referred to as low-grade tumors while Grade III and IV are referred to as high-grade tumors. Historically, inter-

observer variability in assessing parameters such as mitotic index, nuclear pleomorphism and others rendered classification more subjective. However, advances in computer-aided methods have reduced subjectivity in analysing these parameters. Additionally, the inclusion of molecular markers can provide verification of histological tumor lineage. Identifying genomic signatures in combination with objective histopathological subtyping and grading can improve prognosis and inform on the best course of treatment (2).

1.1.1 Pediatric Gliomas

Gliomas are neuroepithelial tumors originating from glial cells. They account for 29-35% of all CNS tumors with two third of gliomas diagnosed as low-grade and the remaining as high-grade gliomas. Glial cells support, protect, and provide nutrients to neurons in the central nervous system. They include three cell types: astrocytes, oligodendrocytes and microglial cells consisting of ependymal and radial glial cells. Tumors that arise from astrocytes, oligodendrocytes, and ependymal cells are known as astrocytoma, oligodendroglioma, and ependymoma, respectively (10). Astrocytomas are the predominant brain tumors in children and can be further divided into several subtypes based on molecular, histological, and clinical parameters, as well as WHO grading (11). Common astrocytoma subtypes ranging from WHO Grade (G) I to IV are classified as follows: pilocytic astrocytoma (GI), subependymal giant cell astrocytoma (SEGA-GI), pleomorphic xanthoastrocytoma (GII), anaplastic astrocytoma (GIII), glioblastoma multiforme (GBM- GIV). Other types of gliomas include ependymomas, oligodendrogliomas, diffused intrinsic pontine glioma (DIPG), optic nerve gliomas, and mixed type gliomas (12). 5-year survival of grade I and II gliomas have 5-year survival rates up to 95% while grade IV gliomas is around 10% and DIPG is less than 1% (13). Gliomas range from benign low-grade gliomas (LGGs) which is operable to aggressive malignant tumors such

as DIPGs and supratentorial GBMs with poor prognosis despite aggressive therapies. The common pediatric glioma types, their location and prognosis are summarized in **Table 1.1**.

LGGs are the most common childhood brain tumors. Although tumor progression is slow and survival rates are as high as 95%, non-resectable tumors at critical locations of the brain remain challenging. Thus, understanding the biology of LGG is necessary in order to develop targeted therapeutic agents. The majority of LGG appear to arise sporadically without a known predisposing pathology. However, SEGA frequency is correlated with the tuberous sclerosis complex, while neurofibromatosis type 1 (NF-1) is a cancer-predisposing syndrome associated with increased frequency of pilocytic astrocytoma, the most prevalent LGG in children. LGG was reported to spontaneously regress, especially in patients with NF-1 (14). While children with LGG showed 30-40% responsiveness to chemotherapy (combination of carboplatin and vincristine) for 3-4 years after treatment, 75% of patients with NF-1 were progression-free for 3-5 years (7). NF-1-associated LGG were linked to a constitutively activate RAS while non-NF-1 associate LGG have loss of BRAF function, leading to activation of the mitogen-activated protein kinase (MAPK) pathway. Additionally, some pediatric LGG (pLGG) have an intragenic duplication of the tyrosine kinase domain of the fibroblast growth factor receptor 1 (FGFR-1) which results in the activation of the phosphoinositide-3-kinase (PI3K) /mechanistic target of rapamycin (mTOR) pathway and increased levels of the MYB transcription factor. These findings led to clinical trials for BRAF and mTOR inhibitors as treatment for pLGG that are currently ongoing (13).

Unlike the improvements seen in the treatment of pLGG over the years, progress in the treatment of HGG has been limited. The histopathology and molecular characteristics of high-grade glioma and DIPG are discussed in detail in the next section.

1.2 Pediatric High-Grade Glioma (pHGG)

1.2.1 Histopathology

Pediatric high-grade gliomas defined by their malignant, diffuse, infiltrating astrocytic characteristics account for 8-12% of all pediatric central nervous system tumors (15). The most common types of pediatric high-grade gliomas include the WHO Grade III anaplastic astrocytoma and WHO Grade IV glioblastoma multiforme (GBM). Anaplastic astrocytoma is characterized by atypical nuclei and increased cellularity and mitotic activity and GBM which is clinically more advanced and aggressive has vascular proliferation and necrosis in addition to Grade III properties. pHGG is widely distributed in the brain while adult HGG are mainly in the cerebral cortex (13). A portion of pediatric glioma patients harbor germline mutation especially in higher grade tumors. The three most prominent cancer predisposition syndromes in pHGG are the Li Fraumeni syndrome (LFS), mismatch repair deficiency and NF-1 mutations (16, 17).

1.2.2 Molecular Features of HGG

A genomic study using 280 pediatric astrocytoma patient samples showed that 10% of pHGG are associated with germline mutations in known cancer predisposition genes. Germline TP53 mutations are prevalent in pHGG, are associated with poor prognosis and the presence of germline tumor protein p53 (TP53) mutations is the main diagnostic criteria for LFS, a highly penetrant syndrome (16). In addition to LFS, mismatch repair deficiencies and mutated NF-1 are other prominent genetic alterations associated with pHGG. Constitutional mismatch repair deficiency is caused by genetic alterations in DNA repair genes including in postmeiotic segregation increased 2 (PMS2), MutS homolog 6 (MSH6), MutS homolog 2 (MSH2), and MutL homolog 1 (MLH1). As a result of mutations in mismatch repair genes the cells are

unable to correct errors during DNA replication, leading to the accumulation of mutations over time and cancer. The NF-1 encoding neurofibromin is an inhibitor of the RAS oncogene. Mutations in this gene therefore lead to activation of the MAP kinase and PI3K/protein kinase B (ATK)/mTOR signaling pathways downstream of RAS (17).

In addition to cancer predisposing mutations, other genetic aberrations are implicated in pHGG that are distinct from those in adult HGG. While adult HGG show high prevalence of isocitrate dehydrogenase 1 (IDH1) mutations, epidermal growth factor receptor (EGFR) amplifications and phosphatase and tensin homolog (PTEN) loss, the main molecular alterations in pHGG include a histone H3 K27M mutation, amplified platelet-derived growth factor receptor (PDGFR) and other receptor tyrosine kinases (RTKs) and deletions of cyclin dependent kinase inhibitor 2A (CDKN2A), TP53 and ADAM metallopeptidase domain 3A (ADAM3A) (13). Pediatric HGG originating in the supratentorial region often harbor glycine 34 residue to an arginine or valine (G34R/V) mutations in the H3F3A gene encoding histone H3.3 (18).

Mutations in histone H3 are a unique characteristic of pediatric high-grade glioma. Specifically, mutations on H3.3 and H3.1 change the lysine 27 residue to a methionine (K27M) or the G34R/V. These two mutations are mutually exclusive and result in clinically and genetically distinct features. G34R/V of histone H3 is more common in the cortex whereas K27M occurs more frequently in midline tumors such as the thalamus or the cerebellum (19).

Ten percent of non-brainstem HGG (NBS-HGG) in children harbor fusions in the neurotrophin receptor tyrosine kinase gene (NTRK). Among them, 40% of NBS-HGG contained NTRK fusion gene in children under three years of age (19). NTRK, an oncogene, is involved in a series of developmental signals and oncogenic events. NTRKs encodes tropomyosin receptor kinase (TRK) which binds neurotrophins, brain-derived neurotrophic factor, and nerve-growth factor. The binding of ligands to TRK triggers homodimerization and

transactivation of the intracellular tyrosine kinase domains. Subsequently, the recruitment of adaptors activates downstream MAPK, PI3K, and protein kinase C (PKC) pathways and drives the transcription of genes responsible for neuronal differentiation and survival which, in turn, leads to rapid tumor growth in young children (20).

1.2.3 Current Therapies and Potential Treatments for pHGG

Current standard of care (SOC) therapy for pHGG in the cerebrum is surgery followed by radiation and chemotherapy. The major treatment modality remains gross total resection (GTR) of the tumor. A study of 85 patients from the Children's Cancer Group showed that maximal safe tumor resection is associated with improved 5-year progression-free survival (PFS) as compared to those with less extensive resection (21). For localized pHGG, focal radiation therapy is the standard post-surgical treatment for children over the age of three. Radiation therapy followed by chemotherapy following surgery resulted in improved prognosis as compared to patients who receive radiation therapy alone (22). These therapies often affect the developing brain and cause deficits in cognition, motor skills, vision, and memory. Neurocognitive deficits arise from neurotoxicity following chemotherapy, craniospinal or whole-brain irradiation (23). Brain surgery may cause infiltration of immune cells resulting in neuroinflammation or impingement in areas of the brain important for cognitive functions (24, 25). Therefore, the development of targeted therapies is critical for improving not only survival but also the quality of life for children with malignancies of the brain.

Current chemotherapeutic drugs for pHGG include prednisone, chloroethyl cyclohexyl nitrosourea, and vincristine that exert anti-inflammatory, DNA alkylation and cell cycle arrest activities, respectively (26). Recently, novel targeted therapies emerged as genomic information provided valuable insights into the biology underlying pHGG. Clinical study with immunotherapy, targeting programmed cell death-1 (PD-1) revealed that immune checkpoints

may be targets in patients with mutations in the mismatch repair genes (malate dehydrogenase 1 (MDH1), MSH2, MSH6, and PMS2) (27). Additionally, histone deacetylase (HDAC) and or demethylase inhibitors showed promising results *in vivo* and have advanced into clinical trials for further evaluation (28). Limitations of these treatments for pHGG are largely due to intra-tumoral genetic heterogeneity and the exclusion of therapeutics agents by the blood brain barrier (13). These challenges have resulted in little progress in the management of pHGG. It is hoped that advances in genomic/proteomic analyses will reveal new targets and lead to novel strategies for combating the disease that could be combined for novel approaches for safely breaching the blood –brain barrier.

1.3 Diffused Intrinsic Pontine Glioma (DIPG)

1.3.1 Histopathology

DIPG is the leading cause of mortality in children with brain tumors. Children with DIPG have a 5-year survival rate of <1%. Even with focal radiation therapy, overall survival is 10-12 months. Additionally, recurrence and/or progression of the disease are highly prevalent after radiation therapy. DIPG has similar histopathological features to GBM but occasionally it can be of a lower grade (II or III). Because of the critical location, the tumor is classified as malignant regardless of the grading. Cancer cells are diffusely infiltrating in the brain stem, most commonly in the pons and the disease occurs almost exclusively in children (13).

1.3.2 Molecular Features of DIPG

As location of the tumor is the most critical feature of DIPG, magnetic resonance imaging (MRI) is the predominant diagnostic technique. Biopsy samples allow for further molecular analysis of the malignancy. Up to 75% of pediatric DIPG harbor histone mutations, mainly in histone 3.1 or 3.3 with some groups showing worse prognosis (29). Similar to midline pHGG,

DIPG frequently harbor K27M mutations. Histone H3, TP53, and ATRX chromatin remodeler (ATRX) mutations are also found in both pHGG and DIPG, whereas activin receptor type 1 (ACVR1) mutations are found exclusively in DIPG (13). ACVR1 is associated with K27M mutations on histone H3.1 or mutations in PI3K. Studies using a zebrafish model showed that ACVR1 activates the bone morphogenetic protein (BMP) signaling pathway that is essential for the development of the dorsal-ventral axis. More studies are needed to exploit the association between DIPG and the role of ACVR1 and the BMP pathway in driving differentiation or proliferation in progenitor or cancer cells. Nevertheless, the high frequency of ACVR1 mutations in DIPG have identified it as a potential target for future treatments (19). Other prevalent mutations of epigenetic modulators in DIPG include histone H3, ATRX, and MYCN (n-myc) (30).

In addition to the frequent mutations listed above, the RB1 and TP53 genes are also often mutated in DIPG. Cell cycle checkpoint regulators are highly amplified in DIPG. In contrast to CDKN2A deletions in NBS-HGG, DIPG have amplifications of the cyclin D1 (CCND) 1, 2, and 3, cyclin-dependent kinase (CDK) 4 and CDK6 genes (19). Missense and truncated TP53 are frequent mutations in both DIPG and NBS-HGG. Mutations in genes involved in RTK/RAS/PI3K signaling include PDGFRA, IGF1R, EGFR, KIT, MET, NTRK1/2/3 and NF1. PDGFRA is the most frequently mutated gene in both NBS-HGG and DIPG. IGF1R amplification is the second highest genetic aberration in DIPG, while EGFR and KIT gene amplifications are more frequent than IGF1R amplifications in NBS-HGG. (13) This wide variation in the mutation landscape is a major challenge in the development of an effective treatment for DIPG malignancies.

1.3.3 Current Therapies and Potential Treatments for DIPG

The current SOC for DIPG are fractionate external beam radiation therapy and post-radiation chemotherapy. Progress in tumor management remains minimal and overall survival remains low for DIPG. Although surgery has been the treatment associated with the best outcome for pHGG, the location of DIPG in the pons of the brainstem renders them inoperable. The lack of progress in the management of this malignancy can be attributed in part to the lack of biopsy samples for biological studies (7). As surgical techniques improve and genomic studies emerge, molecular driven interventions are also becoming possible. Preclinical studies identified the histone demethylase inhibitor, panobinostat as a promising therapeutic candidate for this malignancy where H3.1 or H3.3 K27M mutations are a major mutational driver (80%) in this disease (31). Other HDAC inhibitors such as vorinostat and valproic acid are currently being evaluated in ongoing clinical trials. Moreover, therapeutic agents that target the RTKs including PDGFR, KIT and EGFR are also under investigation either alone, or in combination with each other or vascular endothelial growth factor (VEGF) inhibitors (13).

1.4 The roles of RTK signaling in HGG and DIPG

RTKs are a family of cell-surface receptors that upon extracellular ligand-binding initiate downstream signaling cascades via receptor dimerization and autophosphorylation of the tyrosine kinase domain. The major two downstream pathways activated downstream of ligand binding are the Ras/MAPK/ERK and the PI3K/AKT pathways. RTKs are regulators of proliferation, differentiation, cell survival, invasion, metabolism, migration, cell cycle control, and angiogenesis. RTK signaling is frequently amplified in pHGG and DIPG. The cellular functions regulated downstream of RTK activation are described below.

1.4.1 Epithelial-mesenchymal transition and invasion

pHGG and DIPG are highly drug-resistant due to i) drug exclusion by the blood brain barrier ii) tumor heterogeneity and iii) the ability to undergo epithelial-to-mesenchymal transition (EMT). EMT is a process whereby cells acquire mesenchymal properties such as losing cell-cell adhesion and gaining migratory and invasive characteristics. Many genes involved in EMT such as the TWIST family of transcription factors that are known to be involved in invasion and metastasis to distant sites, also contributes to chemo and radiotherapy resistance. Twist-1 expression was detected at high levels in glioblastomas and was found to be induced by nuclear factor κ-light-chain-enhancer of activated B (NF-κB) (32, 33). Many cytotoxic drugs activate cell death pathways such as p53 but also simultaneously triggered negative regulation of apoptosis such as the NF-κB, TNF-α pathways (34). NF-κB can promote both proapoptotic and antiapoptotic effects(35). Moreover, genes associated with EMT such as zinc finger e-box binding homeobox (ZEB) 1, ZEB2, SIX1 also promote the maintenance of cancer stem cells (CSC) that are responsible for tumor recurrences (36).

Key regulators of the EMT process include zinc finger protein SNAI1 (SNAIL1), SNAIL2 (SLUG), ZEB1, ZEB2, and TWIST. These proteins are transcription factors that downregulate E-cadherin (CDH1) expression and induce expression of N- and /or R-cadherins (CDH2 or CDH4), triggering a series of events that increase drug resistance while also inducing a migratory/invasive phenotype (36, 37). RTKs such as the EGF, fibroblast growth factor (FGF), PDGF, IGF receptors activate a common downstream PI3K/AKT pathway which plays a role in the EMT transition. AKT inhibits glycogen synthase kinase 3 β (GSK3β) preventing GSK3β – mediated phosphorylation of SNAIL or SLUG thereby stabilizing these proteins and promoting EMT (38). pHGG and DIPG have a high frequency of amplification in genes involved in the PI3K/AKT pathway, suggesting that tumor cells acquire mesenchymal

transitions through RTK signaling (19). In addition to the PI3K/AKT pathway, RTKs also signals through the RAS/MAPK pathway. Phospho- ERK 1/2 increase transcription of SNAIL and SLUG (36). Moreover, the TAM family of receptor tyrosine kinases consisting of Tyro3, AXL and Mer, play an important role in EMT and are associated with cancer progression, metastasis, and resistance to therapies. AXL can be activated by other RTKs through heterodimerization (39). Critical mesenchymal transition regulators, SNAIL, SLUG are upregulated in the mesenchymal/pro-angiogenic type of DIPG and are associated with advanced stage tumor and poor survival (40).

1.4.2 Survival and proliferation

RTKs promote cell survival and proliferation via PI3K/AKT and Ras/Raf/MEK/ERK signaling, respectively. Activated ERK phosphorylates transcription factors and cell cycle regulators driving cell division. Ras and Raf can activate both MEK/ERK and the PI3K/AKT signaling, and these pathways are known to crosstalk (41). The PI3K/AKT pathway can provide cell survival signaling via several mechanisms. It can activate the transcription factor NFκB, by phosphorylating and activating IκK, resulting in degradation of the NFκB inhibitor IκB. NFκB, in turn activates transcription of anti-apoptotic proteins such as inhibitor of apoptosis protein (cIAP) and TNF receptor associated factors (TRAFs) (35). In addition, Akt interacts with proteins of the Bcl-2 family key regulators of apoptosis, including the pro-apoptotic Bad and Bax and anti-apoptotic Bcl-2 and Bcl-X_L. Akt phosphorylates bcl2 associated agonist of cell death (Bad) causing its dissociation from Bcl-2 which promotes cell survival (42). An inhibitor of mTOR, Everolimus, is currently in clinical trials for the treatment of DIPG in combination with an EGFR (Erlotinib) and RTK (Dasatinib) inhibitor (NCT02233049).

The gene products of the tumor suppressor genes PTEN and NF1 inhibit the PI3K and the Ras pathways, respectively. PTEN mutation were identified in 25-40% of pHGG and the frequency is as high as 80% in adult glioblastomas (43). In a clinical study that analyzed biospecimens from 70 participants with pHGG, NF1 was found to be mutated in 27% of the specimens (44).

1.4.3 Angiogenesis induction

The vascular endothelial growth factor (VEGF) family consists of 5 ligands (VEGF-A, B, C, D, E) and 3 receptors (VEGFR-1, 2, 3). The well-characterized and main signaling receptor, the RTK VEGFR-2, can be activated by binding VEGF-A, C, D, or E (45). Activation of VEGFR2 signaling results in formation of new vessels or outgrowth of pre-existing vessels and increases vessel permeability (45).

DIPG can be classified into two groups: the mesenchymal and pro-angiogenic type and the oligodendroglial type. Overexpression of VEGF-A and correlation between VEGF-A with drivers of mesenchymal transition (Snail, Slug, YKL-40) are distinct gene expression profiles of the mesenchymal/pro-angiogenic group. Endothelial cell proliferation was seen in 89 and 57% respectively, of the mesenchymal/ pro-angiogenic and oligodendroglial subtypes (40).

Bevacizumab, a VEGF-A inhibitor is a FDA approved treatment for adult glioblastoma; however, a phase III trial investigating bevacizumab as treatment for DIPG or pHGG did not show improvement in progression free-survival or overall survival. However, the drug was well-tolerated, and quality of life was improved in the treated children (46). Recent clinical trials combining the VEGF inhibitor with HDAC, EGFR, and human epidermal growth factor receptor 2 (HER2) inhibitors for the treatment of pediatric gliomas are ongoing (13).

Table 1.1. glioma type and their overall survival and WHO grades

Glioma type	WHO Grade	Prognosis	Location	References
Pilocytic astrocytoma,	I	5-year survival 95.3%	Commonly found in cerebellum.	(47)
Fibrillary astrocytoma, Oligodendroglioma, mixed oligoastrocytoma	II	5-year survival of 34% without treatment but 70% with radiation.	Commonly found in the cerebral hemisphere	
Pleomorphic xanthoastrocytoma (PXA)	II	Overall survival of 75-80% following resection.	Commonly found in the supratentorial region.	(48)
Optic nerve glioma	I	5- year survival 95%.	Optic chiasm	(49)
Anaplastic astrocytoma	III	2- year survival of 34%.	Commonly found in the cerebral hemisphere	(50)
Glioblastoma multiforme (GBM)	IV	2-year survival of 9%	Commonly found in the cerebral hemisphere (frontal and temporal lobes)	(50)
Diffused Intrinsic Pontine Glioma (DIPG)	III/IV	Median survival of 13 months	Pons (brainstem)	(51)

Chapter II: The IGF-System and IGF-Targeted Therapy

2.1 The IGF Signaling System

2.1.1 IGF-Receptors

The IGF-signaling axis consists of the cell surface receptors (Insulin-like growth factor -1 receptor and Insulin-like growth factor -2 receptor (IGF-1R, IGF-2R) and the insulin receptor (IR)); IGF-IR and IR belong to the receptor tyrosine kinase (RTK) superfamily. IGF-1R shared 53% sequence homology with IR. IR is highly involved in metabolism of glucose, protein, and lipids while the IGF-1R regulates cell growth (52). The IGF-1R is synthesized as a single chain pro-receptor and the precursor undergoes post translational modification (glycosylation, dimerization, proteolytic processing) to form the α and β subunits (53). The IGF1R and IR undergo N-linked glycosylation on 11-18 sites. Glycosylation ensures correct folding and processing of the receptor. The variation in glycosylation sites suggests that there is sequence redundancy to minimize detrimental effects of genetic errors; Thomas et al showed that as many as quadruple mutants in N-linked glycosylation remain functional with intact properties such as pro-receptor processing, cell-surface expression, ligand binding and receptor autophosphorylation (54). The IGF-1R and IR function as heterotetramers consisting of 2 α and 2 β subunits. The α and β subunit form a protomer that is homodimerized by disulphide bonding. This is distinct from other RTKs that dimerized upon ligand binding (55). The alpha subunit is part of the extracellular domain that contains the IGF binding sites and the transmembrane β subunit contains the intracellular tyrosine kinase domain flanked by two juxtamembrane region (56). Upon ligand binding, the receptor is conformationally altered and this activates the kinase domain on 1 β subunit and receptor autophosphorylation on specific tyrosine residues. Signaling proteins are then recruited and the juxtamembrane region serves as a docking site for signaling molecules including insulin receptor substrate 1, 2 (IRS-1, IRS2), and SHC adaptor protein 1 (Shc) (Figure 2.1) (55, 57).

The IR transcript undergoes alternative splicing in exon 11 yielding two isoforms, IR-A and IR-B. IR-A lacks 12 amino acid residues in the α-chain as compared to IR-B. This structural difference contributes to the significant decrease in affinity of IR-B for IGF-1 and IGF-2, whereas the differences in affinity to insulin is modest (58). IR-A can bind IGF-2 with higher affinity to mediate proliferative, mitogenic, and transforming effects, whereas, IR-B binds insulin, elicits predominantly metabolic functions and is involved in cell differentiation (59). Under normal physiological state, IR-A is mainly expressed in fetal tissues and in some specific adult tissues such as the brain, whereas IR-B is expressed predominantly in differentiated adult tissues that are involves glucose metabolism such as the liver (60-63). The ratio of IR-A:IR-B plays a critical role in cancer, diabetes, and neurodegenerative diseases (64). While IR and IGF-IR regulate growth and metabolism through the activation of the tyrosine kinase domain, IGF-2R lacks the kinase domain, binds only IGF-2 and prevents IGF-IR signaling by reducing IGF-2 bioavailability. IGF-2R internalizes upon ligand binding and induces trafficking between the trans-Golgi network, endosomes, and lysosomes causing the degradation of the ligand, thereby, attenuating cell proliferation and survival mediated by IGF-1R or IR-A (65). Loss of heterozygosity in the IGF-2R gene was documented in various cancers including liver (66), lung (67), breast (68), prostate (69), and ovarian carcinoma (70, 71). Overexpression of IGF-2R in MDA-MB-231 breast cancer cells reduced IGF-IR signaling *in vitro* and decreased tumor formation and growth *in vivo* (72). These results together suggested that IGF-2R acts as a tumor suppressor gene (65).

IGF-IR and IR also internalizes in a ligand-dependent manner. Additionally, IGF-IR was shown to translocate to the perinuclear and nucleolar regions of the cell via SUMOlyation of three lysine residues on the β-subunit (73, 74). Nuclear IGF-IR acts as a transcriptional co-activator of the LEF/TCF complex, which in turn upregulates cell cycle progression drivers such as cyclin D1 and Axin2 (Figure 2.1) (75). Nuclear IGF-IR is highly associated with

advanced malignancy and therapeutic resistance. In a cohort of 53 patient-derived specimens, nuclear IGF-IR was observed in 7% of low-grade glioma and in 70% of high-grade glioma (76).

2.1.2 Insulin-like Growth Factors and Binding Proteins

The main IGF-IR ligands are IGF-1 and IGF-2 (7-8 kDa) that bind the receptor with high affinity and insulin that binds at 1000-fold lower affinity. While the major role of insulin is in cellular metabolism and the IGFs regulate growth and development at various developmental stages, their signalling pathways are similar. Insulin is produced by pancreatic beta cells whereas the IGFs are predominantly produced by the liver. IGF-1 production is under the control of the growth hormone (GH), and other tissue-specific, nutritional-, and developmental cues (77). IGFs and insulin are synthesized as pre-propeptides that contained an N-terminal signal peptide required for translocation to the endoplasmic reticulum. The signal peptide is subsequently cleaved to form a proprotein. The intermediate products, proinsulin and IGF pro-peptides, are then cleaved at the C-terminal to yield the mature form (78). Mature IGFs contain a hydrophobic site that binds the complementary hydrophobic sites on the receptors and IGF binding proteins (79). IGF-1 and IGF-2 can act locally in an autocrine or paracrine fashion and systemically via endocrine signaling. Local actions are involved in processes such as skeletal development and remodelling (80), physiological and pathological growth of breast tissue (81), while systemic regulation by the growth hormone (GH)/IGF-1/insulin axis modulates longevity, metabolism, and contributes to pathogenesis of age-related diseases including cancer (82). Pathogenic conditions can result from excessive IGFs; thus, free ligands are tightly regulated. Together with transcriptional and translational control of IGF production, the insulin-like growth factor binding proteins (IGFBP) and their proteases play an important role in modulating the accessibility of the ligands.

The IGFBP family consists of six proteins IGFBP-1 to IGFBP-6. IGF-1 in the circulation is bound to IGFBPs. Among them, 75-90% are bound to IGFBP-3 and the acid-labile subunit (ALS), together forming a ternary complex (83). IGFBPs serve diverse functions such as limiting bioavailability of free IGFs, modulating intra and extravascular IGF transport and prolonging half-life of IGFs (84). In a study analyzing IGF-2, IGFBP-1, and IGFBP-3 expression during fetal development in monkeys, it was shown that similarly to humans, IGFBP-3 mRNAs were expressed in a specific spatial/temporal pattern, localized to mature ureteric duct, collecting ducts while IGF-2 mRNA was expressed abundantly in uninduced metanephric blastema and renal mesenchyme during nephrogenesis and renal epithelial development (85). This demonstrated the importance of IGFBPs in localizing IGFs to specific tissue types at a critical time point in embryogenesis for regulating growth and development (85).

IGF/IGFBP affinities are modified by IGFBP proteases allowing the dissociation of the complex by cleaving the N and C terminal domains. IGFBP proteases include kallikreins such as plasmin and thrombin, cathepsins, and matrix metalloproteinases (MMPs) (84). The proteolytic activity reduces the affinity of IGFBP to IGFs, thereby increasing the levels of unbound IGFs and allowing the activation of the IGF-receptor (84). Mutations, glycosylation, and phosphorylation of the cleavage sites can block protease activities (79).

2.1.3 Signaling and Functions

Upon ligand binding, the tyrosine kinase domain of IGF-1R is activated and induces a conformational change that leads to autophosphorylation at Tyr950 which serves as a docking site for various signalling substrates including the IRS proteins (IRS-1 to 4), SHC1, Grb associated binder (GAB), and Crk adaptor proteins (CRK) (86). Src homology 2 (SH2) domain-containing signaling molecules such as Grb2 and p85, the PI3K regulatory subunit, recognize IRS-1, IRS-2, and Shc. Phosphorylated Grb2-son-of-sevenless (SOS) complex subsequently

triggers the downstream Ras- mitogen-activated protein kinase (MAPK) pathway which promotes cell proliferation and differentiation (87, 88). IRS-1 also binds the p85 subunit, activating the PI3K-protein kinase B (Akt)/ mammalian target of rapamycin (mTOR) pathway mediating the anti-apoptotic and cell survival activities (89). It was also shown using triple negative breast cancer cells that focal adhesion kinase (FAK) binds and activates IGF-IR and FAK activation may drive epithelial mesenchymal transition (EMT), cell migration and invasion (90, 91). Cell migration can also be activated by the Janus kinase (JAK)/ signal transducer and transcription (STAT) pathway downstream of the IGF-axis. JAK/STAT signaling was also shown to be involved in promoting cancer stemness (92). The collective effect of this family of activated proteins is to promote the proliferation, invasion, and survival which are important for both the physiological and pathological cell states.

2.1.4 IGF-signaling in the brain

IGF-signaling plays diverse roles during embryonic development and adulthood influencing neuron and brain growth, oligodendrocyte and astrocyte development. IGFs, IGF receptors, and IGFBPs are expressed in the central nervous system and predominantly signal through autocrine and paracrine regulations. Circulating IGFs was shown to cross the blood-brain-barrier (BBB) in adult rats and localize mainly in the forebrain (93). IGF-1 expression in different regions of the brain peaks during postnatal development, whereas IGF-2 is expressed mainly in mesenchymal tissues and peaks during embryonic development (94). IGF-action in the brain is tightly regulated and is cell type, microenvironment, and developmental phase-dependent. For example, IGF-1 stimulates the growth and survival of oligodendrocytes and its precursor and thus plays a critical role in myelin production (95). Using IRS-2-deficient mice compared to age-matched wildtype controls, myelination was shown to be impaired at postnatal day 10 but motor functions and myelination were restored when reaching adult stage, suggesting that IRS-2 is involved in initiation but not maturation of myelination (96). Any

alterations or indirect impact on the IGF-axis may result in pathogenesis in the brain parenchyma.

Furthermore, the IGF-axis plays an important role in memory and learning. Many studies have observed an association between IGF-1 deficiency and a decline in cognitive functions, especially due to aging, both in human and rodents (97). Aleman et al. demonstrated that higher IGF-1 serum levels in healthy old men was correlated with better age-sensitive cognitive measures including perceptual motor skills and mental processing speed(98, 99). A larger study consisted of 186 healthy participants found that higher total level of IGF-1 and total IGF-1/IGFBP-3 ratio but not free IGF-1 level were associated with cognitive decline measured by the Mini-Mental State Examination (MMSE) in a longitudinal study over 2 years (100). Morley et al. discovered that IGF-1 and bioavailable testosterone levels were positively correlated with visual and auditory learning in men (101). In rats, IGF-1 antisense oligonucleotide impaired learning of the conditioned eye-blink response and this effect could be reversed when cerebellar IGF-1 was reverted back to normal (102). Svensson et al. discovered that spatial learning and reference memory measured by the Morris water maze swim test decreased in old but not in young LI-IGF-$1^{-/-}$ mice (liver-specific, inducible inactivation of the IGF-1 gene, using the Cre-LoxP conditional knockout system) (103). In addition to IGF-1, the N-methyl-D-aspartate (NMDA) receptor also plays a role in learning and memory related to aging and are abundant in the hippocampus and the cortex (104). Reduction of the NMDA receptor responses diminished NMDA-depend long term potentiation, and in turn impaired spatial learning (105). Sonntag et al. determined that administration of IGF-1 into 28 months-old Fisher 344xBrown Norway rats resulted in an increase of NMDAR-2A and 2B levels similar to that of the young animal (9-10 months) in the hippocampus (106). Taken together, these results identified IGF-1 as an important neurotrophic hormone for learning and memory.

2.2 Hybrid receptors

As mentioned earlier, the IGF-IR and IRs are heterotetramers consisting of two α and two β subunits, linked by disulphide bridges. However, due to sequence homology, hybrid receptors between IR α–β and IGF-IR α–β dimers can also form. IR-A/IR-B (HIR-AB), IR-B/IGF-IR (HR-B), and IR-A/ IGF-IR (HR-A) hybrids each with characteristic ligand binding preferences and signaling were documented in mammalian cells (61).

In contrast to the 60% sequence homology between IRs and IGF-IR, the sequences of IR-A and IR-B only differ by a 12-amino acid long exon. While IR/IGF-IR hybrids have been well characterized, there is less information on HIR-AB hybrids due to the technical challenge in distinguishing homo and heterodimers. Recent studies by Blanquart et al. demonstrated that HIR-AB can be randomly formed in cells expressing both isoforms by using bioluminescence resonance energy transfer (BRET) (107). HIR-AB bound to insulin with similar affinity to that of the IR-B homodimers (108). The difference between IR-A and IR-B is their affinity to IGF-2. Similar to IR-A, HIR-AB demonstrated high affinities for IGF-2 and insulin, whereas IR-B preferentially binds to insulin (107). Due to the similar pharmacokinetics properties between HIR-AB and IR-A, activation by IGF-2 in cells expressing predominantly IR-A or HIR-AB may contribute to cancer progression (61).

In cultured fibroblasts transfected with insulin and IGF-IR expression plasmid, IR-A and IR-B were found to be randomly associated based on the relative molar ratio of each receptor (109). Bailyes et al. could predict the proportion of hybrid to homodimeric receptors based on the molar ratio of IR:IGF-IR in tissues homogenously expressing the receptors but not in those with heterogeneous cell populations (110). The ligand affinities for HR-A and HR-B are similar to IGF-IR and they bind IGF-1 with higher affinity than insulin as determined by radioimmunoassay, immunoprecipitation and BRET (108) (111). While IGF-1 was consistently found to have high affinity for HR-A and HR-B, there was discrepancy between

their affinities for insulin and IGF-2 (108, 112). Furthermore, a functional study revealed that insulin binding triggers the activation of HR-A but not HR-B in recruiting Crk adaptor protein II (CrkII), an intracellular signaling mediators specific to IGF-IR signalling, suggesting that excess insulin may drive the proliferation, anti-apoptotic, and mitogenic effects mediated downstream of IGF-signaling via HR-A (112).

2.3 Crosstalk between IGF-IR and other signaling pathways.

The IR/IGF-1R signaling pathway is part of a complex network of receptor tyrosine kinases (RTK) and crosstalk with several other RTK such as the epidermal growth factor receptor (EGFR), fibroblast growth factor receptor (FGFR), platelet-derived growth factor receptor (PDGFR), as well as steroid hormones including, estrogen receptor (ER), androgen receptor, and human epidermal growth factor receptor 2 (HER-2) has been documented**.** Knowlden et al. showed that EGFR was phosphorylated and subsequently increased extracellular signal-regulated protein kinase (ERK1/2) expression in the presence of IGF-2 in tamoxifen resistant breast cancer cells but not in wild-type cells and this activation was dependent on proto-oncogene tyrosine-protein kinase Src (c-SRC) that phosphorylates tyrosines 845 and 1101 in EGFR (113). Crosstalk between PDGFR and IGF-IR was also observed in rat liver myofibroblasts. Antibody mediated inhibition of IGFIR diminished IGF-1 and PDGF-induced DNA synthesis as confirmed by BrdU incorporation assay and immunoblotting. This study suggested several possible pathways and mediators that could be involved in the crosstalk including IRS-1, MAPK, PI3K and Phospholipase C γ1 (PLCγ1), but their involvement requires verification. (114).

Crosstalk between ERα and IGF-IR was documented in uterine cells, where IGF-1 induced by estradiol/ER signaling could initiate IGF-IR signaling *in vitro*. Conversely, the transcriptional activity of ER could be induced by IGF-1 in the absence of estradiol, and this was also shown in vivo as IGF-1-induced ER transcriptional activity was observed in the uteri

of ovariectomized mice (115, 116). Lastly, IGF-IR stimulation was shown to activate HER-2 signaling in breast cancer cells resistant to the HER-2-targeted antibody, Trastuzumab. Conversely, inhibition of IGF-IR signaling demolished HER-2 activation, disrupted heterodimerization of both receptors and restored therapeutic sensitivity (117).

IGF-IR signaling has been implicated in resistance to therapies that target other RTK and vice versa (118). The crosstalk between IGF-IR and other RTK remains therefore a challenge to successful therapeutic targeting of the IGF-axis as well as other major growth factors. (For examples of crosstalk between the IGF-IR and other signaling pathways, see **Table 2.1**.

2.4 IGF-Signaling in Cancer (target identification/validation)

2.4.1 IGF-1R and tumor progression

According to the Hallmarks of Cancer proposed by Hanahan and Weinberg, tumor development can be characterize by the ability to sustain proliferative signalling, evade growth suppression, resist cell death, enable replicative immortality, induce angiogenesis, and enable invasion and metastasis (119). The IGF-IR axis has been implicated in driving these phenotypes. Increased expression of IGF-1R was documented in various human malignancies including lung cancer, breast cancer, prostate cancer, glioma, melanoma, and others (62) and upregulation of IGF-1R was associated with metastasis, shorter survival, and poor prognosis (86, 120-122).

Genomic data from the Cancer Genome Atlas showed that among the documented samples, 15% of breast cancer contained genetic alterations in the IGF-axis. IGF-IR is frequently amplified and overexpressed. Moreover, using RNA sequencing, Farabaugh et al. stratified the expression of proteins along the IGF-pathway in different breast cancer subtypes and observed that IGF-IR was expressed at higher levels in Luminal A and B breast cancer, but not in basal or ERBB2^{+} subtypes (123).

As previously mentioned, activation of IGF-IR triggers downstream Ras-MAPK and PI3K-Akt-mTOR pathways contributing to cell proliferation and survival, respectively. IGF-IR also contributes maintenance of stemness in embryonic and germline stem cells under physiological conditions and cancer stem cells under pathological conditions (124). IGF-IR mediated maintenance of cancer stemness was documented in breast (125), colorectal (126), liver (127), lung(128), and brain (129) cancer stem cells. It was shown in lung carcinoma that IGF-IR activation promotes stem cell self-renewal via the regulation of POU class 5 homeobox1 (POU5F1) and the formation of a β-catenin/POU5F1/SOX2 (sex determining region Y-box 2) complex via the PI3K/AKT/GSK3β/β-catenin pathway (128).

Nuclear IGF-IR is associated with advanced stage cancer including metastatic colorectal cancer(130), liver carcinoma(131), breast cancer (132), and pediatric glioma (76). In addition to the transcriptional upregulation of cyclin D1, Axin 2, and IGF-IR genes discussed in the signaling section that ultimately led to cell proliferation and resistance to cell death, nuclear IGF-IR also phosphorylates histone H3 at tyrosine 41 and this recruits the Brg1 chromatin remodelling factor to H3. Brg1 and nuclear IGF-IR in turn, bind to the promotor of Snail family transcriptional repressor 2 (SNAI2), a regulator of the EMT, and induce its expression (75, 133). Consequently, changes in IGF-IR expression or its translocation can have multiple effects on the cell phenotype including acceleration of tumor progression and increased drug resistance, highlighting the importance of therapeutic targeting of IGF-IR.

2.4.2 IR, IR/IGF-IR hybrid receptors and tumor progression

IR, particularly IR-A, was found to be overexpressed in several cancers. Similarly, IGF-IR, IR-A can initiate downstream mitogenic effects upon IGF-2 binding. Physiologically, IR-A is normally expressed in fetal cells including fibroblast and liver cells but increased IR-A expression was documented in breast, lung, and colon cancer (63). Some studies suggested that not only overexpression IR-A contributed to tumor progression, but increased IR-A to IR-B

ratios also play a role. For example, in lung cancer IR-A mRNA expression was increased while IR-B mRNA expression was decreased in cancerous tissue relative to normal lung tissue and an elevation of the IR-A/IR-B ratio was observed (134). Increased IR-A:IR-B ratios were also observed in breast, colon, kidney, liver carcinomas and in glioblastoma and low-grade glioma over 93% of cells had high IR-A/IR-B ratios (134).

Moreover, as many cancers overexpress both IR and IGF-IR, HR-A and HR-B receptors are also abundant. A study analyzing 8 human breast cancer cell lines and 39 patient samples found that over 75% of breast cancers expressed more hybrid receptors than the tetrameric IGF-I receptors. In hybrid receptor-abundant cells, these receptors contributed more to IGF-I induced activation of the IGF-axis than IGF-IR (135, 136). Prevalence of a mixture of IR, IGF-IR, and hybrid receptors on malignant prostate tissue was shown to be significantly greater ($p<0.001$) than benign prostate tissues (137). In osteosarcoma, IR-A, IGF-IR, and HR-A were highly expressed and co-inhibition of all three receptors was shown to be more effective than selectively targeting IGF-IR (138).

2.4.3 IGF ligands/ IGFBP dysregulation and tumor progression

IGF ligands play a paracrine and/or autocrine role in promoting tumor growth. IGF ligands form complexes with the six high-affinity IGF-BPs and the half-life and bioavailability of the ligands are modulated by the IGFBPs (139). High IGF-1 levels were shown to increase the risk of developing various cancers including lung, breast, colorectal, and prostate carcinomas (140). Increased circulating IGF-1 levels were shown to play a role in early stages of transformation and carcinogenesis (62). Wu et al. reported that in liver-specific IGF-1 gene-deleted (LID) mice, there was an increased latency period and a decrease in the percentage of mice that developed chemically and genetically induced mammary tumors (141). Another study used the transgenic adenocarcinoma of mouse prostate (TRAMP) murine model, and found that mice that were homozygous for lit, a mutation that inactivates the growth hormone

release hormone receptor (GHRH-R) and reduces circulating levels of GH and IGF-1 had a significant reduction in the percentage of the prostate gland showing neoplastic changes and improved survival (142). These results suggested that circulating IGF-1 is involved in the onset of tumorigenesis and cancer progression *in vivo* in this model.

Lower IGFBP are associated with increased risk for several cancers including premenopausal breast carcinoma, prostate carcinoma, lung cancer, colorectal carcinoma, lung cancer, endometrial cancer, and bladder cancer (62, 143-145). In a case-controlled study of 1043 lung cancer patients and 11472 controls, a significant reduction in circulating IGFBP-3 was documented in the lung cancer patient group (144). A preclinical study showed that overexpression of tissue inhibitor of metalloproteinase 1 (TIMP-1) increases IGFBP3 levels, which indirectly decreases IGF-2 and inhibits liver hyperplasia in a transgenic murine hepatic tumor model (146).

Moreover, IGF-BP proteases were often active in tumor sites promoting tumor progression and metastasis. IGFs was found to regulate the IGF-BP proteases negatively or positively via binding in fibroblasts and smooth muscle cells (147-149). In breast carcinoma cells, Salahifar et al. discovered a novel product of IGFBP-3 proteolysis that is mediated via a mechanism independent of the IGF-IGF-BP interaction (150). This finding identified a distinct protease secretion mechanism; however, direct evidence on its role in contributing to advance malignancy is still not known. Prostate-specific antigen (PSA) is a serine protease that cleaves IGFBP-3, thereby increasing free IGF-1 and potentiating mitogenic actions (151).

2.5 IGF axis-targeting strategies (receptor, ligand, BP) – preclinical evidence and the clinical experience

As indicated above, the IGF-axis has been validated as a potential therapeutic target for various cancers. Currently, IGF-IR-targeting agents can be categorized into several groups namely, nucleic acid-based approach, antibodies, bispecific antibodies, small molecule

tyrosine kinase inhibitors (TKI) and IGF-ligand targeting agents includes antibodies and the IGF-Trap. The advantages and disadvantages of each approach are summarized in **Table 2.2** (152). Nucleic acid approach using antisense oligonucleotide, RNA interference (RNAi), and dominant negative receptors have been documented in various cancers including glioma (153), breast(154), lung(155) and prostate cancer (156). Antisense oligonucleotide and RNAi strategies introduce a single or double stranded RNA encoding IGF-IR antisense, respectively, to downregulate protein production. The dominant negative receptor approach is based on overexpressing an inactive form of the receptor and preventing ligand-mediated activation of the endogenous receptor (157). These approaches demonstrated high specificity in targeting IGF-IR, however, these methods based on genetic perturbation of the IGF-axis have limited clinical utility (157). Moreover, targeting the IGF-IR does not block the binding of IGF-2 to IR-A which drives mitogenicity in cancer cells. Anti IGF-IR antibodies blocks IGF activation by binding to the α -subunit. This method induces internalization and downregulation of IGF-IR signaling. However, IR co-inhibition causing adverse effects on glucose metabolism, and hyperglycemia as well as activation of compensatory RTK signaling may occur(158, 159). Similar to anti IGF-IR, bispecific antibodies target IGF-IR and an additional gene of interest such as EGFR(160). This technique takes into account pathways that crosstalk with IGF-IR with improved stability to oxidative and thermal stress (161). However, due to their size, steric hindrance and accessibility to the target sites are major challenges associated with this approach. (161). Small molecule TKIs represent another strategy for targeting IGF-IR. Although TKIs are designed to discriminate between different RTKs, cross reactivity of IGF-IR-targeting TKIs with the IR-axis has been documented (158). This may be provide a therapeutic benefit for cancers with increased IR-A expression, but can also target the IR-B, causing hyperinsulinemia and hyperglycemia (162).

In addition to targeting the IGF-IR, removing the IGF ligands from the circulation can also reduce the activation of IGF-signaling. IGF neutralizing antibodies block IGF-IR and IR-A activation by reducing the bioavailability of circulating IGF-ligands without affecting glucose metabolism due to low affinity for insulin. However, efficacy of the antibody depends on IGF-IR expression levels as high levels could outcompete with the antibody for ligand binding (163). Furthermore, reduction of plasma IGF may trigger compensatory feedback mechanisms (164). The IGF-Trap will be discussed in detail in section 2.6. Several IGF-IR targeting antibodies, TKI, and IGF-neutralizing antibodies have advanced to clinical trials. Clinical trial outcomes of these agents are summarized in **Table 2.3** (152) and discussed further in the below.

2.5.1 Targeting the IGF-I Receptor:

2.5.1.1 Antibodies

IGF-1R-targeting antibodies bind to the alpha subunit of the receptor and prevent ligand-binding. In addition, internalization of the receptor reduces expression (158). However, this approach does not block signaling through IR-A. Activation of the IGF-pathway can be bypassed through the binding of IGF-2 to IR-A; thereby induce mitogenic effects (158). A subgroup of this category is a bispecific antibody that targets two antigens. XGFR is a bispecific anti-IGF1R /EGFR antibody that showed inhibition of tumor growth and enhanced immune activation in pancreatic cancer *in vivo* (160).

Among all therapeutic agents targeting the IGF-axis in clinical phase, the majority were anti-IGF-IR antibodies including BIIB022 (Biogen (Cambridge, MA, USA)), Cixutumumab (IMC-A12-ImClone, New York, NY, USA), Dalotuzumab (MK-0646; h7C10-Pierre Fabre (Paris, France) and Merck (Kenilworth, NJ, USA)), Figitumumab (CP-751,871-Pfizer, New York, NY, USA), Ganitumab (AMG 479-Amgen Thousand Oaks, CA, USA), Istiratumab (MM141-Merrimack (Cambridge, MA, USA)), Teprotumumab (R1507-Genmab (Copenhagen,

Denmark) and Roche (Basel, Switzerland)), and Robatumumab (SCH 717454, 19D12-ImmunoGen (Waltham, MA, USA) and Sanofi (Paris, France)). Figitumumab was evaluated in a phase II clinical trial for metastatic prostate cancer and in a in phase III clinical trials for non-small cell lung cancer (NSCLC). The drugs were combined with their respective standard of care treatments. Safety was of concern due to higher rates of serious adverse events related to treatment including diarrhea, decreased appetite, asthenia, hyperglycemia, and no improvement in disease progression and survival was observed (165, 166) . Ganitumab was assessed in metastatic pancreatic cancer (167) and aggressive sarcomas (168). Ganitumab was given as a single agent in sarcomas and approximately 50% of participants had stable disease and 17% showed response over 24 weeks in phase II clinical trial (168). Teprotumumab had a successful phase III clinical trial in patients with thyroid eye diseases and was recently approved by the food and drug administration (FDA) for the treatment of Graves' disease (169). Despite having tolerable safety measures, Dalotuzumab did not improve progression-free survival and overall survival in metastatic colorectal cancer when combined with the standard of care (170). Cixutumumab did not show improved outcome in phase I/II advanced NSCLC or phase II advanced hepatocellular carcinoma (171, 172). Istiratumab (MM-141) targeting IGF-1R and ErbB3 for the treatment of pancreatic cancer showed worse progression- free survival than chemotherapy alone in a phase II clinical trial (173). Robatumumab and BIIB022 were both used as single agents. Although they met tolerable safety measures, they did not show improved outcome in metastatic tumors (174, 175).

2.5.1.2 TKIs

The advantage of small tyrosine kinase inhibitors (TKIs) is that the sequence homology between IGF-1R and IR-A/B kinase domains results in co-inhibition of IR-A and IGF-1R. However, inhibition of IR-A often affects metabolic insulin signaling leading to hyperglycemia (158, 159). Masoprocol (INSM-18, NDGA – InsMed (Bridgewater Township, NJ, USA)),

Linsitinib (OSI-906 – OSI (Farmingdale, NY, USA)), BMS-754807 (BMS (Montreal, QC, Canada)), AXL1717 (Picropodophyllin- Axelar AB (Solna, Sweden)) and XL-228 (Exelixis (Alameda, CA, USA)) were TKIs involved in clinical trials. Unlike anti-IGF-IR antibodies, TKIs were mostly used as a single agent and were well tolerated by patients. Treatments were mostly given orally instead of via intravenous injection. While some showed no improvements in survival and disease progression, XL-228 and AXL1717 had a beneficial effect in phase I trials for solid tumors and relapsed malignant astrocytoma, respectively (176, 177).

2.5.2 Targeting the IGF-ligands:

Targeting the IGF-ligands blocks IGF-1R and IR-A activation but does not affect metabolic functions mediated by the insulin-axis. However, study had shown that it is less effective than IGF-1R antibodies as the neutralizing effect is affected by IGF-1R expression levels (163). Currently the two IGF-neutralizing antibodies, Dusigtumab (MEDI-573-MedImmune, Gaithersburg, MD, USA) and Xentuzumab (BI-836845-Boehringer-Ingelheim, Ingelheim am Rhein, Germany), were in phase I clinical trials and had prolonged stable disease with very little side effects in metastatic breast cancer and advanced solid tumors (178, 179).

2.6 The IGF-Trap:

The validation of the IGF-axis as a therapeutic target has led to the development of the IGF-Trap. The IGF-Trap is a soluble human IGF-IR decoy consisting of the entire extracellular portion of the receptor that binds the IGF-ligands but not insulin with high affinity. The stability and bioavailability of the decoy were improved by the fusion of the Fc domain of human IgG_1 to the extracellular domain of the β subunit (152). Several similar Traps are currently in clinical use. Rilonacept, an interleukin-1 Trap, and the vascular endothelial growth factor (VEGF)-Trap (Aflibercept) are currently in clinical use for the treatment of cryopyrin-associated periodic syndromes and metastatic colorectal cancer, respectively (180, 181) while the TNF-Trap (Entanercept, Enbrel) is used for the treatment of inflammatory conditions. The IGF-Trap

was developed by the Brodt laboratory group in a stepwise manner (152). The truncated receptor was first shown to promote survival and reduce liver metastasis in Lewis lung carcinoma cells (182). The decoy was further genetically engineered to be administered in *vivo*. Wang et al. demonstrated therapeutic advantages in reducing liver metastases in colon and lung carcinomas (183). The IGF-Trap was then generated with the fusion of IGF-IR to the IgG-Fc domain to improve pharmacokinetics of the IGF-Trap. The IGF-Trap not only demonstrated reduction of liver metastases of lung and colon carcinoma but also showed longer half-life and enhanced tumor inhibitory effect such as growth arrest, compared to an anti-IGF-IR antibody at the same concentration (184). The third generation IGF-Trap was bioengineered to eliminate the high-molecular-weight aggregates formed by oligomerization due to disulfide bonds between adjacent Fc fragments. This was done by cysteine - serine substitutions on the IgG_1 Fc fragment and elongating the linker between the IGF-IR extracellular domain and the Fc domain. The IGF-Trap has retained the advantages of the IGF neutralizing antibodies in blocking IGF-IR and IR-A activation without compromising glucose metabolism while improving its therapeutic activity. However, limitation of size, oligomerization, and potential feedback regulation via the hypothalamus-pituitary axis may present challenges to the use of this type of IGF-targeting therapeutic agent (152).

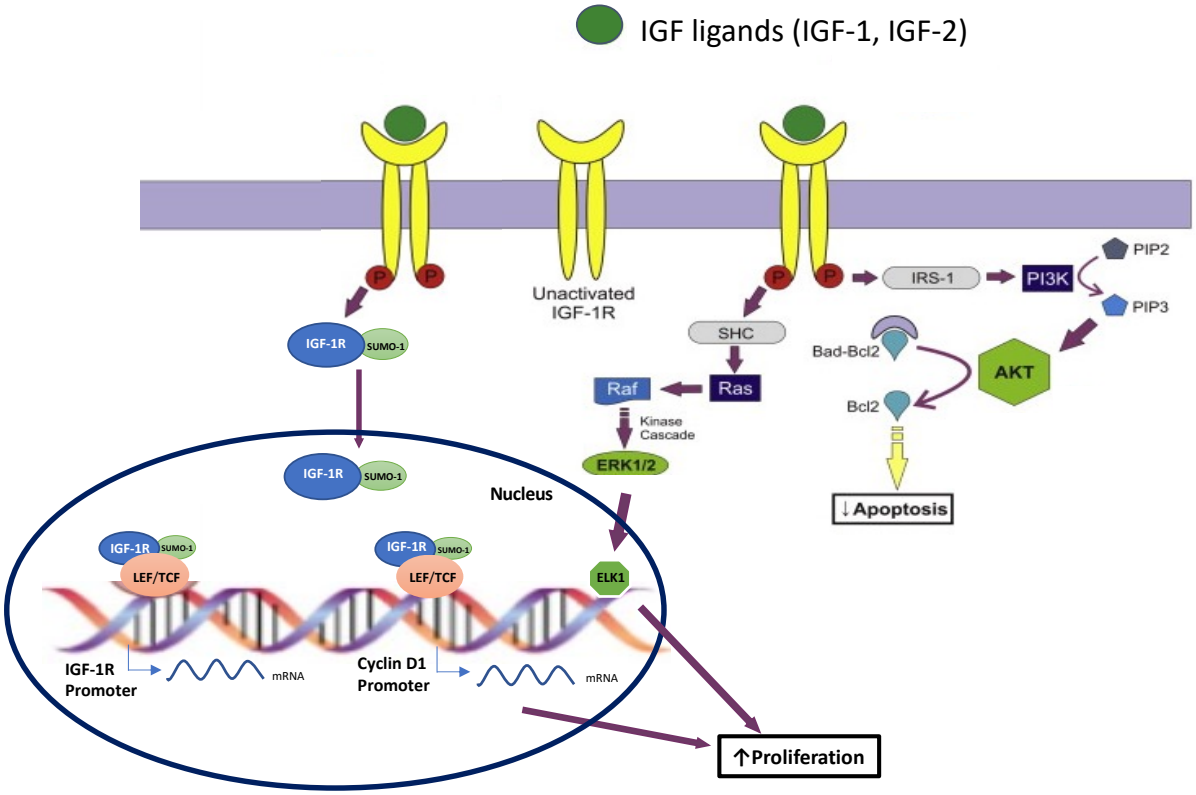

Figure 2.1. IGF-signaling and internalization. The insulin-like growth factor (IGF) system plays a crucial role in tumorigenesis and mediates cell survival, mitogenesis, cell migration and drug resistance. Ligand binding to the IGF1R initiates MEK/ERK and PI3K/ATK signaling. Receptor activation can also lead to nuclear translocation of the receptor where it can act as a transcriptional co-activator for its own promoter but also for cyclin D1 - a key driver of cell cycle progression. Nuclear IGF-1R is associated with advance staged cancer including pediatric high-grade glioma. Blocking ligand binding can inhibit IGF-IR activation and nuclear translocation and is therefore a potential therapeutic strategy for high-grade glioma. (Adapted from Denduluri et al., 2015, and Sarfstein et al., 2013)

Table 2.1. Crosstalk between IGF-IR and other receptor tyrosine kinases.

	Potential mechanism/mediators involved	Response	Physiological or Pathological conditions	Reference
EGFR	MAPK	IGF-2 increased EGFR phosphorylation in tamoxifen resistant breast cancer cells but not wildtype cells.	breast cancer cells	Knowlden et al. 2005
PDGFR	IRS-1, MAPK, PI3K PLC gene	IGF-IR is essential for mediating PDGFR-dependent mitogenic activity.	Liver myofibroblasts	Novosyadlyy et al. 2006
ER	Akt, MAPK	ERα can be activated by IGF-IR signaling in an estradiol independent manner.	Uterine cells, Uterus (*in vivo*)	Klotz et al. 2002
HER-2	Heterodimerization of IGFIR and HER-2	IGF-IR signaling simultaneously activates HER-2 in HER-2 targeted antibody resistant cells.	Breast cancer cells	Nahta et al. 2005

Table 2.2. Pros and cons of IGF-Targeting strategies from pre-clinical and clinical experience.

Target	Approach	Advantage	Disadvantage	Reference
IGF1R	Nucleic acid approach	High specificity via mRNA degradation	Toxicity, challenges in drug delivery and uptake Compensatory signaling through IR-A Low translational potential	Bohula et al. 2003
	Antibodies	Induce internalization and downregulation of IGF1R	Adverse effects on glucose metabolism Hyperglycemia activation of IR-A by IGF-2 nuclear translocation of IGF-IR Compensatory receptor tyrosine kinase (RTK) signaling	Buck et al. 2010 Osher et al. 2019
	Bispecific antibodies	Neutralizing two or more targets improved protein stability to oxidative and thermal stress Inhibit compensatory signaling by other RTKs	Steric hindrance large, reduced intra-tumoral penetration	Runcie et al. 2018, Schanzer et al. 2016
	TKI	Cross reactivity with IR	Affects metabolic insulin signaling via IR-B hyperglycemia short half-life	Osher et al. 2019, Quinn et al. 2014
IGF-ligands	Antibodies	Block IGF-IR and IR-A activation Low affinity for insulin minimizes adverse effects on glucose metabolism Reduced ligand bioavailability in the serum	Efficacy depends on IGF-IR expression levels Reduced plasma IGF levels may trigger compensatory feedback mechanisms	Tian et al. 2014
	Traps	Block IGF-IR and IR-A activation Low affinity for insulin minimizes adverse effects on glucose metabolism Reduce ligand bioavailability in the serum Fc fusion proteins increase serum half-life	Size may limit diffusion into the tumor site Oligomerization due to disulfide bonds may affect manufacturability Could potentially trigger a compensatory feedback mechanism upon long-term administration	Tian et al. 2014 Beck et al. 2011

Table 2.3. Outcomes of IGF-1R Clinical Trials

Target	Drug	Phase	Disease	Single agent or combination	Efficacy and Survival (Improved / Not significant/ Hazardous)	Safety (Well tolerated/ Tolerable/ Hazardous)	Quality of life (Treatment method and frequency)	Reference
IGF1R Antibodies	Figitumumab (CP-751,871)	II	Metastatic castration-resistant prostate cancer	docetaxel/prednisone	Hazardous PFS HR:1.44	Hazardous Tx vs CNT SAE: 41% vs 15%	tx given intravenous twice daily. CNT: every 3 weeks	De Bono et al. 2014
		III	NSCLC	Chemotherapy (paclitaxel and carboplatin)	Hazardous Median OS HR: 1.18 PFS HR: 1.10	Hazardous Tx vs CNT SAE: 66% vs 51%	tx given intravenously on day 1 of each 3-week cycle for up to 6 (~ 1 year). CNT: every 3 weeks	Langer et al. 2014
	Ganitumab (AMG 479)	III	Metastatic pancreatic cancer	Gemcitabine	Not significant (12mg/kg / 20mg/kg) Median OS HR: 1.00/0.97 PFS HR: 1.00/ 0.97	Tolerable SAE: 68% (12mg/kg) vs 59% (20mg/kg) vs 56% (placebo)	CNT: 3 times each 28-day cycle Additional tx given intravenously 2 times each 28-day cycle.	Fuchs et al. 2015
		II	Ewing family tumors or desmoplastic small round cell tumors	Single	Improved ORR: 6% SD: 49% CBR: 17%	Tolerable 63% Tx attributable adverse events 45% experienced SAE. 0% discontinuation of Tx due to Tx related AEs	Tx given intravenously every two weeks	Tap et al. 2012
IGF1R Antibodies	Teprotumumab (R1507)	III	Thyroid eye disease	Single	Improved Response at week 24: 69% vs 20% Therapeutic effects at week 6: 43% vs 4%	Tolerable Hyperglycemia in patients with diabetes but controlled by adjusting medication	Tx given intravenously every 3 weeks. (8 infusions in total)	Smith et al. 2017
	Dalotuzumab (MK-0646; h7C10)	II/III	Metastatic colorectal cancer	Cetuximab and irinotecan	Hazardous	Tolerable SAE:	Tx given IV either 10mg/kg once weekly or 7.5mg/kg every second week in	Sclafani et al. 2015

					PFS HR: 1.33/ 1.13 (10mg/kg/week, 7.5mg/kg/2 week) OS HR: 1.41/ 1.26	49.6% vs 42% vs 38.3% (10mg/kg/week, 7.5 mg/kg/2 week, placebo)	addition to cetuximab and irinotecan treatments.	
	Cixutumumab (IMC-A12)	I/II	Advanced NSCLC	Erlotinib	Not significant SD: 5/18 (28%) Median PFS:39 days Range:21-432+ days	Well tolerated Majority AE are G1 or 2. No significant higher increased incidence of rash and fatigue compare to other studies with EGFR combination therapy.	Tx given 4 times during the 28-day cycles in addition to erlotinib.	Weickhardt et al. 2012
		II	Advanced hepatocellular carcinoma	Single	Not significant. 4-month PFS 30% vs 42% (placebo CNT of sorafenib trial)	Hazardous 46% hyperglycemia, 25% became diabetic 1 treatment related mortality	Tx given intravenously weekly.	Abou-Alfa et al. 2014
	Robatumumab (SCH 717454, 19D12)	II	Relapse osteosarcoma and Ewing sarcoma	Single	No significant in osteosarcoma Improved in a small subset of Ewing sarcoma patients receiving treatment for >4 years	Well tolerated Drug-related SAE: 3% (resectable osteosarcoma) 6% non-resectable osteosarcoma, 7% Ewing sarcoma	Tx given ever 2 weeks.	Anderson et al. 2016
	Istiratumab (MM141)	II	Metastatic PDAC	Chemotherapy Paclitaxel/gemcitabine	Hazardous Median PFS HR: 1.88 Median PS HR:1.36	Tolerable No significant difference in SAE (>G3) Higher low-grade AE (39.5% vs 24.4%) in Tx group	Tx given IV every 2 weeks combined with CNT treatment.	Kundranda et al. 2020
	BIIB022 (Biogen)	I	Relapsed or refractory solid tumors	Single	Not significant No complete or partial responses. 59% stable disease. 29% progressive disease,	Well tolerated Low incidence of grade 3 toxicities but no grade 4 or 5	Tx given IV every 3 week.	Von Mehren et al. 2014
IGF1R Antibodies	AVE1642 (EM164)	I	Advanced solid tumors	Docetaxel/gemcitabine/erlotinib/ doxorubicin	Improved 3 response 22 durable stabilizations 44% disease control rate Vs previous study using docetaxel 17% in melanoma and 7% with gemcitabine in leiomyosarcoma	Tolerable 36/52 (62%) experience Gr3 or 4 AE (neutropenia 16/58. 13/19 SAE possibly related to Tx. 3 pts experience SE leading to death. Similar to docetaxel alone	Tx given intravenously once every 21-day cycle.	Macaulay et al. 2012
IGF1R TKI	Linsitinib (OSI-906)	III	Locally advanced or metastatic ACC	single	Not significant OS HR:0.94	Well tolerated	Tx given orally twice daily.	Quinn et al. 2014

					PFS HR:0.83 3 pts partial response, 8 prolonged PFS	TEAE: 97.8% vs 93.8% (Tx :P) GR5: 5.6% vs 10.4% GR4: 10.1 vs2.1 Gr3: 45.6 vs 31.3		
	BMS-754807	I	Solid tumors	Single	Not significant 7/19 SD>100 days (SCLC, osteosarcoma)	Well tolerated. 1/19 had Gr3 AE All other AE ≤Gr2	Tx given once daily.	Desai et al. 2010
	XL-228	I	Solid tumors, multiple myeloma	Single	Improved 41% SD >12weeks (56% NSCLC)	Well tolerate Drug-related AE: Gr 3 or 4 neutropenia and hyperglycemia	Tx given IV once a week.	Smith et al. 2010
	AXL1717 (Picropodophyllin)	I	Relapse Malignant astrocytoma	single	Improved 4/9 SD, 1/9 PR (OS 20-33 months vs 15 months median survival after diagnosis)	Well tolerated. Main SAE: neutropenia 5/9	Tx given orally twice daily.	Aiken et al. 2017
		II	advance/metastatic NSCLC	single	Not significant OS, PFS and their HR not statistically significant as compared to docetaxel.	Well tolerated Less incidence of treatment-related Gr3/4 neutropenia compared to docetaxel.	Tx given orally everyday.	Bergqvist et al. 2017
	Masoprocol (INSM-18, NDGA	II	Non-metastatic hormone-sensitive prostate cancer	Single	Not significant Lengthens median PSADT Does not induce significant PSA declines	Well tolerated Low incidence of Gr3 events.	Tx give orally everyday.	Friendlander et al. 2012
IGF-neutralizing antibody	BI836845	I b/2	HR+ locally advanced or metastatic breast cancer	Exemestane and everolimus	Improved 12/21 (57%) disease control 4/21 (19%) PR Median PFS: 9.4 months	Well tolerated. Most AE are Gr ½. No drug-related AE led to discontinuation.	Tx given intravenously once every week additional to exemestane and everolimus.	Cortes et al. 2016
	Dusigtumab / MEDI-573	I	Advanced solid tumors	Single	Improved. No partial or complete responses 33% SD	Well tolerated. Most AE were ≤ grade 2	Tx given every intravenously every week.	Haluska et al. 2014

NSCLC: non-small-cell lung cancer, OS: overall survival, HR: hazard ratio, PFS: progression-free survival, ORR: objective response rate, SAE: serious adverse events PSA: prostate-specific antigen, PSADT: prostate-specific antigen doubling time, SD: stable disease, CBR: clinical benefit rate (complete +partial response + stable disease ≥ 24 weeks), ACC: adrenocortical carcinoma, TEAE: treatment emerged adverse event. SCLC: small cell lung cancer. PR: partial response, HR: hormone receptor, Tx: Treatment

Chapter 3. Targeting the IGF-axis in pediatric high-grade glioma inhibits cell cycle progression and cell survival

Yinhsuan Michely Chen[1,2&], Matthew Leibovitch[2&], Michele Zeinieh[4], Nada Jabado[1,2,4] and Pnina Brodt[1,2,3,5*]

[1]Department of Medicine, Division of Experimental Medicine, McGill University, [2]The Research Institute of the McGill University Health Center, Montreal, QC H4A 3J1, [3]Department of Surgery, [4]Department of Paediatrics and Human Genetics, [5]Department of Oncology, McGill University, Montreal, QC, Canada

Running title: IGF1R signaling and activity in pediatric high-grade glioma

[&]These authors contributed equally to this manuscript

*To whom all inquiries should be addressed at**:** Research Institute of the McGill University Health Centre, 1001 Décarie Blvd, Glen Site, Room E.02.6220 Montréal, QC H4A 3J, Canada,

Telephone: (514) 934-1934 (Ext. 36692) Email: pnina.brodt@mcgill.ca

Author Contributions: YM Chen and M. Leibovitch: Data curation, formal analysis, investigation, methodology, manuscript writing, M. Zeinieh: Resources, technical support, N Jabado : Resources, supervision, analysis, P. Brodt: Conceptualization, resources, formal analysis, supervision, funding acquisition, investigation, manuscript writing and editing.

The authors have no conflict of interest to declare

3.1 ABSTRACT

Pediatric high-grade gliomas (pHGG) accounts for approximately 8-12% of primary brain tumors in children. Prognosis is poor with a median survival of 9-15 months. IGF-1 receptor (IGF-1R) gene amplifications have been identified in high-grade gliomas and may contribute to its highly aggressive phenotype, but the effect of IGF inhibitors on pHGG is yet to be determined. In the present study, we analyzed the response of patient-derived pediatric high-grade glioma cells to a novel IGF-1R inhibitor, the IGF-Trap. Using immunohistochemistry, we found that IGF-1R was localized to both the nucleus and cell membrane in different pHGG PDX lines under basal conditions. In response to ligand binding, nuclear transport of the receptor increased, and this was associated with transcriptional upregulation of both the receptor and cyclin D1, suggesting that IGF-1R could regulate its own expression and cell cycle progression in these cells. IGF-1 increased the proliferation of the pHGG cells DIPG13 and SGJ2 and this could be blocked by the addition of the IGF-Trap. The IGF-Trap also reduced colony formation in optimal growth medium and blocked the ability of IGF-1 to rescue these cells from starvation-induced apoptosis. Taken together, these results identify IGF-1R as a transcriptional activator and mediator of cell cycle progression, cellular proliferation, and survival in pHGG and identify the IGF-axis as a potential target in high-grade pediatric gliomas.

Key words: Pediatric glioma, IGF signaling, the IGF-Trap, nuclear translocation.

Importance of manuscript: The role of the IGF axis in pediatric high-grade glioma (pHGG) progression is not well understood. Our aim was to analyze IGF signaling in clinically relevant pHGG models and assess the potential of a newly engineered IGF-1R signaling inhibitor, the IGF-Trap, to block IGF-dependent cellular functions in these cells. Using PDX–derived pHGG cells

maintained under conditions that preserved stemness, we report here that the IGF-1R could regulate pHGG growth via two parallel pathways. While ligand binding activated ERK and PI3K/Akt signaling, the receptor also translocated to the nucleus, where it could activate cyclin D1 transcription to drive cell cycle progression. Blockade of ligand binding by the IGF-Trap inhibited both pathways reducing cell survival and proliferation and inhibiting cell cycle progression. There are currently limited treatment options for pHGG and the prognosis remains dismal. Our data identify the IGF-axis as a potential target in this deadly disease.

3.2 INTRODUCTION

Brain cancer is the second most common cancer and the leading cause of cancer-related death in children. Although advances have been made in the classification and treatment of this disease, based on molecular stratification, the prognosis for high-grade gliomas (WHO Grade III and IV) remains poor. While the cause remains unknown, genetic mutations including gene amplifications and deletions increase the risk of developing brain tumors. Among them gene alterations in receptor tyrosine kinases and other cell cycle regulators are highly prevalent in hemispheric pediatric high-grade gliomas (pHGG) while Lys_{27}Met substitutions in histone H3 (H3 K27M) is a signature mutation of diffuse midline gliomas (1). Previous studies have shown that the insulin-like growth factor-1 receptor (IGF-1R) gene is amplified at high frequency in pediatric high-grade gliomas and is the second most frequently amplified gene in diffuse intrinsic pontine glioma (DIPG). Moreover, nuclear localization of IGF-1R was associated with advanced stage pHGG (2).

Insulin-like growth factors (IGF-1 and IGF-2) are mediators of cell growth and differentiation. IGF-1 is essential for early brain development, where it was shown to promote neuronal proliferation and glial cell survival (3). Its levels in the brain were shown to decrease drastically after the perinatal period (3). IGF-signalling is triggered when IGF ligands bind to the cell surface IGF-1 receptor, activating downstream signal transduction cascades including the PI3K/Akt and MEK/ERK signaling that mediate cell survival and proliferation. Ligand binding also triggers receptor modification by small ubiquitin-like modifier protein–1 (SUMO-1) and nuclear translocation via vesicular transport (4). Nuclear IGF-1R can bind to the enhancer-like regions of several promoter, activating transcription of various genes including its own and that of cyclin D1. Thus, receptor activation can regulate cell cycle progression and cell proliferation that are critical for tumor progression and metastasis, via several different pathways.

The IGF-Trap is a soluble form of IGF-1R that inhibits IGF-signaling by binding to the IGF ligands, reducing their bioavailability and impeding receptor activation. While IGFBPs have higher affinity to IGF-ligands than IGF-IR, IGFBPs have a short half-life *in vivo* (5, 6) and are therefore not ideal for clinical applications. The bioengineering and optimization of this novel IGF inhibitor were described in detail previously (7, 8). In pre-clinical studies, the IGF-Trap could inhibit the growth of several very aggressive tumors including triple negative breast cancer cells and metastatic colon and lung carcinoma cells (7, 9). A new, highly effective variant of the IGF-Trap was recently produced with increased anti –tumorigenic potency (10). Its effect on glioma growth has not yet been evaluated.

There is a compelling body of evidence implicating the IGF axis in glioma progression. Studies based on pre-clinical glioma models including our own, have identified this receptor as a therapeutic target in this disease (11, 12). However, there is presently a lack of animal models for pHGG, and scant information on it role in this highly aggressive disease. A recent study revealed a significant association between high/moderate IGF-1R expression and poor survival in pHGG and found that IGF-1R increased the radio-resistance of pHGG cells, identifying it as a potential target for increased therapeutic efficacy (13). The objective of this study was to investigate IGF signaling in clinically relevant pHGG models and assess the therapeutic potential of the IGF-Trap in the treatment of these cancers.

3.2 METHODS

Cells:

The patient- derived primary tumor cell lines (DIPG13, BT245, HSJ19 and HSJ51) were described in detail previously(14). DIPG13 and BT245 were kind gifts from Dr. Michelle Monje (Stanford University, CA) and Dr. Keith Ligon (Dana-Farber Cancer Institute, Boston, Mass); they were received in September 2014 and November 2015, respectively. HSJ-019 and HSJ-051 resections were obtained in September 2015 and July 2016, respectively from the Department of Neurosurgery of the St. Justine Hospital (Montreal QC, Canada) and PDX lines developed at the Research Institute of the McGill University Health Center (MUHC RI). These cells were all authenticated using the Microsatellite Geneprint 10 analysis (Genome Qeubec) upon receiving and periodiocally after 4 (HSJ-19), 7 (HSJ-51), or 9 (DIPG13, BT245) passages. To preserve stemness, the cells were plated on laminin-coated culture dishes and maintained in Neurocult NSC proliferation media (STEMCELL Technologies- Vancouver, BC, CA) containing 0.0002% heparin and supplemented with 10ng/ml basic fibroblast growth factor (bFGF, Wisent-St. Bruno, QC, CA) and 20ng/ml epidermal growth factor (EGF, Peprotech- Cranbury, NJ, USA) (Sigma-Oakville, ON, CA). The tumor-derived cell lines were confirmed to match original samples by STR fingerprinting(14). The SJ-GBM2 cells (also known as SJG2, the designation used throughout this manuscript) are part of the NCI Pediatric Preclinical Testing Program (PPTP) cell line panel. These cells were maintained in DMEM/F12 medium (Wisent- St. Bruno, QC, CA) with 10% fetal bovine serum (FBS).

Reagents and Antibodies:

Recombinant human IGF-1 was from R&D Systems (Toronto, ON, CA). Rabbit monoclonal anti IGF-1R (ab182408) and p-IGF-1R (Y-1161; ab39398) antibodies were from Abcam (Cambridge,

MA, USA). Antibodies to ERK (9102S), p-ERK (9101S), GAPDH (2118S) Akt (9272S) p-Akt (3787S) and Cyclin D1 were all from Cell Signaling (Beverly, MA, USA). Antibody to tubulin (T9028) was from Sigma. Secondary antibodies Alexa Fluor 488-goat-anti-rabbit was from Life technologies (Burlington, ON, CA) and DAPI from Invitrogen (Burlington, ON, CA). The MEK inhibitor (PD98059) was from Calbiochem (Sigma-Aldrich Canada, Oakville, Ont) and Dynasore from EMD Millipore.

Expression levels of IGF-1R and ligands in PDXs:

RNA sequencing data was sourced from Krug et al (15). Gene expression was quantified by the number of primary alignment reads (MAPQ>3) falling into exonic regions of IGF-1, IGF-2, and IGF-IR and counts were normalized to mapped reads per kilobase of transcript per million (RPKM). Additional information can be found in Supplementary text. Sequencing files are available under Gene Expression Omnibus (GEO): GSE128745.

IGF-1R activation and signaling

Cells were cultured in complete medium for 24 hours followed by starvation media (DMEM/F12 medium) for 16 hours prior to stimulation with 50 (DIPG13) or 10 (SJG2) ng/ml IGF-1, in the presence or absence of IGF-Trap (2:1 IGF-Trap:IGF-1 molar ratio). Following stimulation, the cells were placed on ice, rinsed twice with ice cold PBS and lysed directly on the plate with the RIPA lysis buffer (50mM Tris (pH 7.4), 1mM EDTA, 150mM NaCl, 1% (w/v) NP-40, 2mM Na_3VO_4, 5mM NaF, 0.25% sodium deoxycholate and a protease inhibitor cocktail (Roche, Mississauga, ON, CA)). The lysates were transferred to 1.5 ml tubes, vortexed for 30 seconds and incubated on ice for 5 minutes. Tubes were centrifuged at 13000 x g for 10 minutes at 4^0C and supernatants were transferred to clean 1.5 ml tubes. Cell lysates were quantified using the BCA assay and analyzed by Western blotting.

RNA extraction and qPCR

Cells were cultured in complete media (DIPG13) or in DMEM/F12 containing 1 % FBS (SJG2) for 48 hours. Total cellular RNA was extracted using Trizol (Life Technologies, Burlington, ON, Canada) and qPCR was performed using standard procedures, as we previously described (16), the primers described in Supplementary Table 3.1 and the FASTSTART Universal SYBR Green reagent (Roche Pharmaceuticals, Bedford, MA) according to manufacturer's instructions. The Applied Biosystems 7500 Fast real-time cycler was used to analyze the samples.

Immunocytochemistry (ICC):

Cells were seeded on laminin-coated coverslips (2 x 10^4 cells/coverslip), incubated for 48 hrs at 37°C, fixed for 20 min at RT in 3.7% paraformaldehyde in 5% sucrose and washed repeatedly in PBS. Cells were permeabilized in 0.1 or 0.2% Triton X-100. The coverslips were incubated in blocking medium (5% serum in PBS) followed by incubation for 1 hr at RT with the indicated primary antibodies and a 30 min incubation at RT with the appropriate Alexa Fluor-conjugated secondary antibody. The coverslips were counterstained with DAPI and mounted in ProLong Gold mounting reagent. Images were analyzed using a Zeiss LSM780 laser scanning confocal microscope equipped with an AxioCam camera.

Subcellular fractionation

Cells were cultured for 18 hr in basal media (DMEM/F12) depleted of growth supplements and growth factors and then stimulated with 10 or 50 ng/ml IGF-1 for the duration indicated. Dynasore (30 μM) was added 4 hours prior to addition of IGF-1. The cells were lysed on ice with a hypotonic buffer (20mM HEPES, 1mM EDTA, 1 mM EGTA, 1mM DTT, protease inhibitors, phosphatase inhibitors) containing 0.2% NP40. The lysates were centrifuged at 4°C for 20 sec at 15,000 rpm, the supernatants containing the cytoplasmic fractions collected and the pellets containing nuclei

washed twice with hypotonic buffer and resuspended in a high salt buffer (420mM NaCl, 20 mM HEPES, 1mM EDTA, 1mM EGTA, 20% glycerol, 1mM DTT, 0.5 mM PMSF) containing protease and phosphatase inhibitor cocktails and incubated on a rotating shaker for 30 min at 4°C. Lysates were centrifuged for 20 min at 15,000 rpm and the supernatants containing the nuclear fractions collected. Both fractions were stored at -80°C until used.

Immunoblotting:

Immunoblotting was performed as we described in detail previously (17). Briefly, cells were lysed in RIPA lysis buffer. Following centrifugation at 13,000 x g for 10 minutes, lysates were separated by SDS-PAGE using 8 or 10 % polyacrylamide gels and transferred onto polyvinylidene difluoride (PVDF) or nitrocellulose membranes. Membranes were blocked in 5% BSA in TBST (Tris buffered saline with 0.1% Tween) for 1 hr followed by incubation, first at 4°C overnight, with the primary antibody and then for 1 hr at RT with HRP-conjugated anti-rabbit or anti-mouse immunoglobulin secondary antibodies (Jackson ImmunoResearch- West Grove, PA, USA), as appropriate. Signal detection and densitometry were performed using ImageQuant Las4000.

Analysis of cell proliferation in real time

DIPG13 and SJG2 cells were seeded in 24 or 48-well plates and incubated in complete medium at 37°C overnight. Prior to analysis, the cells were maintained in culture medium depleted of growth factors or specific supplements as indicated, and supplemented with 10 (SJG2) or 50 (DIPG13) ng/ml IGF-1. The cells were placed in the Incucyte live cell imaging system (Essen Bioscience, Ann Arbor, MI, USA) and images acquired every 6 hours for 4 days and analyzed using the phase confluence Incucyte setting.

MTT Assay:

SJG2 cells were seeded in 96-well plates and incubated overnight at 37°C in complete medium. Cells were washed and cultured in growth supplement-depleted medium, as indicated, in the presence or absence of 10ng/ml IGF-1 and with or without the indicated concentrations of the IGF-Trap. The MTT reagent was added and incubated for 3-4 hours at 37°C, the formazan crystals dissolved in DMSO, and absorbance recorded at 570 nm.

Apoptosis Assay:

Cells were seeded in 96-well plates and incubated overnight at 37°C in complete medium. The medium was then replaced with growth supplements-depleted medium as indicated, and the cells incubated in the presence or absence of IGF-1, and with or without the indicated concentrations of IGF-Trap. The Annexin V red reagent (Essen Bioscience-Ann Arbor, MI, USA) was added, and cells analysed in the Incucyte live cell imaging system. Images were acquired every 3 hours for 5 days and the Incucyte Integrated Analysis software used to analyze the data.

Cloning assay:

DIPG13 (500 cells/well) were seeded onto laminin coated 6 wells plates and cultured in complete medium, with or without 50ng/ml IGF-1 and in the presence or absence of IGF-Trap (1:1 molar ratio to IGF-1) . The medium was replenished every 4 days for up to 15 days, at which time colonies were fixed in 4% paraformaldehyde and stained with 0.5% crystal violet. Colonies were counted and sized using a Nikon Eclipes Ts2 microscope and the NIS-Elements software.

Cell Cycle analysis.

Cell cycle was analyzed by flow cytometry. Cells in 6-well plates ($5x10^4$ cells/well) were starved (in DMEM/F12) overnight for 18 hours before treatment for 24 hours with the indicated concentrations of IGF-1, IGF-Trap or both, vehicle (PBS) or complete medium (as positive

control). Cells were collected, centrifuged at 1000 rpm for 5 minutes, washed twice with PBS and fixed for 20 minutes in chilled 70% ethanol. Cells were stained with propidium iodide (20 μg/ml), treated with RNase A (100 μg/ml) for 2 hours at 4°C in the dark, and debris removed using a cell strainer (100 μm) before the analysis. Cell cycle phases were determined by acquiring at least 10^4 events using the FACSCanto (BD Biosciences, San Jose, CA, USA) and the data analyzed using the ModFit software (Verity Software House, Topsham, ME, USA).

3.4 RESULTS

The role of the IGF axis in pHGG progression is not yet well understood. Our aim was to evaluate IGF signaling in clinically relevant pHGG models. We began by evaluating the response to IGF-1 in several patient-derived xenograft (PDX) pHGG cell lines. We first compared expression levels of IGF-1R and its ligands in a library of pHGG PDXs RNA-sequencing data(18) and selected DIPG13 for further study based on a transcriptomic profile of high IGF-1R and mid/low IGF-ligand expression (Supplementary Figure 3.1). These cells have an undifferentiated phenotype and harbor the characteristic H3.3 K27M mutation frequently identified in midline tumors(1, 14). They are therefore representative of traits characteristic of the clinical disease. In addition, we also used the SJG2 cells derived from a grade IV pediatric glioblastoma expressing wild type H3 and harboring a Met fusion gene. This cell line is representative of the H3/IDH WT subgroup of pHGG that contains largely hemispheric tumors (19). We began by measuring expression of the IGF-1R and its ligands in DIPG13 and SJG2 cells using qPCR and found that both expressed measurable levels of the receptor and both ligands, although IGF-1R and IGF-2 mRNA levels were 25-fold and 4 fold higher, respectively in DIPG13 cells while SJG2 cells expressed 3 fold higher levels of IGF-1 (**Figure 3.1A-C**).

3.4.1 IGF-1R signaling in DIPG13 cells can be blocked by the IGF-Trap. Having confirmed high IGF-1R expression levels in DIPG13 cells, we next analyzed IGF-1R-initiated signaling in these cells. We found that following stimulation with 50 ng/ml IGF-1, IGF-1R was rapidly activated in these cells, triggering ERK and PI3K/Akt activation (**Fig 3.1D**).

We previously reported on the bioengineering, characterization and optimization of an IGF-1R signaling inhibitor - the IGF-Trap. The IGF-Trap binds IGF-1 and IGF-2 with high affinity, reducing their bioavailability to the membrane receptor and inhibiting receptor activation and signaling (7, 10). When the effect of the IGF-Trap on receptor activation in DIPG13 cells was analyzed, we found that ligand-induced IGF-1R activation and downstream signaling were significantly inhibited in the presence of the IGF-Trap (**Fig 3.1F**).

We obtained different results for SJG2 cells. While receptor activation in the presence of exogenous IGF-1 was observed in these cells, no increase in Akt or ERK phosphorylation were observed and in fact, a reduction in their activation levels was evident over time (**Fig 3.2A & B**). This may be due to the high basal Akt and ERK activation levels in these cells resulting from either autocrine IGF-1R activation by endogenously produced IGF-1 and/or downstream of the Met amplification and translocation in these cells. As expected, IGF-1R activation in the cells was inhibited in the presence of the IGF-Trap but this did markedly alter signaling in comparison to cells treated with IGF-1 only. (**Supplementary Figure 3.2**).

3.4.2 In response to ligand binding, the IGF-1R is also transported to the nucleus in pHGG cells. Nuclear transport of IGF-1R has been identified as an adverse prognostic factor in different cancers and observed in pHGG (2). We sought to determine whether ligand binding also induced nuclear transport of IGF-1R in DIPG13 cells. We first analyzed the subcellular distribution of the receptor under basal conditions, using immunocytochemistry (ICC) and observed both

membranous and nuclear IGF-1R in these cells (**Fig. 3.3A**). This was also seen in other grade IV glioblastoma PDX-derived cells including lines BT2545, HSJ19 and HSJ51(14) (**Fig. 3.3B**), suggesting that nuclear translocation of this receptor was broadly relevant to pHGG pathology.

3.4.3 Ligand–binding increases nuclear transport of IGF-1R and this is blocked by the IGF-Trap. To assess how nuclear translocation of IGF-1R is affected by ligand binding, we analysed the cells following treatment with IGF-1 using ICC and subcellular fractionation. In DIPG13 cells treated with 50 ng/ml IGF-1 in minimal medium, ICC revealed increased nuclear IGF-1R levels, as compared to controls (**Fig 3.3C&D**). This was confirmed by subcellular fractionation of the cells, followed by Western blotting, where an increase in IGF-1R levels in the nuclear fraction was observed within 10 minutes of IGF-1 stimulation (**Fig. 3.3E, F & G**), indicating that ligand-mediated IGF-1R activation triggered nuclear transport of the receptor in these cells. The increase in nuclear transport was blocked in the presence of the IGF-Trap (**Fig 3.3C, D & F**), confirming that receptor activation was essential to increased nuclear transport. Moreover, Dynasore, a blocker of dynamin-mediated coated vesicle formation and a potent inhibitor of the endocytic pathway inhibited ligand-mediated nuclear translocation of IGF-1R (**Fig 3.3G**), suggesting that receptor internalization via the endocytic pathway was essential to nuclear IGF-1R transport in these cells.

3.4.4 Nuclear IGF-1R activates gene transcription in DIPG13 cells. Nuclear IGF-1R was previously reported to auto-regulate its own transcription, as well as increase transcription of other genes including cyclin D1(20). We tested the effect of ligand-induced IGF-1R activation on IGF-1R and Cyclin D1 transcription, using quantitative PCR and found that both genes were transcriptionally upregulated in DIPG13 cells following IGF-1 stimulation (**Fig 3.4A & B**).

Western blotting confirmed increased cyclin D1 production in these cells, although we did not detect a measurable increase in IGF-1R protein levels in the total cell lysates (**Fig 3.4C & D**), possibly due to the increased presence of IGF-1R in the nuclear fraction.

3.4.5 Transcriptional activation of Cyclin D1 and IGF-1R is ERK activation independent. To ascertain that transcriptional activation of cyclin D1 and IGF-IR is mediated by nuclear IGF-1R independently of the MEK/ERK activation pathway, we treated IGF-1-stimulated cells with the MEK inhibitor PD98059. We confirmed the blockade of ERK signaling in the presence of this inhibitor. However, in the presence of IGF-1, transcriptional activation of cyclin D1, as assessed by qPCR and Western blotting was not significantly altered, suggesting that it was likely due to direct regulation by nuclear IGF-1R (**Fig 3.4F&G**). As expected, increased cyclin D1 expression was also inhibited in the presence of the IGF-Trap (**Fig 3.4E**).

3.4.6 IGF-1-induced nuclear transport of IGF-1R has distinct transcriptional effects in SJG2 cells. IGF-1 also increased nuclear transport of IGF-1R in SJG2 cells and this was blocked by the IGF-Trap and Dynasore (**Fig 3.5 A-E**). However, in these cells, no significant increase in cyclin D1 transcription was observed for up to 6 hr post stimulation. IGF-1R mRNA levels increased by 50% but this was not reflected in a significant increase in protein levels (**Figure 3.5F-I**).

3.4.7 IGF-1R signaling promotes survival and proliferation of pediatric high-grade glioma cells. Having observed IGF-1R signaling and nuclear transport in the pHGG cells, we next evaluated the consequences of receptor activation on cellular functions known to be regulated by the IGF-1R. The effect of IGF-1R signaling blockade by the IGF-Trap was also evaluated

3.4.7.1 ***Increased proliferation of pHGG in the presence of IGF-1 is blocked by the IGF-Trap*****.** Proliferation was measured in real time using the Incucyte system. DIPG13 cells were incubated for 96 hours, with or without 50 ng/ml IGF-1 and in the absence or presence of the IGF-

Trap that was added at molar ratios of 1:1 or 2:1 (IGF-Trap:IGF-1). We observed that proliferation significantly increased in the presence of IGF-1 and this was inhibited by the IGF-Trap (**Fig 3.6A&B**). We used the MTT assay to measure proliferation of SJG2 cells in the presence of 10 ng/ml IGF-1 (**Fig 3.6C&D**). While IGF-1 did not significantly increase the proliferation of SGJ2 cells in the presence of low FBS concentrations, the proliferation was still significantly reduced in the presence of IGF-Trap (**Fig. 3.6C&D**), suggesting that it blocked autocrine IGF signaling.

3.4.7.2 ***IGF-Trap can reduce colony formation by DIPG13 cells.*** IGF-1R is known to regulate tumor cell clonogenicity (21). We tested the effect of the IGF-Trap on colony formation by DIPG13 cells seeded in 6 well plates at a density of 400 cells/well in optimal growth medium supplemented with 50 ng/ml IGF-1. We found a significant reduction in the number and size of DIPG13 colonies in the presence of IGF-Trap (**Fig 3.6E-G).**

3.4.7.3 The ***IGF-Trap increases pHGG apoptosis.*** To test the ability of IGF-1 to rescue the pHGG cells from apoptosis, the cells were maintained in medium depleted of growth factors (DIPG13) or serum (SJG2) in the presence or absence of IGF-1. Incorporation of a fluorescently labelled Annexin V reagent by these cells was measured using the real-time Incucyte system. IGF-1 rescued DIPG13 from starvation induced apoptosis and this could be reversed by IGF-Trap (**Fig 3.6H&I**). Exogenous IGF-1 had a minor rescue effect on SJG2 cells, but the addition of IGF-Trap, nevertheless, increased the apoptotic index for these cells (**Fig 3.6J).**

3.4.7.4 IGF-1 increases cell cycle progression in DIPG13 cells and this is blocked by the IGF-Trap. Finally, having established that IGF-1R transcriptionally activated cyclin D1, we asked whether this affected cell cycle progression in DIPG13 cells. Cells were cultured in medium depleted of all growth supplements, treated with IGF-1 (or supplements, as positive control) for

24 hr in the presence or absence of IGF-Trap, and cell cycle analysis performed by flow cytometry. As expected, we found that starvation halted cell cycle progression in these cells and induced apoptosis. The addition of IGF-1 enhanced G_1-S transition, restoring it to levels similar to those observed in complete medium, and this was reversed by the addition of the IGF-Trap (**Fig 3.6K&L**) confirming the role of IGF-1 as a driver of cell cycle progression in these cells.

3.5 DISCUSSION

The aims of this study were to evaluate IGF-responsiveness in human pediatric high-grade glioma cells and assess the sensitivity of the cells to a novel IGF-inhibitor, the IGF-Trap. We selected for the study two pHGG PDXs with distinct genomic perturbations, representing different clinical subtypes and we confirmed their IGF-1R expression and responsiveness. In addition, we confirmed nuclear IGF-1R localization in several pHGG diffuse midline PDXs, consistent with findings by Clément at al that identified nuclear IGF-1R localization as a signature of pediatric high-grade gliomas (2).

IGF-signaling is known to trigger the MEK/ERK and PI3K/Akt pathways that result in increased cell proliferation and survival, respectively. We confirmed that in response to IGF-1, the receptor is activated in both DIPG13 and SJG2 cells and showed that the proliferation of DIPG13 cells increased and they could also be rescued from starvation-induced apoptosis in the presence of IGF-1. Because patient-derived xenografts are cultured in defined media with low or no serum to maintain stemness, optimal conditions for the IGF-1-mediated effects had to first be determined, and were found to be cell type-specific. Under these conditions, we did not find a significant increase in SJG2 proliferation in response to IGF-1. Intriguingly, however, the proliferation of both DIPG13 and SJG2 cells was inhibited by the IGF-Trap. This is likely due to the higher

expression of IGF-1 in SJG2 cells that could drive autocrine IGF-1R signaling, even in the absence of exogenous IGF-1.

In both DIPG13 and SJG2 cells, IGF-1 stimulation resulted in nuclear translocation of the receptor, and this upregulated IGF-1R and cyclin D1 expression in DIPG13 cells, independently of MEK/ERK activation and resulted in enhanced G_1-S transition in minimal medium supplemented with IGF-1 only. We did not, however, observe cyclin D1 upregulation in SJG2 cells treated with IGF-1, suggesting that the cellular context determines the transcriptional activity of the nuclear IGF-1R. Of relevance, recent results of a meta-analysis of over 1000 pediatric high-grade gliomas and DIPG cases identified amplifications in cell cycle genes including CCND1, CDK4, and CDK6 among the genetic aberrations in subclonal populations of DIPG (22, 23), suggesting that cell cycle drivers may be potential targets in this incurable disease (23). Hence, combining IGF-axis and CDK4/6 inhibitors may hold promise for DIPG treatment (22).

The standard of care for pediatric brain tumors is currently a combination of surgery, chemotherapy and radiation therapy, modalities that are associated with severe toxicity and have had limited curative effect. Although there is only scant information on the effect of IGF axis targeting in pHGG, several reports suggest that a systematic analysis of the beneficial effects of IGF-inhibitors is warranted. Thus, Bielen et al using pediatric glioblastoma cell lines showed that the specific IGF-1R small molecule inhibitor NVPAEW541 or receptor silencing by siRNA decreased cell viability and induced G1 arrest in the cells and that co-treatment of the cells with the PDGFR inhibitor imatinib and NVP-AEW541 resulted in a highly synergistic interaction *in vitro*. This combination therapy also reduced the growth of the pGBM *in vivo* (24), identifying IGF-1R as a potential target in this disease and suggesting that combinatorial therapy with other RTK inhibitors may optimize the response. More recently, Simpson et al have shown that IGF-1R

targeting increased the radio-sensitivity of pHGG cells, likely through perturbation of the DNA damage response (13). Of relevance, IGF-1R was also identified as a therapeutic target in medulloblastoma, a highly aggressive pediatric malignancy of the cerebellum (25, 26). Collectively, the results suggest that IGF-1R targeting may have beneficial therapeutic effects in pediatric brain malignancies, including pHGG. IGF-targeting drugs are generally well tolerated and to date, no deleterious effects were observed in animals treated with the IGF-Trap(7, 10). Our results warrant further investigation of the sensitivity of pHGG PDX implanted orthotopically in the brain to IGF-Trap treatment pending successful delivery of this drug to the brain with the aid of technologies that enable transient opening of the blood brain barrier.

3.6 Acknowledgements. The authors gratefully acknowledge the assistance of the molecular imaging core facility of the Research Institute of the McGill University Health Center and in particular Dr. Min Fu and Ms. Shibo Feng. This work was made possible by grant PSR-SIIRI-998 from the Ministère de l'Economie et de l'Innovation du Québec and a grant from the McGill University Health Center (MUHC) Foundation (to PB). Michely Chen was partially supported by a fellowship from the Research Institute of the MUHC.

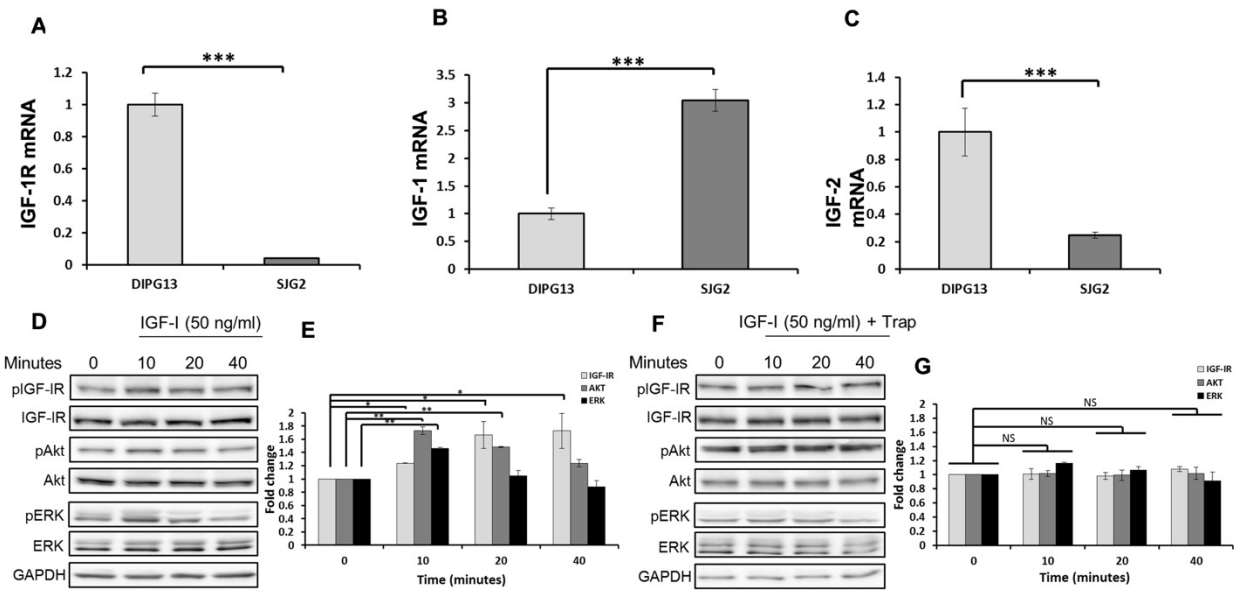

Figure 3.1. IGF-IR expression and signaling in pHGG cells. Shown in **(A-C)** are results of qPCR analysis performed on RNA extracted from cells cultured in the respective optimal media, as described in Methods. Results are based on 3 analyses and are expressed reative to mRNA levels in DIPG13 cells that were assigned a value of 1. Shown in (**D**), are representative results of Western blotting performed following culture of DIPG13 cells in growth-supplements depleted medium overnight followed by incubation of the cells with (or without) 50 ng/ml IGF-1 for the duration indicated. Shown in (**F**) are representative results of Western blotting performed on lysates of DIPG13 cells cultured as in (**D**) in the presence of IGF-Trap added at a molar ratio of 2:1 to IGF-1. Shown in the bar graphs (**E & G**) are the means and SE (n=4) expressed as fold change in activation levels relative to basal levels (time 0) that were assigned a value of 1. * $p \leq 0.05$, ** $p \leq 0.01$, *** $p \leq 0.001$, NS- Not significant.

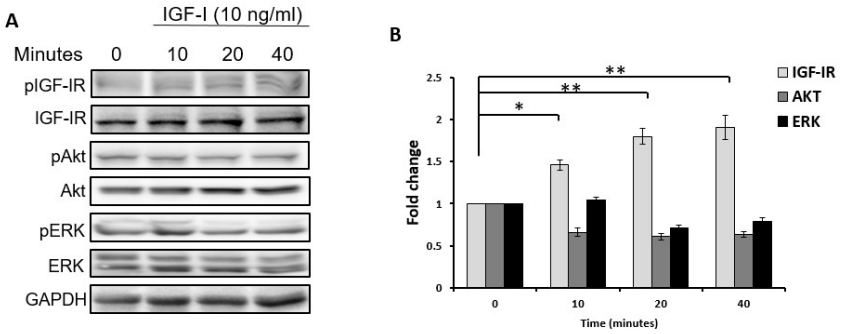

Figure 3.2. **Exogenous ligand activates IGF-1R but not downstream signaling in SJG2 cells**. Shown in **(A)** are results of a representative Western blot following stimulation of serum starved SJG2 cells with 10 ng/ml IGF-1 and in **(B)** results of densitometry expressed as ratios to basal levels (time 0)(n=3). * $p \leq 0.05$.

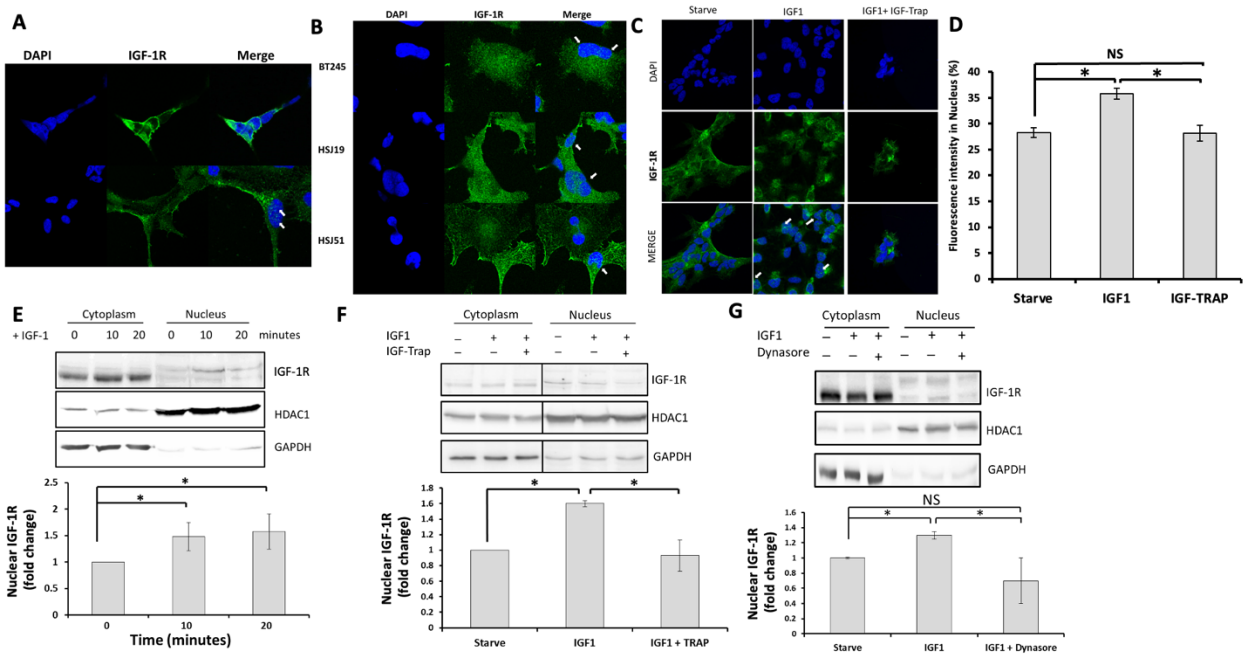

Figure 3.3. The IGF-1R is transported to the nucleus in response to ligand binding and this is blocked by the IGF-Trap. pHGG cells were seeded on laminin coated coverslips, permeabilized (or not) with 0.1% Triton X and cellular IGF-1R distribution analyzed by immunocytochemistry (ICC). Shown in **(A)** are images of DIPG13 cells immunostained with antibodies to IGF-1R without (Top) or with (bottom) prior permeabilization. Punctate IGF-1R clusters in the DAPI-stained nuclei (blue) are indicated with white arrowheads. Nuclear IGF-1R was also observed in several other grade IV pHGG, as shown in **(B)**. To determine whether IGF-1 could increase nuclear translocation of IGF-1R, DIPG13 cells in minimal medium were treated with 50ng/ml of IGF-1 for 20 min and the subcellular distribution analyzed. Shown in **(C & D)** are results of ICC where IGF-1R is indicated by arrowheads in (**C**) and mean fluorescence intensity measured in the nuclei based on a total of 5-9 images per condition shown in the bar graph (**D**). Shown in **(E-G)** are results of Western blotting performed on subcellular DIPG13 fractions isolated following treatment of the cells with IGF-1 only **(E)** and in the presence (or absence) of IGF-Trap (**F**) or Dynasore (**G**). GAPDH and HDAC1 were used as markers for the cytosolic and nuclear fractions, respectively. Shown in the bar graphs (bottom) are results of densitometry expressed as fold change in nuclear IGF-1R levels relative to levels at time 0 that were assigned a value of 1 (n=3). * $p \leq 0.05$, NS- Not significant.

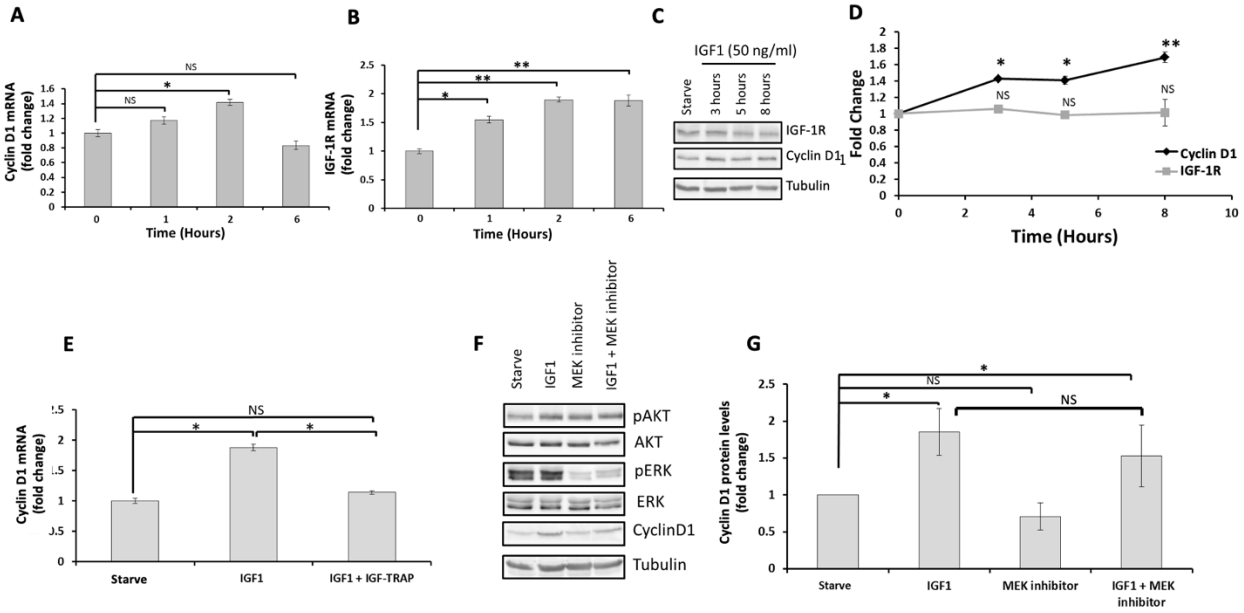

Figure 3.4. **Ligand-induced and MEK/ERK-signaling independent cyclin D1 and IGF-1R upregulation in DIPG13 cells.** DIPG13 cells were starved overnight and stimulated with 50ng/ml IGF-I. RNA was collected at the indicated intervals and analyzed by qPCR. Shown in (**A & B**) are qPCR results for Cyclin D1 and IGF-1R mRNA, respectively, in (**C**) representative results of Western blotting performed on these cells showing increased Cyclin D1 protein levels in the presence of IGF-1 and in the bar graph (**D**) results of densitometry expressed as fold change in Cyclin D1 and IGF-1R levels relative to levels at time 0 that were assigned a value of 1 (n=3). Shown in (**E**) are results of qPCR performed on cells stimulated with 50ng/ml IGF-I in the presence or absence of the IGF-Trap (**D**), in (**F**) a representative result of Western blotting performed following a 16 hr stimulation with 50ng/ml IGF-I with or without 20 μM of the MEK inhibitor PD98059 and in the bar graph **(G)** results of Western blotting expressed as means of fold change (±SE) relative to control levels (serum free conditions) that were assigned a value of 1 (n=3). * $p \leq 0.05$, ** $p \leq 0.01$, NS- Not significant.

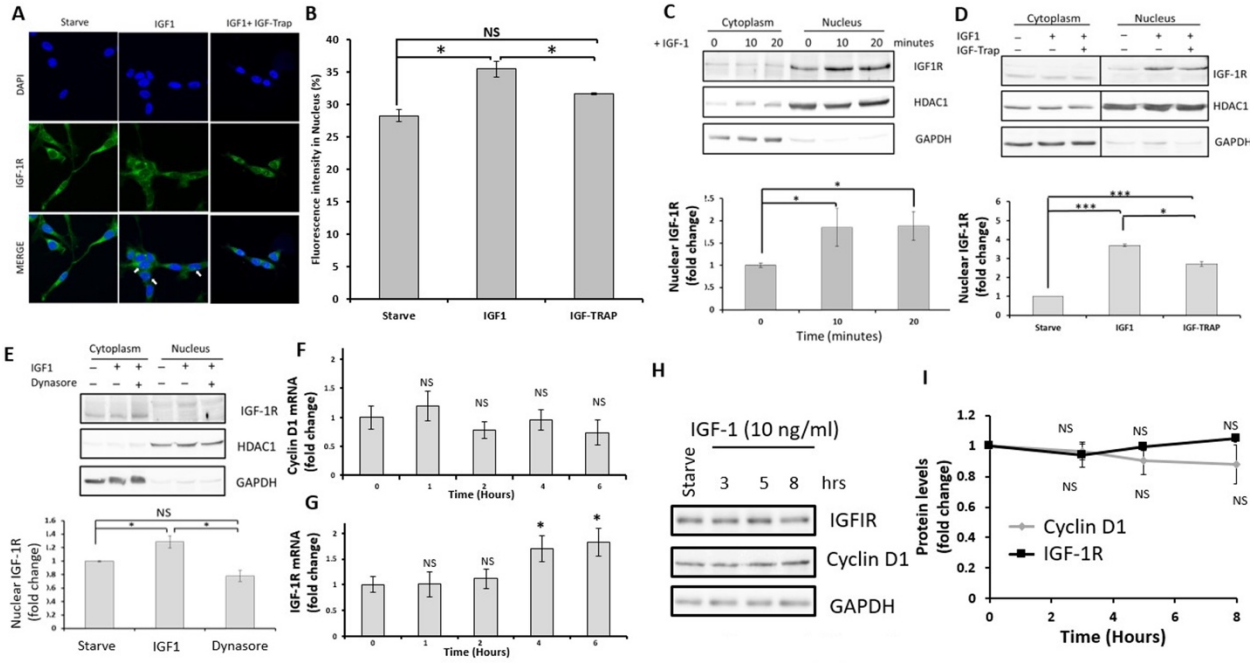

Figure 3.5. IGF-1 triggers nuclear translocation but does not regulate Cyclin D1 transcription in SJG2 cells. SJG2 cells were seeded on coverslips, permeabilized with 0.1% and cellular IGF-1R distribution analyzed by immunocytochemistry (ICC). Shown in **(A)** are images of SJG2 permeabilized cells immunostained with antibodies to IGF-1R. Punctate IGF-1R clusters in the DAPI-stained nuclei (blue) are indicated with white arrowheads and quantification shown in (**B**). Western blots shown in (**C**) were performed on subcellular fractions obtained after overnight serum-starvation followed by addition of 10 ng/ml IGF-1 for 20 minutes (**C**) and in the absence or presence of IGF-Trap added at 2:1 ratio with IGF-1 (**D**), or Dynasore added at a concentration of 30 μM)(**E**)**.** Shown in (**F & G**) are qPCR results obtained for Cyclin D1 (**F**) and IGF-1R (**G**) transcripts and in (**H and I**) results of Western blotting performed on lysates of cells stimulated with 10 ng/ml IGF-1. Results of densitometry (**I**) are expressed as fold change in the indicated protein levels relative to levels at time 0 that were assigned a value of 1 (n=3). * $p \leq 0.05$, *** $p \leq 0.001$, NS- Not significant

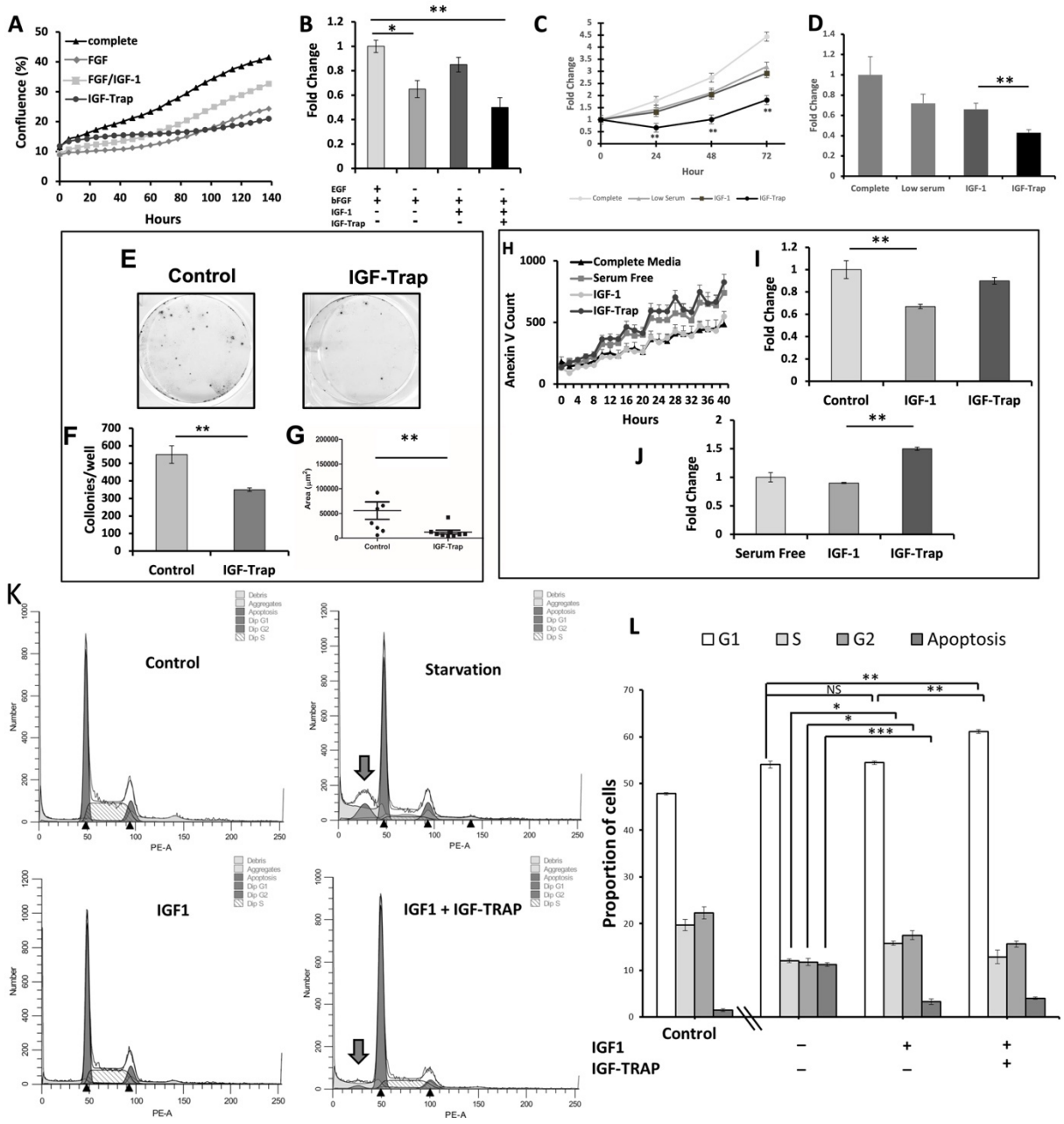

Figure 3.6. The IGF-Trap alters the tumor cell survival and growth-promoting effects of IGF-1. Cells were seeded in 24 well plates and cultured in minimal media containing (or not) 50 (DIPG13) or 10 (SJG2) ng/ml IGF-1. Shown in (**A**) are results obtained with DIPG13 cells using the Incucyte system and in the bar graph (**B**) the results expressed as means (±SE) relative to cells culture in optimal defined medium that were assigned a value of 1. Shown in (**C**) are results of an MTT assay performed with SJG2 cells that were cultured in serum-low medium and with or without IGF-1 and IGF-Trap for the indicated duration and in (**D**) results of an Incucyte assay performed with SJG2 cells expressed as a ratio to values at time 0. The effect of IGF-1 on tumor cell clonogenicity (**E-G**) was measured following seeding of DIPG13 cells in 6-well plates at a density of 400 cells/plate in optimal growth medium containing also 50 ng/ml IGF-1 and in the presence or absence of IGF-Trap for 15 days. Shown in **(E)** are representative images of crystal

violet-stained colonies (n=3), in **(F)** the number of colonies expressed as means (±SE) of 3 plates and in **(G)** the size of individual colonies as measured using an ocular grid. Apoptosis was analyzed in DIPG13 and SJG2 cells that were cultured in growth factor and serum depleted medium, respectively, supplemented (or not) with IGF-1 and in the presence or absence of IGF-Trap. The Incucyte system was used to monitor incorporation of fluorescently labelled Annexin V in real-time. Shown in (**H**) are representative Incucyte generated plots for DIPG13 cells (n=3) and in the bar graph **(I)** the results expressed as means (±SE) relative to cells in basal conditions that were assigned a value of 1. Shown in (**J**) are the results obtained for SJG2 cells expressed as mean fold change relative to cells in full medium (n=3). To analyze cell cycle progression, DIPG13 cells were starved in minimal DMEM/F12 medium for 18 hours and then incubated for 24 hrs in complete medium or in DMEM/F12 containing 50 ng/ml IGF-1. The cells were fixed, stained with proprium iodide and cell cycle analysis performed by flow cytometry. Shown are representative flow cytometry histograms **(K)** where a arrow denotes apoptosis. Shown in the bar graphs (**L**) are the calculated proportions of cells at different cell cycle phases including the proportions of apoptotic cells. Results are based on three independent experiments and are expressed as mean percentages (± SE) of total cells analyzed**.** *$p<0.05$, **$p<0.01$, ***$p<0.001$.

3.7 Supplementary:

3.7.1 Supplementary methods:

RNAseq analysis of pHGG PDX.

Read processing, alignment, and gene expression analysis were as described previously (18). Briefly, sequences were cleaned up by discarding adaptor sequences, first four nucleotides of each read and short reads (<30bp) and followed by quality control metrics. Alignment of reads was carried out by mapping to the reference genome and selecting only for reads mapping to 9 or less locations. Gene expression levels were quantified by the number of primary alignments reads (MAPQ>3) falling into exonic regions and counts were normalized to mapped reads per kilobase of transcript per million (RPKM).

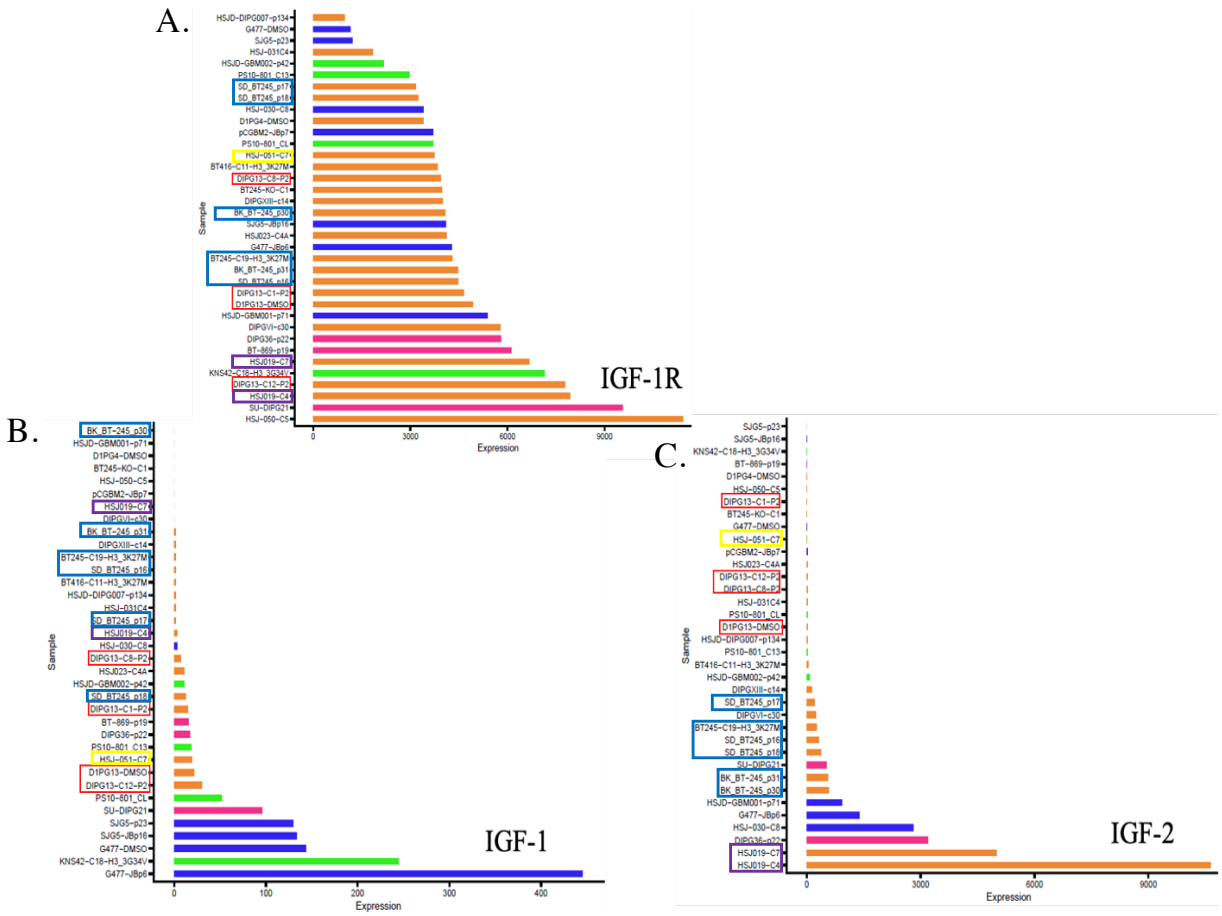

Supplementary Figure 3.1. **RNAseq data identify DIPG13 PDX as candidate for IGF-axis targeting**. Expression of (A) IGF-IR, (B) IGF-1, (C) IGF-2 across pediatric high-grade glioma PDXs was quantified by RNA sequencing. Gene expression levels were quantified by the number of primary alignment reads of the exonic regions and counts were normalized to mapped reads per kilobase of transcript per million (RPKM). The RNA-seq data were sourced from Krug et al(18). Sequencing files are available under Gene Expression Omnibus (GEO): GSE128745. Orange bars denote PDX with H3.3K27M, pink bars denote H3.1K27M, blue bars denote histone WT and green bars denote H3.3G34R/V gliomas. The framed PDXs BT245, HSJ-19, and HSJ-51 were also used in this study. Data from multiple passages of DIPG13, BT245, and HSJ-19 are shown.

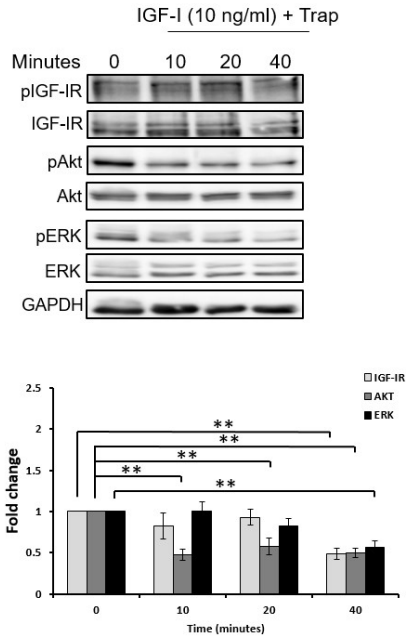

Supplementary Figure 3.2. **The IGF-Trap does not alter signaling in SJG2 cells**. Shown on top are representative results of Western blotting performed following stimulation of serum starved SJG2 cells with 10 ng/ml IGF-1 in the presence of IGF-Trap added at a molar ratio of 2:1 to IGF-1. Shown in the bar graphs (bottom) are the means and SE based on 3 experiments. * - $p < 0.01$

Supplementary Table 3.1. Primer sequences for qPCR.

Gene	Direction	Primer 5'---> 3'
GAPDH	Forward	GGATTTGGTCGTATTGGGCG
	Reverse	ATGGAATTTGCCATGGGTGG
IGF-1R	Forward	CGCACCAATGCTTCAGTTCC
	Reverse	TGCCAGCGCACAATGTAGTA
IGF-1	Forward	CTCTTCAGTTCGTGTGTGGA
	Reverse	CAGCCTCCTTAGATCACAGC
IGF-2	Forward	TGGCATCGTTGAGGAAGTGCT
	Reverse	ACGGGGTATCTGGGGAAGTT
Cyclin D1	Forward	TGAGGAGCCCCAACAACTTC
	Reverse	CCGGGTCACACTTGATCACT

References:

1. Cacciotti C, Fleming A, Ramaswamy V. Advances in the molecular classification of pediatric brain tumors: a guide to the galaxy. J Pathol. 2020;251(3):249-61.
2. Clément F, Martin A, Venara M, de Luján Calcagno M, Mathó C, Maglio S, et al. Type 1 IGF Receptor Localization in Paediatric Gliomas: Significant Association with WHO Grading and Clinical Outcome. Hormones and Cancer. 2018;9(3):205-14.
3. Wrigley S, Arafa D, Tropea D. Insulin-Like Growth Factor 1: At the Crossroads of Brain Development and Aging. Front Cell Neurosci. 2017;11:14.
4. Sehat B, Tofigh A, Lin Y, Trocmé E, Liljedahl U, Lagergren J, et al. SUMOylation mediates the nuclear translocation and signaling of the IGF-1 receptor. Science signaling. 2010;3(108):ra10.
5. Löfqvist C, Niklasson A, Engström E, Friberg LE, Camacho-Hübner C, Ley D, et al. A pharmacokinetic and dosing study of intravenous insulin-like growth factor-I and IGF-binding protein-3 complex to preterm infants. Pediatric research. 2009;65(5):574-9.
6. Baumann G. Growth Hormone (GH). In: Martini L, editor. Encyclopedia of Endocrine Diseases. New York: Elsevier; 2004. p. 383-9.
7. Wang N, Rayes RF, Elahi SM, Lu Y, Hancock MA, Massie B, et al. The IGF-Trap: novel inhibitor of carcinoma growth and metastasis. Molecular cancer therapeutics. 2015.
8. Vaniotis G, Moffett S, Sulea T, Wang N, Elahi SM, Lessard E, et al. Enhanced anti-metastatic bioactivity of an IGF-TRAP re-engineered to improve physicochemical properties. Sci Rep. 2018;8(1):17361.
9. Tsui J, Qi S, Perrino S, Leibovitch M, Brodt P. Identification of a Resistance Mechanism to IGF-IR Targeting in Human Triple Negative MDA-MB-231 Breast Cancer Cells. Biomolecules. 2021;11(4).
10. Vaniotis G, Moffett S, Sulea T, Wang N, Elahi SM, Lessard E, et al. Enhanced anti-metastatic bioactivity of an IGF-TRAP re-engineered to improve physicochemical properties. Scientific Reports. 2018;8(1):17361.
11. Samani AA, Nalbantoglu J, Brodt P. Glioma Cells With Genetically Engineered IGF-I Receptor Downregulation Can Persist in the Brain in a Dormant State. Frontiers in oncology. 2020;10:555945.
12. Samani AA, Yakar S, LeRoith D, Brodt P. The role of the IGF system in cancer growth and metastasis: overview and recent insights. Endocrine reviews. 2007;28(1):20-47.
13. Simpson AD, Soo YWJ, Rieunier G, Aleksic T, Ansorge O, Jones C, et al. Type 1 IGF receptor associates with adverse outcome and cellular radioresistance in paediatric high-grade glioma. British journal of cancer. 2020;122(5):624-9.
14. Harutyunyan AS, Krug B, Chen H, Papillon-Cavanagh S, Zeinieh M, De Jay N, et al. H3K27M induces defective chromatin spread of PRC2-mediated repressive H3K27me2/me3 and is essential for glioma tumorigenesis. Nature communications. 2019;10(1):1262.
15. Krug B, De Jay N, Harutyunyan AS, Deshmukh S, Marchione DM, Guilhamon P, et al. Pervasive H3K27 Acetylation Leads to ERV Expression and a Therapeutic Vulnerability in H3K27M Gliomas. Cancer Cell. 2019;35(5):782-97.e8.
16. Burnier JV, Wang N, Michel RP, Hassanain M, Li S, Lu Y, et al. Type IV collagen-initiated signals provide survival and growth cues required for liver metastasis. Oncogene. 2011;30(35):3766-83.
17. Zhang D, Brodt P. Type 1 insulin-like growth factor regulates MT1-MMP synthesis and tumor invasion via PI 3-kinase/Akt signaling. Oncogene. 2003;22(7):974-82.
18. Krug B, De Jay N, Harutyunyan AS, Deshmukh S, Marchione DM, Guilhamon P, et al. Pervasive H3K27 Acetylation Leads to ERV Expression and a Therapeutic Vulnerability in H3K27M Gliomas. Cancer Cell. 2019;35(5):782-97 e8.

19. Mackay A, Burford A, Carvalho D, Izquierdo E, Fazal-Salom J, Taylor KR, et al. Integrated Molecular Meta-Analysis of 1,000 Pediatric High-Grade and Diffuse Intrinsic Pontine Glioma. Cancer Cell. 2017;32(4):520-37.e5.
20. Sarfstein R, Werner H. Minireview: nuclear insulin and insulin-like growth factor-1 receptors: a novel paradigm in signal transduction. Endocrinology. 2013;154(5):1672-9.
21. Brodt P, Fallavollita L, Khatib AM, Samani AA, Zhang D. Cooperative regulation of the invasive and metastatic phenotypes by different domains of the type I insulin-like growth factor receptor beta subunit. J Biol Chem. 2001;276(36):33608-15.
22. Aziz-Bose R, Monje M. Diffuse intrinsic pontine glioma: molecular landscape and emerging therapeutic targets. Curr Opin Oncol. 2019;31(6):522-30.
23. Hoeman C, Shen C, Becher OJ. CDK4/6 and PDGFRA Signaling as Therapeutic Targets in Diffuse Intrinsic Pontine Glioma. Frontiers in oncology. 2018;8:191.
24. Bielen A, Perryman L, Box GM, Valenti M, de Haven Brandon A, Martins V, et al. Enhanced efficacy of IGF1R inhibition in pediatric glioblastoma by combinatorial targeting of PDGFRalpha/beta. Mol Cancer Ther. 2011;10(8):1407-18.
25. Ajeawung NF, Wang HY, Gould P, Kamnasaran D. Advances in molecular targets for the treatment of medulloblastomas. Clin Invest Med. 2012;35(5):E246.
26. Reiss K. Insulin-like growth factor-I receptor - a potential therapeutic target in medulloblastomas. Expert Opin Ther Targets. 2002;6(5):539-44.

Chapter Preface:

In Chapter 3, we described our data that identified the IGF-axis as a potential target and the IGF-Trap as a potent agent for the treatment of pHGG *in vitro*. However, pHGG lack established *in vivo* models for the assessment of therapeutic efficacy in animals. Although there are some differences in the molecular characteristics of pediatric and adult HGG, the IGF-axis is also highly amplified in the adult counterpart. We sought to evaluate the therapeutic efficacy and optimize the delivery of the IGF-Trap to the brain and used human and mouse models of adult HGG to this end namely, the adult U87-MG and murine GL261 cell lines that have been used extensively *in vivo*; In Chapter 4, we describe the effects of the IGF-Trap on the growth of these tumor cells *in vivo* as well as the initial results with 2 novel, non-invasive IGF-Trap delivery methods for the treatment of brain malignancies.

Chapter 4. Evaluation of Strategies for Increasing Brain Delivery of the IGF-Trap

Yinhsuan Michely Chen[1,2], Masakazu Hashimoto [2,4], Shu Qi [2], Stephanie Perrino[2] and Pnina Brodt [1,2,4,5]

Affiliations:

1. Department of Medicine, Division of Experimental Medicine, McGill University, Montreal, QC H3A 0G4, Canada
2. The Research Institute of the McGill University Health Center, Montreal, QC H4A 3J1, Canada
3. Department of Surgery, McGill University, Montreal, QC H3A 0G4, Canada
4. Department of Oncology, McGill University, Montreal, QC H3A 0G4, Canada

4.1 Abstract:

BACKGROUND: Glioblastoma Multiforme is the most common primary brain tumor in adults. Prognosis remains poor for this malignancy. Although the cause remains unknown, genetic mutations including gene amplifications and alterations in the receptor tyrosine kinase pathways were identified in over 85% of glioblastoma patients. IGF-I receptor (IGF-IR) gene amplifications have been identified in glioblastoma and overexpression of IGF-IR confers a poorer prognosis. Cell membrane IGF-1R mediates cellular proliferation in response to the ligands IGF-1 and IGF-2 and can act as a survival factor, rescuing cells from drug-induced apoptosis.

AIM: The goal of this study was to evaluate the therapeutic efficacy and optimize the delivery of an IGF-inhibitor, the IGF-Trap, for the treatment of high-grade gliomas, using preclinical models.

RESULTS: Evaluation of the therapeutic efficacy and IGF-Trap delivery strategies in

preclinical glioblastoma models were carried out in a stepwise manner. IGF-Trap was first evaluated *in vitro,* and inhibition of proliferation confirmed. Next, the IGF-Trap efficacy in vivo was tested using subcutaneously injected murine glioblastoma GL261 and human glioblastoma U87 cells and a significant decrease in tumor growth was observed. Similar results were observed when these glioblastoma cells were implanted orthotopically into the brain. While the blood-brain-barrier excludes substances outside of the brain, the IGF-Trap was delivered via a cannula and showed deceleration of tumor development and improvement in survival. Nanoparticle encapsulated IGF-Trap increased bioavailability in the brain and in the body. Combination therapy of transcranial magnetic stimulation and the IGF-Trap was evaluated as an additional method of drug delivery. 33% of mice presented minimal tumor in the combination group while all mice in other groups at 4 weeks and the two that responded to treatment showed prolonged survival.

CONCLUSION: This study identified the IGF-Trap as an effective therapeutic agent for the treatment of glioblastoma and two delivery methods that enhances uptake in the brain. The results provided insights to potential treatment approaches for glioblastoma.

4.2 Introduction:

Glioblastoma Multiforme is the most prevalent primary brain tumor in adults. Glioblastoma occurs at higher rates in persons older than 55 years of age and a 5-year survival rate of 5% (1). Morphological and molecular characterization of glioblastoma identified the malignancy as poorly differentiated and highly heterogeneous. Altered oncogenic pathways include copy number alterations in the tyrosine kinase receptor signaling pathways, epigenetic changes in the retinoblastoma (RB) pathway and genetic mutation as well as copy number alterations in the tumor suppressor p53 pathway (2). The tyrosine kinase receptor family such as the epidermal growth factor receptor (EGFR), platelet-derived growth factor receptor (PDGFR), insulin-like growth factor 1 receptor (IGF-IR) were found to be frequently amplified

and the common downstream PI3K/Akt pathway was found to be altered in 86-89.6% which makes them a popular therapeutic target for glioblastoma treatment (3). IGF-IR was shown to be overexpressed and associated with poorer survival in glioblastoma patients (4). IGF-signaling was also shown to be involved in resistance of glioblastoma cells to EGFR (5) and PDGFR inhibitors (6). The goal of this study is to assess the therapeutic potential of an insulin-like growth factor (IGF)-signaling inhibitor for the treatment of glioblastoma.

Insulin-like growth factors (IGF-1 and IGF-2) are proteins that are involved in cell growth and differentiation. IGF-signalling is triggered by the binding of IGF ligands to the cell surface IGF-I receptor, thereby activating downstream signaling cascades including the PI3K/Akt and MEK/ERK pathways that are involved in cell survival and cell cycle progression, respectively. Additionally, binding of the IGF ligands to the IGF-1R is critical for transporting IGF-1R to the nucleus. Thus, IGF-signaling promotes cellular proliferation and resistance to apoptosis, two mechanisms that are critical for tumor progression and metastasis (7, 8).

In our laboratory, the IGF-Trap, an IGF-1R targeting fusion protein, was developed. The IGF-Trap is a soluble form of IGF-1R that inhibits IGF-signaling by binding to the IGF ligands and thus preventing receptor activation. Previous studies have shown that the IGF-Trap could inhibit the growth of several very aggressive tumors *in vivo* including triple negative breast cancer cells and colon/lung carcinoma cells (9). A new, highly effective variant of the IGF-Trap was recently produced (10) but its effect on glioma growth has not yet been assessed.

One major obstacle to effective treatment of glioma is drug delivery to the brain, as drug exclusion by the blood-brain barrier (BBB) limits drug access to the tumor. BBB is a semi-permeable layer of endothelial cells that protects the brain from foreign substances. In this study, IGF-Trap delivery to intra-cerebral tumors will be optimized using transcranial magnetic stimulation (TMS) and by nanoparticle encapsulation of the IGF-Trap. TMS is a non-invasive approach that uses electromagnetic waves that stimulates the neurons thereby inducing

the release of glutamate (11). This process was simulating the underlying mechanism of abnormal neuronal depolarization that were found to increase permeability of the BBB. In a recent study, the TMS-induced BBB opening allows the IGF-Trap to extravasate into the surrounding extravascular space (12). Additionally, trimethyl chitosan was used as the nanoparticle which was shown to exert advantages with the permanent positively charged moiety such as improved solubility and enhanced absorptive meditated transcytosis for better uptake into the brain (13). Several studies have demonstrated increased bioavailability of therapeutic agents for glioblastoma treatments; however, to our knowledge, no studies on the therapeutic efficacy with the trimethyl chitosan encapsulated agent was investigated. In this study, we assessed and optimized the delivery of IGF-Trap for the treatment of glioblastoma in a preclinical model.

4.3 Methods:

Cells:

Human U87-MG cells were obtained from the ATCC cell collection and murine GL261 syngeneic to the Bl/6 strain from the DTP/DCTD/NCI Tumor Repository. The cells were MAP and mycoplasma tested by the NCI diagnostic laboratory and confirmed negative. They were subsequently regularly tested for mycoplasma contamination using the mycoplasma PCR test throughout this study. The cells were cultured in DMEM (Wisent) (U87) (Wisent) and RPMI (Wisent) (GL261) with 10% FBS and antibiotics.

Mice

All mouse experiments were carried out in strict accordance with the guidelines of the Canadian Council on Animal Care (CCAC) ‘‘Guide to the Care and Use of Experimental Animals’’ and under the conditions and procedures approved by the Animal Care Committee of McGill University (AUP number: 5733). C57Bl/6 is a commonly used inbred mouse strain in drug discovery research and GL261 is a glioblastoma cell line syngeneic to C57Bl/6 (14).

The immunodeficient NOD-*scid* IL2Rgamma^{null} (NSG) mice (The Jackson Laboratory) were used to carry out experiments on human U87-MG cells.

MTT Assay:

Cells were seeded in 96-well plates and incubated at 37^{o}C for 24 hr. Cells were deprived of FBS (Wisent) and conditions with and without 10ng/ml of IGF-1, IGF-Trap at indicated molar ratios were added and incubated up to 96hr. Every 24 hr, 10uL of 5mg/ml MTT (Sigma) reagent was added to each well and solubilized by DMSO. Absorbance at 570 nm was measured with the Infinite 200 PRO microplate reader (TECAN).

Subcutaneous Injection:

U87 or GL261 (1 x 10^6 cells/ mouse) was injected subcutaneously into the flank of 7-10 wk old male mice. 100µg of IGF-Trap was given twice weekly via intravenous injection. Tumor size was measured with a caliper. Mice were sacrificed when the tumor reached end point when the length reaches 1.5cm.

Intracranial tumor implantation and cannulation:

U87 MG (2 x 10^5 cells/mouse) and GL261 (1 x 10^5 cells/mouse) were implanted orthotopically into the right cerebral striatum using a Stoelting stereotactic apparatus at coordinates -2, -1, -3.5 of bregma. Intracerebral tumor growth was monitored using optical imaging following the injection of RediJect-D-lcuiferin (PerkinElmer) i.p. into the mice. Images ere acquired with the IVIS 200 scanner. (PerkinElmer). A cannula (328OPM/Spc, Plastics One) was implanted above the tumor injection site for subsequent treatments.

Transcranial Magnetic Stimulation:

Mice were anesthetized and a circular coil (Brainsway Ltd.) was placed on top of the head using a protocol that was described in detail elsewhere (12) and a coil adapted for mouse treatment. Repetitive TMS was applied at 1Hz, 130% of the resting motor threshold as

measured in the ipsilateral forelimb movement. Each stimulation was administered for a duration of 50 sec, followed by 1min rest and this was repeated 5 times (250 pulses in total).

4.4 Results:

4.4.1 The IGF-Trap inhibits cell proliferation *in vitro*.

The goal of this project was to evaluate and optimize delivery of the IGF-Trap for intra-cerebral treatment of glioblastoma in pre-clinical mouse models. We chose GL261 and U87 as murine and human glioblastoma models, respectively.

U87 and GL261 were documented to express IGF-IR and are rapidly proliferating cells. U87 comparatively expresses lower IGF-IR levels (15); however, we have previously reported that antisense mediated silencing of IGF-IR in these cells markedly reduced their ability to form intracerebral tumors (16). We also confirmed high IGF-IR protein expression in GL261 cells **(Fig 4.1.)** . To test sensitivity of these cells to the IGF-Trap, we first analyzed its effect on glioma cell proliferation *in vitro* using the MTT assay. The cells were incubated in serum- low medium (1% FBS) and 10ng/ml IGF-1 were added to induce proliferation. IGF-Trap was added (or not) at molar ratios of 1:1 or 1:2 (IGF-1: IGF-Trap). We found that IGF-1 increased cell proliferation of both cells under serum low conditions and treatment with IGF-Trap significantly decreased the proliferation of both cells. **(Fig. 4.2).**

4.4.2 The IGF-Trap attenuates subcutaneous growth of GL261 and U87 *in vivo*.

To evaluate the therapeutic effect of IGF-Trap *in vivo*, we first used a subcutaneous model where tumor growth can be more easily monitored. GL261 and U87 cells were injected in the flank in syngeneic C57Bl/6 males and NSG males respectively and mice were treated twice weekly i.v. with 5 mg/kg IGF-Trap or vehicle (PBS) for control. Tumors were measured with a caliper and tumor volumes calculated (volume = length ^{2} x width / 2). IGF-Trap

significantly inhibited growth of both GL261 and U87 cells *in vivo* and improved long term survival in GL261 injected mice **(Fig. 4.3).**

4.4.3 The IGF-Trap delivered via an intracranial cannula inhibits the growth glioma cells increasing long-term survival of the mice.

We next evaluated the Therapeutic efficacy of IGF-Trap when administered directly into the brain to treat orthotopically implantation GL261 and U87 cells. To ensure that the IGF-Trap can be delivered in proximity to the tumor site, a cannula was implanted directly above the tumor injection site. GL261 and U87 expressed a GFP-luciferase tag enabling assessment of intracerebral tumor growth via optical imaging.

GL261 (100,000 cells/mouse) were implanted intracerebrally into male NSG mice and the mice were randomized three days later. IGF-Trap (5μg per treatment) was injected twice weekly directly into the brain via the implanted cannula starting on day 3. We found that while all mice in the control group (4/4) developed tumors that were detectable from day 14 onwards, tumors in the IGF-Trap- treated group were undetectable by optical imaging in 4/5 mice for up to 17 days post tumor cell injection**.** Moreover, while tumors in the control group progressed rapidly, the detectable tumor in the IGF-Trap-treated group regressed after prolonged treatment, while the remaining mice had stable disease **(Fig. 4.4A&B).** This resulted in an extension to animal survival in the treatment group with median survival times of 54 and 63 days respectively, in the control and treated groups **(Fig. 4.4C).** However, the survival outcome was not statistically significant.

A similar experiment was performed with U87 cells. Male NSG mice were implanted intra-cerebrally with 200,000 cells and randomized on day 3. IGF-Trap (5μg/treatment) was administered via a cannula twice weekly starting on day 3. We found that the IGF-Trap treatment significantly reduced the growth rate of the intracerebral tumors **(Fig. 4.5 A)** and increased the median survival time from 49 (control group) to 97 (IGF-Trap treated group) days ($p<0.05$ using the Gehan-Brewslow-Wilcoxon test) **(Fig. 4.5B)**.

4.4.4 Nanoparticles encapsulated IGF-Trap increases bioavailability in the brain.

Direct intracerebral drug administration is not practicable clinically. Having observed significant effects of the IGF-Trap on glioma growth when administered directly into the brain, we sought to optimize delivery of this inhibitor to the brain when administered intravenously and used a nanoparticle encapsulation to this end. The IGF-Trap was labeled with a CF680 fluorescent dye for easy detection and encapsulated in trimethyl-chitosan based nanoparticles (NP) (17). To test whether the NP encapsulation increased IGF-Trap uptake in the brain, we injected 100μg of IGF-Trap either free or NP encapsulated intravenously and used optical imaging to monitor the distribution of the IGF-Trap over 24 hr. As expected (10), we observed a high concentration of the labelled IGF-Trap in the livers of all mice. However, at 5 minutes post injection a detectable signal was also observed in the brains. However, while the signal persisted in the brains of NP-Trap injected mice for at least 24 hr, it was no longer detectable in IGF-Trap injected mice 4 hr. post injection (**Fig. 4.6**), suggesting a sustained retention of the encapsulated IGF-Trap in the brain. This was also evident when the fluorescent signal intensity was measured and normalized signal intensity at 5 min. While 90% of signal detected at 5 min was retained at 24 hr following NP-Trap injection, less than 50% of the naked IGF-Trap was still detectable at that time **(Fig. 4.6B**). E*x vivo* imaging of brains resected at 1 hr post injection confirmed these findings. We observed a significantly stronger fluorescent signal in mice injected with NP-Trap as compared to the naked IGF-Trap (**Fig. 4.6C and D**).

4.4.5 The effect of transcranial magnetic stimulation on glioma treatment with the IGF-Trap.

We also evaluated the effect of combining IGF-Trap treatment with transcranial magnetic stimulation (TMS), as means of transiently opening the blood brain barrier for IGF-Trap diffusion into the brain parenchyma. Mice were injected intra-cerebrally with 10^5 GL261 cells

and treated twice weekly with 5 mg/kg IGF-Trap intravenously starting on day 3 post tumor injection. TMS was administered immediately prior to tumor injection consisted of 5 rounds of stimulation 1 min each at 1Hz. We observed that while all mice in the control (vehicle – treated) and IGF-Trap treated groups developed tumors that progressed rapidly only 67% (4/6) mice treated with TMS + IGF-Trap developed tumors **(Fig. 4.7)**. All treatments were terminated on Day 56, following which time, tumor progression was observed in the TMS+IGF-Trap treated group. Interestingly, while 33% in the combination therapy group with late-onset tumor development demonstrated survival improvement, 20% (1/5) of the IGF-Trap alone group also showed survival improvement.

4.5 Discussion:

We have shown that glioblastoma cells were sensitive to IGF-Trap treatment *in vitro* and *in vivo*. This is consistent with a study by Zamykal et al where an anti-IGF-IR antibody, IMC-A12, was shown to inhibit the intracerebral growth of U87 cells. The authors of that study suggested that this was due to the anti-angiogenic effect of the antibody (18). The effect of the IGF-Trap on angiogenesis remains to be evaluated.

We sought to use a non-invasive method for transiently breaching the blood brain barrier in order to deliver the IGF-Trap to the brain via intravenous injection for the treatment of intracerebral tumors. Previous studies evaluated drug delivery using trimethyl-chitosan based nanoparticles *in vitro* and *in vivo*. Other groups reported increased bioavailability and biodistribution of a test agent in the brain (19) upon autopsy. We used longitudinal live-imaging over 24 hr and also analyzed the brains of injected mice *ex vivo* at 1hr post injection. We found that nanoparticle-encapsulated IGF-Trap was detectable in the brain for up to 24hr post injection and a higher fluorescent signal was observed in the brains of mice injected with trimethyl-chitosan encapsulated IGF-Trap analyzed ex vivo. The values recorded for encapsulated IGF-Trap were probably an underestimation (by a factor of 2) of the signal

because they could not be adjusted for the fluorescent quenching effect of the nanoparticles based on the standard curve. In previous studies, trimethyl chitosan particles have been used to encapsulate retinoic acid for enhanced drug delivery to treat glioblastoma *in vitro* (20). However, our study is the first to show that these particles can be used for the delivery of large biologics such as the 425 kDa IGF-Trap. Chitosan based NP were also used to enhance bioavailability of orally delivered cancer drugs such as 5-fluorouracil (21), paclitaxel (22), and cytarabine (23), and were shown to improve the intestinal absorption of insulin *in vivo* (24). In another study, cytarabine encapsulated in chitosan microspheres was embedded in a poly(lactide-co-glycolide) film and subcutaneously injected into rats at a concentration of 34.5μg/kg. The cytarabine concentration peaked at 48 hr and was detectable in the plasma for 13 days (23). This result suggested that the control released advantages of chitosan-based NP in delivering therapeutic agents could be further enhanced with the incorporation of a comatrix, thus validating the chitosan-based NP approach as a potent and versatile method for drug delivery.

TMS was previously shown to facilitate extravasation of the IGF-Trap from the circulation into the extracellular space in rats (12). However, its utility for drug delivery to treat brain tumors has not yet been confirmed. Here we report that while all non-treated and IGF-treated mice developed tumors by 21 days post tumor injection, 2/6 IGF-Trap treated mice remained tumor-free for up to 56 days and the duration of treatment and only developed detectable tumors on day 63 after cession of treatment, suggesting that further optimization of this combination treatment is required. TMS treatment had no adverse effects in any of the treated mice confirming the safety of this procedure. TMS was FDA approved for major depressive disorder and approximately 60% of patients responded during maintenance treatment (25). We showed that 20% (1/5) of the IGF-Trap treatment group demonstrated survival improvement. Cancerous glial cells are known to release glutamate that causes

excitotoxic death to surrounding brain cells (26). Moreover, documentation on BBB disruption in high-grade tumors is often a sign of other physiological changes such as angiogenesis (27). These may alter the permeability of the BBB and thus resulted in a survival advantage even without TMS. The use of this technique for drug delivery for the treatment of brain malignancies will require further optimization.

In summary, IGF-Trap was shown to inhibit growth of glioblastoma cells *in vitro* and *in vivo*. Trimethyl chitosan encapsulated IGF-Trap showed increased biodistribution in the brain for a longer period and at greater levels. Combination therapy of TMS and IGF-Trap decreased tumor growth, but the effect was partial. While our results suggest that both nanoparticle encapsulation and TMS could potentially be beneficial for the delivery of the IGF-Trap and similar large molecule biologics to the brain for the treatment of brain malignancies, further studies are needed to confirm the therapeutic efficacy of trimethyl chitosan encapsulated IGF-Trap and optimize the TMS protocol for IGF-Trap delivery.

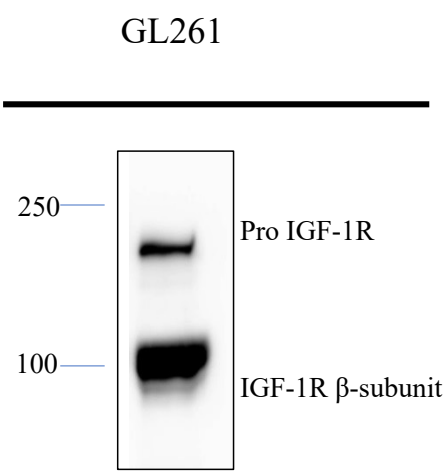

Figure 4.1. High IGF-IR expression in GL261. Cultured GL261 cells were lysed, and 20 μg of protein lysate loaded onto 7% polyacrylamide gels for analysis by Western blotting. Shown are results of a representative WB.

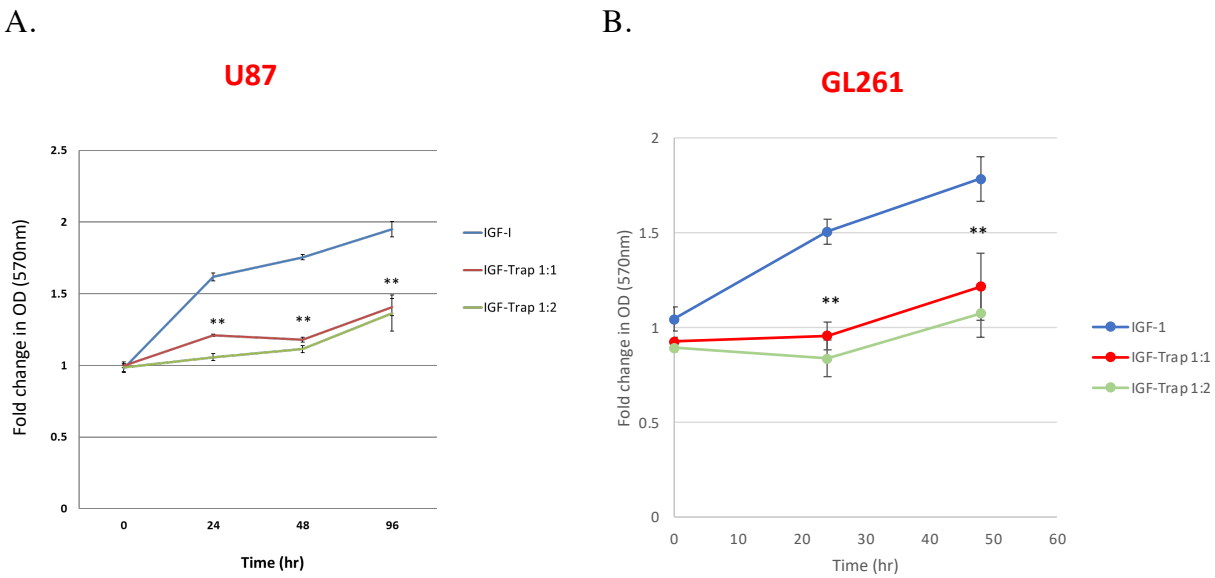

Figure 4.2. IGF-Trap inhibits growth of U87-MG and GL261 cells *in vitro*. Proliferation of U87-MG **(B)** and GL261 **(C)** cells was measured using the MTT assay. The cells were cultured in low (1%) FBS medium supplemented with 10 ng/ml IGF-1 and with and without IGF-Trap used at 1:1 or 1:2 (IGF-1: IGF-Trap) molar ratio. Shown are means of fold change in OD (570 nm) ±SD based on 3 experiments.

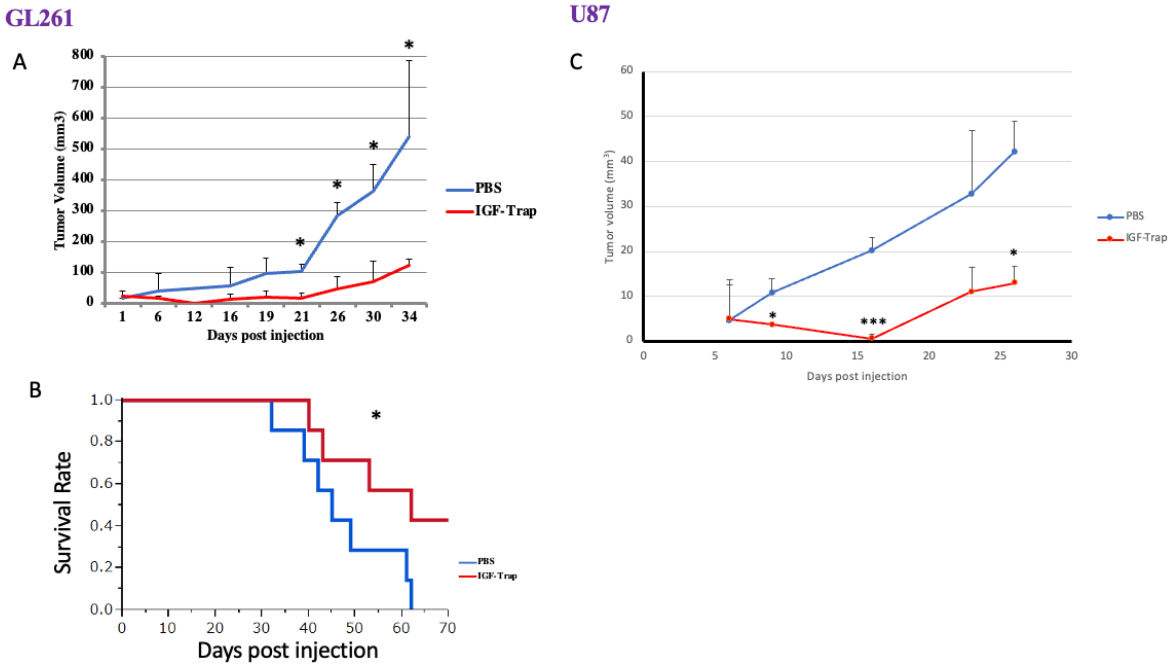

Figure 4.3. The effect of the IGF-Trap on glioblastoma growth in vivo. GL261 and U87-GM cells (10^6 per mouse) were injected subcutaneously into syngeneic C57BL/6 and NSG mice, respectively. Treatment with 5 mg/kg IGF-Trap i.v. began when the tumors were palpable and continued twice weekly until the length of the tumor reached 1.5cm. Tumors were measured twice weekly using a caliper. Shown in **(A)** are the growth curves for mice injected with GL261 cells. Values are expressed as means of tumor volumes ±SD (n=14) and in **(B)** Kaplan Meier survival curves for these mice. Shown in **(C)** are the tumor growth curves for U87-GM injected mice (n= 10). *- $p<0.05$

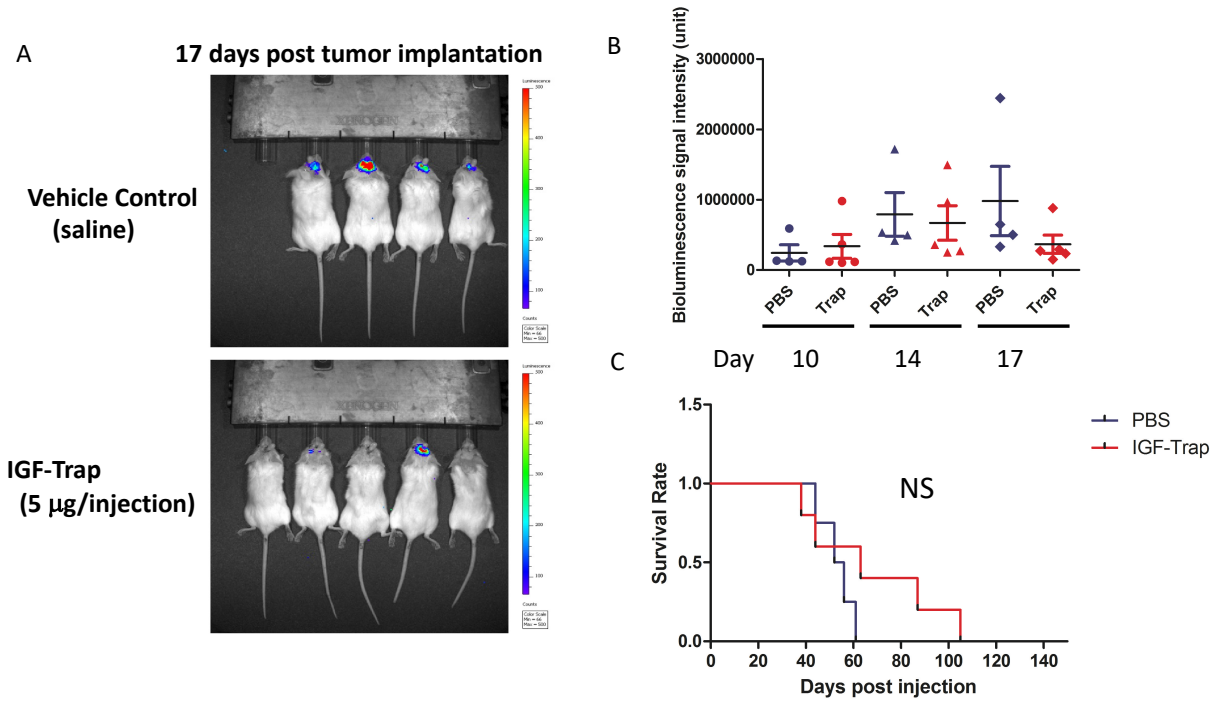

Figure 4.4. Effect of IGF-Trap treatment on intracerebral growth of GL261 tumors. GFP-luciferase tagged GL261 cells (10^5 cells/mouse) were injected orthotopically in the cerebral cortex (x, y, z=-2mm, -1mm, -3.5mm to Bregma). A cannula was inserted directly above the tumor injection site and used to administer 5mg IGF-Trap twice weekly directly into the tumor area until the mice were moribund. Tumor growth was monitored using optical imaging. Shown in **(A)** are optical images acquired on day 17 post tumor inoculation, in **(B)** the bioluminescence signal intensity measured for individual mice in each group and the plotted signal intensity from days 10, 14, 17 and in **(C)** Kaplan Meier survival curves showing extended survival of the IGF-Trap injected mice. NS- not significant.

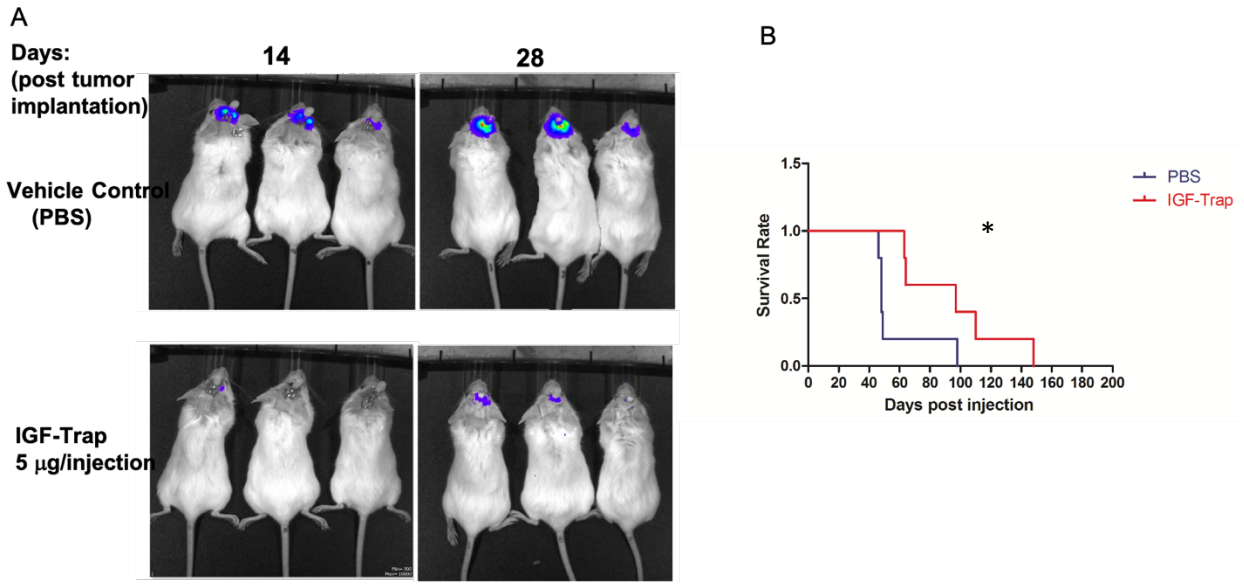

Figure 4.5. IGF-Trap administered intra-cerebrally inhibits the growth of orthotopically implanted U87 tumors. GFP-luciferase tagged U87-MG cells ($2X10^5$/mouse) were injected orthotopically in the cerebral cortex (x, y, z=-2mm, -1mm, -3.5mm to Bregma). A cannula was inserted at the same time, directly above the tumor and 5 mg IGF-Trap injected through the cannula twice weekly. Tumor growth was monitored using optical imaging. Shown in **(A)** are images of cerebral tumors acquired at the indicated intervals post tumor inoculation and in **(B)** Kaplan Meier survival curves. *- $p< 0.05$

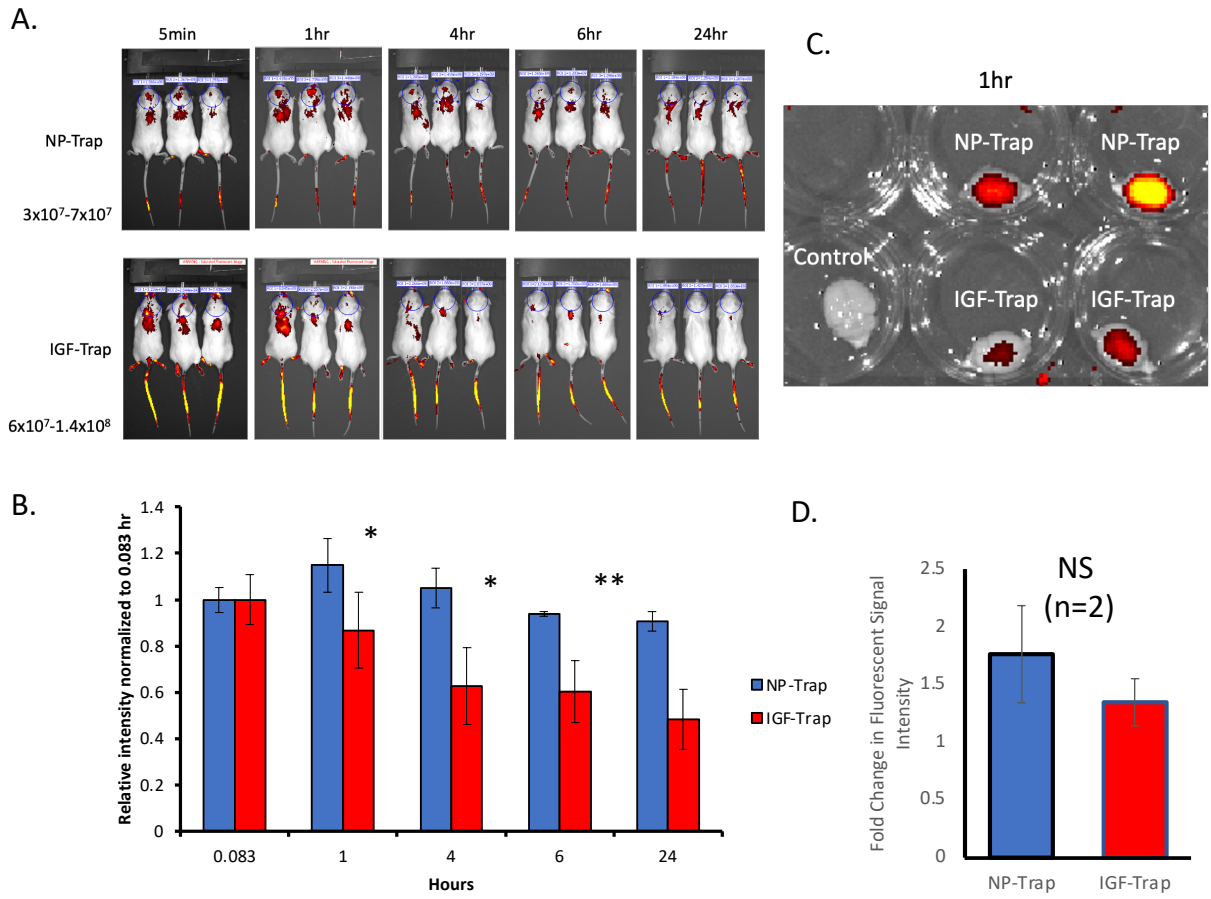

Figure 4.6. IGF-Trap encapsulation in tri-methyl chitosan nanoparticles increases uptake and stability of IGF-Trap in the brain. IGF-Trap was labeled with a CF680 dye with and encapsulated in tri-methyl chitosan nanoparticles. NP-Trap and the "naked" IGF-Trap were injected intravenously, and the distribution was monitored for up to 24 hr. as indicated. Shown in **(A)** are images of the injected mice in **(B)** mean fluorescent signal intensity ±SD normalized to a non-injected control mouse and to levels detected at 0.083 hr in *-$p<0.05$ **-$p<0.01$, in **(C)** Ex vivo images of brains resected 1 hr post IGF-Trap injection and in **(D)** quantification of the average fluorescence intensity of the ex vivo brains resected 1hr post injection (C) and normalized to the non-injected, control brain at 1hr. NS-not significant.

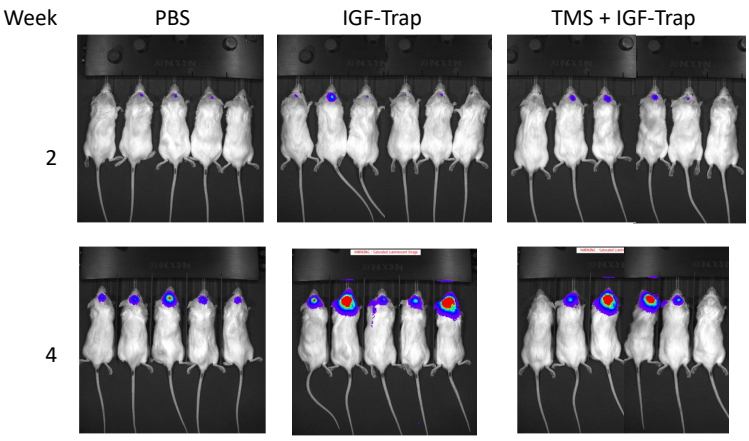

Figure 4.7. The effect of combined transcranial magnetic stimulation (TMS) and IGF-Trap administration on the intracerebral growth of GL261 tumors. GL261 cells (10^5/mouse) were injected intra-cerebrally using a stereotactic instrument. Mice were inoculated twice weekly i.v. with 5 mg/kg IGF-Trap with or without prior administration of 5 rounds of 1Hz pulses 1 min each. Control mice received injections of vehicle (PBS) only. Shown in **(A)** are optical images acquired at the indicated time post tumor inoculation.

4.6 References:

1. Alexander BM, Cloughesy TF. Adult Glioblastoma. J Clin Oncol. 2017;35(21):2402-9.

2. Crespo I, Vital AL, Gonzalez-Tablas M, Patino Mdel C, Otero A, Lopes MC, et al. Molecular and Genomic Alterations in Glioblastoma Multiforme. Am J Pathol. 2015;185(7):1820-33.

3. Pearson JRD, Regad T. Targeting cellular pathways in glioblastoma multiforme. Signal Transduction and Targeted Therapy. 2017;2(1):17040.

4. Maris C, D'Haene N, Trépant AL, Le Mercier M, Sauvage S, Allard J, et al. IGF-IR: a new prognostic biomarker for human glioblastoma. British journal of cancer. 2015;113(5):729-37.

5. Ma Y, Tang N, Thompson RC, Mobley BC, Clark SW, Sarkaria JN, et al. InsR/IGF1R Pathway Mediates Resistance to EGFR Inhibitors in Glioblastoma. Clin Cancer Res. 2016;22(7):1767-76.

6. Song K, Yuan Y, Lin Y, Wang YX, Zhou J, Gai QJ, et al. ERBB3, IGF1R, and TGFBR2 expression correlate with PDGFR expression in glioblastoma and participate in PDGFR inhibitor resistance of glioblastoma cells. Am J Cancer Res. 2018;8(5):792-809.

7. Samani AA, Yakar S, LeRoith D, Brodt P. The role of the IGF system in cancer growth and metastasis: overview and recent insights. Endocrine reviews. 2007;28(1):20-47.

8. Seccareccia E, Brodt P. The role of the insulin-like growth factor-I receptor in malignancy: an update. Growth Hormone & IGF Research. 2012;22(6):193-9.

9. Wang N, Rayes RF, Elahi SM, Lu Y, Hancock MA, Massie B, et al. The IGF-Trap: novel inhibitor of carcinoma growth and metastasis. Molecular cancer therapeutics. 2015.

10. Vaniotis G, Moffett S, Sulea T, Wang N, Elahi SM, Lessard E, et al. Enhanced anti-metastatic bioactivity of an IGF-TRAP re-engineered to improve physicochemical properties. Sci Rep. 2018;8(1):17361.

11. Vazana U, Veksler R, Pell GS, Prager O, Fassler M, Chassidim Y, et al. Glutamate-mediated blood–brain barrier opening: implications for neuroprotection and drug delivery. Journal of Neuroscience. 2016;36(29):7727-39.

12. Vazana U, Schori L, Monsonego U, Swissa E, Pell GS, Roth Y, et al. TMS-Induced Controlled BBB Opening: Preclinical Characterization and Implications for Treatment of Brain Cancer. Pharmaceutics. 2020;12(10):946.

13. Caprifico AE, Foot PJS, Polycarpou E, Calabrese G. Overcoming the Blood-Brain Barrier: Functionalised Chitosan Nanocarriers. Pharmaceutics. 2020;12(11).

14. Sanchez VE, Lynes JP, Walbridge S, Wang X, Edwards NA, Nwankwo AK, et al. GL261 luciferase-expressing cells elicit an anti-tumor immune response: an evaluation of murine glioma models. Scientific Reports. 2020;10(1):11003.

15. Drukala J, Urbanska K, Wilk A, Grabacka M, Wybieralska E, Del Valle L, et al. ROS accumulation and IGF-IR inhibition contribute to fenofibrate/PPARα -mediated inhibition of Glioma cell motility in vitro. Molecular Cancer. 2010;9(1):159.

16. Samani AA, Nalbantoglu J, Brodt P. Glioma Cells With Genetically Engineered IGF-I Receptor Downregulation Can Persist in the Brain in a Dormant State. Frontiers in oncology.

2020;10:555945.

17. Etrych T, Lucas H, Janoušková O, Chytil P, Mueller T, Mäder K. Fluorescence optical imaging in anticancer drug delivery. J Control Release. 2016;226:168-81.

18. Zamykal M, Martens T, Matschke J, Günther HS, Kathagen A, Schulte A, et al. Inhibition of intracerebral glioblastoma growth by targeting the insulin-like growth factor 1 receptor involves different context-dependent mechanisms. Neuro Oncol. 2015;17(8):1076-85.

19. Ramalingam P, Ko YT. Enhanced oral delivery of curcumin from N-trimethyl chitosan surface-modified solid lipid nanoparticles: pharmacokinetic and brain distribution evaluations. Pharm Res. 2015;32(2):389-402.

20. Liu J-L, Li J, Zhang L-Y, Zhang P-L, Zhou J-L, Liu B. Preparation of N, N, N-trimethyl chitosan-functionalized retinoic acid-loaded lipid nanoparticles for enhanced drug delivery to glioblastoma. Tropical Journal of Pharmaceutical research 2017;18(8):1765-22.

21. Ouchi T, Banba T, Fujimoto M, Hamamoto S. Synthesis and antitumor activity of chitosan carrying 5-fluorouracils. Die Makromolekulare Chemie. 1989;190(8):1817-25.

22. Miwa A, Ishibe A, Nakano M, Yamahira T, Itai S, Jinno S, et al. Development of novel chitosan derivatives as micellar carriers of taxol. Pharmaceutical research. 1998;15(12):1844-50.

23. Blanco MD, Gómez C, Olmo R, Muñiz E, Teijón JM. Chitosan microspheres in PLG films as devices for cytarabine release. International Journal of Pharmaceutics. 2000;202(1):29-39.

24. Pan Y, Li Y-j, Zhao H-y, Zheng J-m, Xu H, Wei G, et al. Bioadhesive polysaccharide in protein delivery system: chitosan nanoparticles improve the intestinal absorption of insulin in vivo. International Journal of Pharmaceutics. 2002;249(1):139-47.

25. Connolly KR, Helmer A, Cristancho MA, Cristancho P, O'Reardon JP. Effectiveness of transcranial magnetic stimulation in clinical practice post-FDA approval in the United States: results observed with the first 100 consecutive cases of depression at an academic medical center. J Clin Psychiatry. 2012;73(4):e567-73.

26. Sontheimer H. A role for glutamate in growth and invasion of primary brain tumors. J Neurochem. 2008;105(2):287-95.

27. Provenzale JM, Mukundan S, Dewhirst M. The role of blood-brain barrier permeability in brain tumor imaging and therapeutics. AJR Am J Roentgenol. 2005;185(3):763-7.

Chapter 5. GENERAL DISCUSSION

5.1 Summary of data

The overall goal of this project was to evaluate the therapeutic effect of the IGF-Trap in glioma models and identify and optimize effective IGF-Trap delivery methods for the treatment of brain malignancies.

We found that the IGF-Trap blocked IGF-IR mediated functions including proliferation, colony formation, cell survival, and cell cycle progression in response to IGF-1 in the pHGG glioma model. Moreover, nuclear localization of IGF-IR was confirmed in several pHGG PDXs. IGF-1 induces nuclear translocation of IGF-IR. Subsequently, nuclear IGF-IR acts as a transcriptional co-activator that auto-regulates its own transcription and enhance transcription of other genes such as cyclin D1 in an ERK activation-independent manner. Nuclear translocation mediated by the IGF ligands and downstream transcriptional activity can be inhibited by the IGF-Trap.

In addition, using a murine (GL261) and an adult human (U87) glioblastoma model that demonstrated dependency on IGF-signaling for tumor growth and development, the therapeutic effects of the IGF-Trap was evaluated in a stepwise manner. First, we showed that the IGF-Trap inhibited proliferation *in vitro* in both models. Subsequently, we found that tumor growth subcutaneously was inhibited by the IGF-Trap. Next, GL261 and U87 were implanted orthotopically in the brain using a stereotactic instrument. To ensure access to the tumor microenvironment, the IGF-Trap was administered through a cannula inserted in proximity to the tumor injection site. Using this direct delivery method, the IGF-Trap significantly inhibited tumor growth in the brain and extended long-term survival of mice injected with both tumor types. To overcome the BBB exclusion, trimethyl chitosan-based nanoparticles were used to encapsulate the IGF-Trap, as means of increasing delivery across the BBB. This method significantly increased the retention of the IGF-Trap in the brain.

We also tested the effect of TMS when used in conjunction with IGF-Trap administration intravenously and found that administering TMS prior to the injection of IGF-Trap had a beneficial effect and delayed tumor development in 33% of the mice increasing their survival time, while injection of IGF-Trap alone did not have a measurable beneficial effect. The combination therapy was well-tolerated by the mice and none of them showed signs of illness attributable the TMS treatment. The technique, however, requires further optimization to enhance the therapeutic efficacy of the combination therapy.

These results identified IGF-IR and the IGF-Trap as a molecular target and a potential therapeutic agent for high-grade glioma, respectively. Additionally, trimethyl chitosan-based nanoparticle and TMS were identified as potentially useful methods for the delivery of large molecule biologics.

5.2 Implications of the study:

pHGG have molecular characteristics that are distinct amplification from the adult counterpart (185). However, in both, IGF-IR gene amplifications were identified. IGF-IR is the second most amplified gene, specifically in DIPG, that occur exclusively in children (13). This type of midline glioma is inoperable and maximal resection of tumor is the standard of care, as well as the initial and best treatment for gliomas to date (186). Moreover, IGF-IR has been identified as a molecular target in pHGG due to its role in promoting radio-resistance and contributing to worse prognosis (187). IGF-IR inhibitors and inhibitors of its downstream effectors enhanced radiosensitivity of pediatric high-grade glioma (187-190). Furthermore, nuclear IGF-IR was highly associated with advanced grade glioma in children (76). Therefore, IGF-IR is a potential treatment target for pHGG. To date, few studies have explored the therapeutic potential of IGF-IR targeting in pHGG. Bielen et al. revealed the synergistic effect of combining an IGF-IR inhibitor, NVP-AEW541, with a PDGFR inhibitor, imatinib, in attenuating tumor growth and inhibiting activation of the downstream cascades *in vivo* (191).

Our study identifies IGF-IR as a therapeutic target in pHGG and provides mechanistic insight into IGF-IR signaling and functions in promoting tumor progression in pHGG. Our data also show that IGF-IR targeting drugs can be effective as single agents in the treatment of pHGG.

GL261 and U87 are established cell lines of murine and adult glioblastomas, respectively. Samani et al. showed that glioma cells with an IGF-IR antisense RNA mediated stable reduction in IGF-IR expression levels had a significantly reduced ability to grow in the brain (153). Insensitivity to radio- or chemotherapy treatment in glioblastoma is very common. This can be attributed to its genetic heterogeneity and stemness that is driven by the IGF-signaling and the hedgehog pathways (192). These results identified IGF-IR as a potential therapeutic target for glioblastoma. In our study, we observed that the IGF-Trap decreased tumor growth rate and improved survival of GL261 and U87 – injected mice. In some treated mice, tumor growth was initially suppressed but the tumors eventually progressed possibly due to the acquisition of resistance. In another study , it was also observed that continuous treatment of breast cancer cells with the IGF-Trap led to the emergence of resistant cells due to upregulation of bFGFR1 expression (193) – a receptor also upregulated in glioblastoma (194). It is possible therefore, that combination therapy with IGF-IR and FGFR inhibitors may be required for sustained suppression of glioblastoma growth.

Drug delivery to the brain remains a major challenge due to the blood brain barrier and strategies for transiently breaching the BBB are actively sought (195-197). We used Trimethyl chitosan-based (TRIOZAN) nanoparticles to encapsulate the IGF-Trap in an effort to increase IGF-Trap diffusion through the BBB. We found that TRIOZAN- encapsulation increased IGF-Trap retention in the brain as compared to non-encapsulated IGF-Trap, suggesting that it may be a useful vehicle for drug delivery for the treatment of brain malignancies.

Therapeutic effects of TMS have been clinically proven in challenging psychiatric disorders including major depressive disorder and treatment resistant depression (198). The

benefit of TMS in the treatment of brain malignancies remains, however, to be demonstrated. Of note, the release of the neurotransmitter, glutamate, through the activation of NMDA receptors upon TMS stimulation was found to transiently increase BBB permeability (199). This discovery may open the way to optimization of drug delivery across the BBB for the treatment of various central nervous system diseases. A pilot study of 15 patients with glioblastoma showed increase BBB permeability especially around the tumor bed (199). However, cancerous cells are known to release glutamate that causes excitotoxic death to surrounding brain cells in order to expand in the brain (200). It was also documented in high-grade tumors that the BBB is disrupted and this is often a sign of other physiological changes such as angiogenesis (201). In our study, TMS was adapted for the first time to use in mice but has not been tested in animals with deformed brain structures. We observed delayed tumor formation and survival advantage with TMS and IGF-Trap combination therapy. However, IGF-Trap alone also improved survival slightly, suggesting that some breach of the BBB may have occurred in tumor –bearing mice.

5.3 Recommendations for Future Research:

We have demonstrated that pHGG, specifically DIPG, responded well to the IGF-Trap. However, there are few established *in vivo* models of pHGG, due partially to the slow growing nature of the PDXs. To further examine the therapeutic efficacy of the IGF-Trap, validation with an *in vivo model* will be required.

Additionally, we showed that the trimethyl chitosan-based nanoparticle encapsulated IGF-Trap had improved bioavailability in the brain. Localization of the IGF-Trap in the brain parenchyma using immunohistochemistry is ongoing. In addition, evaluation of the therapeutic effect of nanoparticle-encapsulated IGF-Trap is in progress.

Lastly, in the murine model of glioblastoma, a response to the combination TMS/IGF-Trap therapy was observed. However, the data did not reach statistical significance due to the

large intra-group variability and small sample size. Optimization of the positioning of electromagnetic pulses is underway to improve the efficacy and reduce intra-group variability of the response to this therapy.

5.4 Conclusion:

In conclusion, we identified IGF-Trap as a potent therapeutic agent for blockade of tumor promoting functions downstream of IGF-signaling and nuclear translocation in pHGG. Moreover, the IGF-Trap inhibited tumor growth and improved survival of GL261 and U87-bearing mice. Trimethyl chitosan-based nanoparticle and TMS showed promising results in overcoming the BBB to drug delivery. Further optimization of these delivery strategies and their use in combination with IGF-IR inhibitors could have important translational implications for the clinical management of glioblastoma.

5.5 References:

1. Baba AI, Catoi C. Chapter 14, NERVOUS SYSTEM TUMORS. Bucharest, Romania: The Publishing House of the Romanian Academy

; 2007.

2. Kros JM. Grading of gliomas: the road from eminence to evidence. Journal of neuropathology and experimental neurology. 2011;70(2):101-9.

3. Martin AM, Raabe E, Eberhart C, Cohen KJ. Management of pediatric and adult patients with medulloblastoma. Current treatment options in oncology. 2014;15(4):581-94.

4. Packer RJ, Gajjar A, Vezina G, Rorke-Adams L, Burger PC, Robertson PL, et al. Phase III study of craniospinal radiation therapy followed by adjuvant chemotherapy for newly diagnosed average-risk medulloblastoma. J Clin Oncol. 2006;24(25):4202-8.

5. Gajjar A, Chintagumpala M, Ashley D, Kellie S, Kun LE, Merchant TE, et al. Risk-adapted craniospinal radiotherapy followed by high-dose chemotherapy and stem-cell rescue in children with newly diagnosed medulloblastoma (St Jude Medulloblastoma-96): long-term results from a prospective, multicentre trial. Lancet Oncol. 2006;7(10):813-20.

6. Kühl J, Müller HL, Berthold F, Kortmann RD, Deinlein F, Maass E, et al. Preradiation chemotherapy of children and young adults with malignant brain tumors: results of the German pilot trial HIT'88/'89. Klin Padiatr. 1998;210(4):227-33.

7. Packer RJ. Childhood brain tumors: accomplishments and ongoing challenges. Journal of child neurology. 2008;23(10):1122-7.

8. Kieran MW, Chisholm J, Casanova M, Brandes AA, Aerts I, Bouffet E, et al. Phase I study of oral sonidegib (LDE225) in pediatric brain and solid tumors and a phase II study in children and adults with relapsed medulloblastoma. Neuro Oncol. 2017;19(11):1542-52.

9. LoRusso PM, Rudin CM, Reddy JC, Tibes R, Weiss GJ, Borad MJ, et al. Phase I trial of hedgehog pathway inhibitor vismodegib (GDC-0449) in patients with refractory, locally advanced or metastatic solid tumors. Clin Cancer Res. 2011;17(8):2502-11.

10. Gladson CL, Prayson RA, Liu WM. The pathobiology of glioma tumors. Annual review of pathology. 2010;5:33-50.

11. Marko NF, Weil RJ. The molecular biology of WHO grade I astrocytomas. Neuro Oncol. 2012;14(12):1424-31.

12. Diwanji TP, Engelman A, Snider JW, Mohindra P. Epidemiology, diagnosis, and optimal management of glioma in adolescents and young adults. Adolesc Health Med Ther. 2017;8:99-113.

13. Glod J, Rahme GJ, Kaur H, H Raabe E, Hwang EI, Israel MA. Pediatric Brain Tumors: Current Knowledge and Therapeutic Opportunities. J Pediatr Hematol Oncol. 2016;38(4):249-60.

14. Schmandt SM, Packer RJ, Vezina LG, Jane J. Spontaneous regression of low-grade

astrocytomas in childhood. Pediatric neurosurgery. 2000;32(3):132-6.

15. Fangusaro J. Pediatric high grade glioma: a review and update on tumor clinical characteristics and biology. Frontiers in oncology. 2012;2:105.

16. Muskens IS, de Smith AJ, Zhang C, Hansen HM, Morimoto L, Metayer C, et al. Germline cancer predisposition variants and pediatric glioma: a population-based study in California. Neuro Oncol. 2020.

17. Michaeli O, Tabori U. Pediatric High Grade Gliomas in the Context of Cancer Predisposition Syndromes. Journal of Korean Neurosurgical Society. 2018;61(3):319-32.

18. Jones C, Baker SJ. Unique genetic and epigenetic mechanisms driving paediatric diffuse high-grade glioma. Nat Rev Cancer. 2014;14(10):10.1038/nrc3811.

19. Wu G, Diaz AK, Paugh BS, Rankin SL, Ju B, Li Y, et al. The genomic landscape of diffuse intrinsic pontine glioma and pediatric non-brainstem high-grade glioma. Nature genetics. 2014;46(5):444-50.

20. Cocco E, Scaltriti M, Drilon A. NTRK fusion-positive cancers and TRK inhibitor therapy. Nat Rev Clin Oncol. 2018;15(12):731-47.

21. Finlay JL, Boyett JM, Yates AJ, Wisoff JH, Milstein JM, Geyer JR, et al. Randomized phase III trial in childhood high-grade astrocytoma comparing vincristine, lomustine, and prednisone with the eight-drugs-in-1-day regimen. Childrens Cancer Group. Journal of Clinical Oncology. 1995;13(1):112-23.

22. Sposto R, Ertel IJ, Jenkin RD, Boesel CP, Venes JL, Ortega JA, et al. The effectiveness of chemotherapy for treatment of high grade astrocytoma in children: results of a randomized trial. A report from the Childrens Cancer Study Group. Journal of neuro-oncology. 1989;7(2):165-77.

23. Askins MA, Moore BD, 3rd. Preventing neurocognitive late effects in childhood cancer survivors. Journal of child neurology. 2008;23(10):1160-71.

24. Mazzocco MM, Pennington BF, Hagerman RJ. The neurocognitive phenotype of female carriers of fragile X: additional evidence for specificity. J Dev Behav Pediatr. 1993;14(5):328-35.

25. Travis ZD, Sherchan P, Hayes WK, Zhang JH. Surgically-induced brain injury: where are we now? Chinese Neurosurgical Journal. 2019;5(1):29.

26. El-Ayadi M, Ansari M, Sturm D, Gielen GH, Warmuth-Metz M, Kramm CM, et al. High-grade glioma in very young children: a rare and particular patient population. Oncotarget. 2017;8(38):64564-78.

27. Bouffet E, Larouche V, Campbell BB, Merico D, de Borja R, Aronson M, et al. Immune Checkpoint Inhibition for Hypermutant Glioblastoma Multiforme Resulting From Germline Biallelic Mismatch Repair Deficiency. J Clin Oncol. 2016;34(19):2206-11.

28. Bavle A, Chintagumpala M. Pediatric high-grade glioma: a review of biology, prognosis, and treatment. Journal of Radiation Oncology. 2018;7(1):7-15.

29. Lowe BR, Maxham LA, Hamey JJ, Wilkins MR, Partridge JF. Histone H3 Mutations: An Updated View of Their Role in Chromatin Deregulation and Cancer. Cancers. 2019;11(5).

30. Buczkowicz P, Hawkins C. Pathology, Molecular Genetics, and Epigenetics of Diffuse Intrinsic Pontine Glioma. Frontiers in oncology. 2015;5:147-.

31. Grasso CS, Tang Y, Truffaux N, Berlow NE, Liu L, Debily MA, et al. Functionally defined therapeutic targets in diffuse intrinsic pontine glioma. Nature medicine. 2015;21(6):555-9.

32. Elias MC, Tozer KR, Silber JR, Mikheeva S, Deng M, Morrison RS, et al. TWIST is expressed in human gliomas and promotes invasion. Neoplasia. 2005;7(9):824-37.

33. Pham CG, Bubici C, Zazzeroni F, Knabb JR, Papa S, Kuntzen C, et al. Upregulation of Twist-1 by NF-kappaB blocks cytotoxicity induced by chemotherapeutic drugs. Mol Cell Biol. 2007;27(11):3920-35.

34. Nakanishi C, Toi M. Nuclear factor-kappaB inhibitors as sensitizers to anticancer drugs. Nat Rev Cancer. 2005;5(4):297-309.

35. Lin B, Williams-Skipp C, Tao Y, Schleicher MS, Cano LL, Duke RC, et al. NF-kappaB functions as both a proapoptotic and antiapoptotic regulatory factor within a single cell type. Cell Death Differ. 1999;6(6):570-82.

36. Meel MH, Schaper SA, Kaspers GJL, Hulleman E. Signaling pathways and mesenchymal transition in pediatric high-grade glioma. Cellular and molecular life sciences : CMLS. 2018;75(5):871-87.

37. Kalluri R, Weinberg RA. The basics of epithelial-mesenchymal transition. The Journal of clinical investigation. 2009;119(6):1420-8.

38. Wang Y, Shi J, Chai K, Ying X, Zhou BP. The Role of Snail in EMT and Tumorigenesis. Current cancer drug targets. 2013;13(9):963-72.

39. Scaltriti M, Elkabets M, Baselga J. Molecular Pathways: AXL, a Membrane Receptor Mediator of Resistance to Therapy. Clin Cancer Res. 2016;22(6):1313-7.

40. Puget S, Philippe C, Bax DA, Job B, Varlet P, Junier MP, et al. Mesenchymal transition and PDGFRA amplification/mutation are key distinct oncogenic events in pediatric diffuse intrinsic pontine gliomas. PloS one. 2012;7(2):e30313.

41. McCubrey JA, Steelman LS, Chappell WH, Abrams SL, Wong EW, Chang F, et al. Roles of the Raf/MEK/ERK pathway in cell growth, malignant transformation and drug resistance. Biochimica et biophysica acta. 2007;1773(8):1263-84.

42. Chang F, Lee JT, Navolanic PM, Steelman LS, Shelton JG, Blalock WL, et al. Involvement of PI3K/Akt pathway in cell cycle progression, apoptosis, and neoplastic transformation: a target for cancer chemotherapy. Leukemia. 2003;17(3):590-603.

43. Diaz AK, Baker SJ. The genetic signatures of pediatric high-grade glioma: no longer a one-act play. Seminars in radiation oncology. 2014;24(4):240-7.

44. Ijaz H, Koptyra M, Gaonkar KS, Rokita JL, Baubet VP, Tauhid L, et al. Pediatric high-grade glioma resources from the Children's Brain Tumor Tissue Consortium. Neuro-Oncology. 2019;22(1):163-5.

45. Apte RS, Chen DS, Ferrara N. VEGF in Signaling and Disease: Beyond Discovery and Development. Cell. 2019;176(6):1248-64.

46. Hummel TR, Salloum R, Drissi R, Kumar S, Sobo M, Goldman S, et al. A pilot study of bevacizumab-based therapy in patients with newly diagnosed high-grade gliomas and diffuse intrinsic pontine gliomas. Journal of neuro-oncology. 2016;127(1):53-61.

47. Tabash MA. Characteristics, survival and incidence rates and trends of pilocytic astrocytoma in children in the United States; SEER-based analysis. Journal of the neurological sciences. 2019;400:148-52.

48. Ida CM, Rodriguez FJ, Burger PC, Caron AA, Jenkins SM, Spears GM, et al. Pleomorphic Xanthoastrocytoma: Natural History and Long-Term Follow-Up. Brain pathology (Zurich, Switzerland). 2015;25(5):575-86.

49. Rakotonjanahary J, De Carli E, Delion M, Kalifa C, Grill J, Doz F, et al. Mortality in Children with Optic Pathway Glioma Treated with Up-Front BB-SFOP Chemotherapy. PloS one. 2015;10(6):e0127676.

50. Lam S, Lin Y, Auffinger B, Melkonian S. Analysis of survival in pediatric high-grade brainstem gliomas: A population-based study. Journal of pediatric neurosciences. 2015;10(3):199-206.

51. Kebudi R, Cakir FB, Agaoglu FY, Gorgun O, Ayan I, Darendeliler E. Pediatric diffuse intrinsic pontine glioma patients from a single center. Child's nervous system : ChNS : official journal of the International Society for Pediatric Neurosurgery. 2013;29(4):583-8.

52. Xu Y, Kong GK, Menting JG, Margetts MB, Delaine CA, Jenkin LM, et al. How ligand binds to the type 1 insulin-like growth factor receptor. Nature communications. 2018;9(1):821.

53. Ullrich A, Gray A, Tam AW, Yang-Feng T, Tsubokawa M, Collins C, et al. Insulin-like growth factor I receptor primary structure: comparison with insulin receptor suggests structural determinants that define functional specificity. The EMBO journal. 1986;5(10):2503-12.

54. Elleman TC, Frenkel MJ, Hoyne PA, McKern NM, Cosgrove L, Hewish DR, et al. Mutational analysis of the N-linked glycosylation sites of the human insulin receptor. The Biochemical journal. 2000;347 Pt 3(Pt 3):771-9.

55. Maruyama IN. Mechanisms of activation of receptor tyrosine kinases: monomers or dimers. Cells. 2014;3(2):304-30.

56. Jacobs S, Kull FC, Cuatrecasas P. Monensin blocks the maturation of receptors for insulin and somatomedin C: identification of receptor precursors. Proceedings of the National Academy of Sciences. 1983;80(5):1228-31.

57. Denduluri SK, Idowu O, Wang Z, Liao Z, Yan Z, Mohammed MK, et al. Insulin-like growth factor (IGF) signaling in tumorigenesis and the development of cancer drug resistance. Genes & Diseases. 2015;2(1):13-25.

58. Denley A, Wallace JC, Cosgrove LJ, Forbes BE. The insulin receptor isoform exon 11- (IR-A) in cancer and other diseases: a review. Hormone and metabolic research = Hormon- und Stoffwechselforschung = Hormones et metabolisme. 2003;35(11-12):778-85.

59. Sciacca L, Prisco M, Wu A, Belfiore A, Vigneri R, Baserga R. Signaling Differences from the A and B Isoforms of the Insulin Receptor (IR) in 32D Cells in the Presence or Absence of IR Substrate-1. Endocrinology. 2003;144(6):2650-8.

60. Escribano O, Beneit N, Rubio-Longás C, López-Pastor AR, Gómez-Hernández A. The Role of Insulin Receptor Isoforms in Diabetes and Its Metabolic and Vascular Complications. Journal of diabetes research. 2017;2017:1403206.

61. Belfiore A, Frasca F, Pandini G, Sciacca L, Vigneri R. Insulin receptor isoforms and insulin receptor/insulin-like growth factor receptor hybrids in physiology and disease. Endocrine reviews. 2009;30(6):586-623.

62. Samani AA, Yakar S, LeRoith D, Brodt P. The role of the IGF system in cancer growth and metastasis: overview and recent insights. Endocrine reviews. 2007;28(1):20-47.

63. Frasca F, Pandini G, Scalia P, Sciacca L, Mineo R, Costantino A, et al. Insulin receptor isoform A, a newly recognized, high-affinity insulin-like growth factor II receptor in fetal and cancer cells. Molecular and cellular biology. 1999;19(5):3278-88.

64. Belfiore A, Malaguarnera R, Vella V, Lawrence MC, Sciacca L, Frasca F, et al. Insulin Receptor Isoforms in Physiology and Disease: An Updated View. Endocrine Reviews. 2017;38(5):379-431.

65. Brown J, Jones EY, Forbes BE. Interactions of IGF-II with the IGF2R/cation-independent mannose-6-phosphate receptor mechanism and biological outcomes. Vitamins and hormones. 2009;80:699-719.

66. De Souza AT, Hankins GR, Washington MK, Orton TC, Jirtle RL. M6P/IGF2R gene is mutated in human hepatocellular carcinomas with loss of heterozygosity. Nature genetics. 1995;11(4):447-9.

67. Hankins GR, De Souza AT, Bentley RC, Patel MR, Marks JR, Iglehart JD, et al. M6P/IGF2 receptor: a candidate breast tumor suppressor gene. Oncogene. 1996;12(9):2003-9.

68. Kong FM, Anscher MS, Washington MK, Killian JK, Jirtle RL. M6P/IGF2R is mutated in squamous cell carcinoma of the lung. Oncogene. 2000;19(12):1572-8.

69. Hu CK, McCall S, Madden J, Huang H, Clough R, Jirtle RL, et al. Loss of heterozygosity of M6P/IGF2R gene is an early event in the development of prostate cancer. Prostate cancer and prostatic diseases. 2006;9(1):62-7.

70. Rey JM, Theillet C, Brouillet JP, Rochefort H. Stable amino-acid sequence of the mannose-6-phosphate/insulin-like growth-factor-II receptor in ovarian carcinomas with loss

of heterozygosity and in breast-cancer cell lines. International journal of cancer. 2000;85(4):466-73.

71. Huang Z, Wen Y, Shandilya R, Marks JR, Berchuck A, Murphy SK. High throughput detection of M6P/IGF2R intronic hypermethylation and LOH in ovarian cancer. Nucleic acids research. 2006;34(2):555-63.

72. Lee JS, Weiss J, Martin JL, Scott CD. Increased expression of the mannose 6-phosphate/insulin-like growth factor-II receptor in breast cancer cells alters tumorigenic properties in vitro and in vivo. International journal of cancer. 2003;107(4):564-70.

73. Sarfstein R, Werner H. Minireview: nuclear insulin and insulin-like growth factor-1 receptors: a novel paradigm in signal transduction. Endocrinology. 2013;154(5):1672-9.

74. Sehat B, Tofigh A, Lin Y, Trocmé E, Liljedahl U, Lagergren J, et al. SUMOylation mediates the nuclear translocation and signaling of the IGF-1 receptor. Science signaling. 2010;3(108):ra10.

75. Warsito D, Sjöström S, Andersson S, Larsson O, Sehat B. Nuclear IGF1R is a transcriptional co-activator of LEF1/TCF. EMBO reports. 2012;13(3):244-50.

76. Clément F, Martin A, Venara M, de Luján Calcagno M, Mathó C, Maglio S, et al. Type 1 IGF Receptor Localization in Paediatric Gliomas: Significant Association with WHO Grading and Clinical Outcome. Hormones and Cancer. 2018;9(3):205-14.

77. Vogel T, editor Insulin/IGF-Signalling in Embryonic and Adult Neural Proliferation and Differentiation in the Mammalian Central Nervous System2013.

78. Chan SJ, Keim P, Steiner DF. Cell-free synthesis of rat preproinsulins: characterization and partial amino acid sequence determination. Proc Natl Acad Sci U S A. 1976;73(6):1964-8.

79. Foulstone E, Prince S, Zaccheo O, Burns JL, Harper J, Jacobs C, et al. Insulin-like growth factor ligands, receptors, and binding proteins in cancer. J Pathol. 2005;205(2):145-53.

80. Wang Y, Bikle DD, Chang W. Autocrine and Paracrine Actions of IGF-I Signaling in Skeletal Development. Bone Res. 2013;1(3):249-59.

81. Rasmussen AA, Cullen KJ. Paracrine/autocrine regulation of breast cancer by the insulin-like growth factors. Breast Cancer Research and Treatment. 1998;47(3):219-33.

82. Vitale G, Pellegrino G, Vollery M, Hofland LJ. ROLE of IGF-1 System in the Modulation of Longevity: Controversies and New Insights From a Centenarians' Perspective. Front Endocrinol (Lausanne). 2019;10:27.

83. Jogie-Brahim S, Feldman D, Oh Y. Unraveling insulin-like growth factor binding protein-3 actions in human disease. Endocr Rev. 2009;30(5):417-37.

84. Wetterau LA, Moore MG, Lee KW, Shim ML, Cohen P. Novel aspects of the insulin-like growth factor binding proteins. Mol Genet Metab. 1999;68(2):161-81.

85. Lee CI, Goldstein O, Han VKM, Tarantal AF. IGF-II and IGF Binding Protein (IGFBP-1, IGFBP-3) Gene Expression in Fetal Rhesus Monkey Tissues during the Second and Third Trimesters. Pediatric Research. 2001;49(3):379-87.

86. Iams WT, Lovly CM. Molecular Pathways: Clinical Applications and Future Direction of Insulin-like Growth Factor-1 Receptor Pathway Blockade. Clin Cancer Res. 2015;21(19):4270-7.

87. Sasaki N, Rees-Jones R, Zick Y, Nissley S, Rechler M. Characterization of insulin-like growth factor I-stimulated tyrosine kinase activity associated with the beta-subunit of type I insulin-like growth factor receptors of rat liver cells. Journal of Biological Chemistry. 1985;260(17):9793-804.

88. Annunziata M, Granata R, Ghigo E. The IGF system. Acta diabetologica. 2011;48(1):1-9.

89. Hakuno F, Takahashi S-I. 40 YEARS OF IGF1: IGF1 receptor signaling pathways. Journal of Molecular Endocrinology. 2018;61(1):T69-T86.

90. Taliaferro-Smith L, Oberlick E, Liu T, McGlothen T, Alcaide T, Tobin R, et al. FAK activation is required for IGF1R-mediated regulation of EMT, migration, and invasion in mesenchymal triple negative breast cancer cells. Oncotarget. 2015;6(7):4757-72.

91. Andersson S, D'Arcy P, Larsson O, Sehat B. Focal adhesion kinase (FAK) activates and stabilizes IGF-1 receptor. Biochem Biophys Res Commun. 2009;387(1):36-41.

92. Matsui WH. Cancer stem cell signaling pathways. Medicine (Baltimore). 2016;95(1 Suppl 1):S8-s19.

93. Reinhardt RR, Bondy CA. Insulin-like growth factors cross the blood-brain barrier. Endocrinology. 1994;135(5):1753-61.

94. D'Ercole AJ, Ye P, Calikoglu AS, Gutierrez-Ospina G. The role of the insulin-like growth factors in the central nervous system. Mol Neurobiol. 1996;13(3):227-55.

95. McMorris FA, Mozell RL, Carson MJ, Shinar Y, Meyer RD, Marchetti N. Regulation of oligodendrocyte development and central nervous system myelination by insulin-like growth factors. Ann N Y Acad Sci. 1993;692:321-34.

96. Freude S, Leeser U, Müller M, Hettich MM, Udelhoven M, Schilbach K, et al. IRS-2 branch of IGF-1 receptor signaling is essential for appropriate timing of myelination. J Neurochem. 2008;107(4):907-17.

97. Sonntag WE, Ramsey M, Carter CS. Growth hormone and insulin-like growth factor-1 (IGF-1) and their influence on cognitive aging. Ageing Res Rev. 2005;4(2):195-212.

98. Aleman A, de Vries WR, de Haan EH, Verhaar HJ, Samson MM, Koppeschaar HP. Age-sensitive cognitive function, growth hormone and insulin-like growth factor 1 plasma levels in healthy older men. Neuropsychobiology. 2000;41(2):73-8.

99. Aleman A, Verhaar HJ, De Haan EH, De Vries WR, Samson MM, Drent ML, et al. Insulin-like growth factor-I and cognitive function in healthy older men. J Clin Endocrinol

Metab. 1999;84(2):471-5.

100. Kalmijn S, Janssen JA, Pols HA, Lamberts SW, Breteler MM. A prospective study on circulating insulin-like growth factor I (IGF-I), IGF-binding proteins, and cognitive function in the elderly. J Clin Endocrinol Metab. 2000;85(12):4551-5.

101. Morley JE, Kaiser F, Raum WJ, Perry HM, 3rd, Flood JF, Jensen J, et al. Potentially predictive and manipulable blood serum correlates of aging in the healthy human male: progressive decreases in bioavailable testosterone, dehydroepiandrosterone sulfate, and the ratio of insulin-like growth factor 1 to growth hormone. Proceedings of the National Academy of Sciences of the United States of America. 1997;94(14):7537-42.

102. Castro-Alamancos MA, Torres-Aleman I. Learning of the conditioned eye-blink response is impaired by an antisense insulin-like growth factor I oligonucleotide. Proc Natl Acad Sci U S A. 1994;91(21):10203-7.

103. Svensson J, Diez M, Engel J, Wass C, Tivesten A, Jansson JO, et al. Endocrine, liver-derived IGF-I is of importance for spatial learning and memory in old mice. Journal of Endocrinology. 2006;189(3):617-27.

104. Ishii T, Moriyoshi K, Sugihara H, Sakurada K, Kadotani H, Yokoi M, et al. Molecular characterization of the family of the N-methyl-D-aspartate receptor subunits. J Biol Chem. 1993;268(4):2836-43.

105. Clayton DA, Mesches MH, Alvarez E, Bickford PC, Browning MD. A hippocampal NR2B deficit can mimic age-related changes in long-term potentiation and spatial learning in the Fischer 344 rat. J Neurosci. 2002;22(9):3628-37.

106. Sonntag WE, Bennett SA, Khan AS, Thornton PL, Xu X, Ingram RL, et al. Age and insulin-like growth factor-1 modulate N-methyl-D-aspartate receptor subtype expression in rats. Brain Res Bull. 2000;51(4):331-8.

107. Blanquart C, Achi J, Issad T. Characterization of IRA/IRB hybrid insulin receptors using bioluminescence resonance energy transfer. Biochem Pharmacol. 2008;76(7):873-83.

108. Benyoucef S, Surinya KH, Hadaschik D, Siddle K. Characterization of insulin/IGF hybrid receptors: contributions of the insulin receptor L2 and Fn1 domains and the alternatively spliced exon 11 sequence to ligand binding and receptor activation. The Biochemical journal. 2007;403(3):603-13.

109. Frattali AL, Pessin JE. Relationship between alpha subunit ligand occupancy and beta subunit autophosphorylation in insulin/insulin-like growth factor-1 hybrid receptors. J Biol Chem. 1993;268(10):7393-400.

110. Bailyes EM, Navé BT, Soos MA, Orr SR, Hayward AC, Siddle K. Insulin receptor/IGF-I receptor hybrids are widely distributed in mammalian tissues: quantification of individual receptor species by selective immunoprecipitation and immunoblotting. The Biochemical journal. 1997;327 (Pt 1)(Pt 1):209-15.

111. Slaaby R, Schäffer L, Lautrup-Larsen I, Andersen AS, Shaw AC, Mathiasen IS, et al. Hybrid receptors formed by insulin receptor (IR) and insulin-like growth factor I receptor

(IGF-IR) have low insulin and high IGF-1 affinity irrespective of the IR splice variant. J Biol Chem. 2006;281(36):25869-74.

112. Pandini G, Frasca F, Mineo R, Sciacca L, Vigneri R, Belfiore A. Insulin/insulin-like growth factor I hybrid receptors have different biological characteristics depending on the insulin receptor isoform involved. J Biol Chem. 2002;277(42):39684-95.

113. Knowlden JM, Hutcheson IR, Barrow D, Gee JMW, Nicholson RI. Insulin-Like Growth Factor-I Receptor Signaling in Tamoxifen-Resistant Breast Cancer: A Supporting Role to the Epidermal Growth Factor Receptor. Endocrinology. 2005;146(11):4609-18.

114. Novosyadlyy R, Dudas J, Pannem R, Ramadori G, Scharf J-G. Crosstalk between PDGF and IGF-I receptors in rat liver myofibroblasts: implication for liver fibrogenesis. Laboratory Investigation. 2006;86(7):710-23.

115. Klotz DM, Hewitt SC, Ciana P, Raviscioni M, Lindzey JK, Foley J, et al. Requirement of estrogen receptor-α in insulin-like growth factor-1 (IGF-1)-induced uterine responses and in vivo evidence for IGF-1/estrogen receptor cross-talk. Journal of Biological Chemistry. 2002;277(10):8531-7.

116. Janssen JA, Varewijck AJ. IGF-IR targeted therapy: past, present and future. Frontiers in endocrinology. 2014;5:224.

117. Nahta R, Yuan LX, Zhang B, Kobayashi R, Esteva FJ. Insulin-like growth factor-I receptor/human epidermal growth factor receptor 2 heterodimerization contributes to trastuzumab resistance of breast cancer cells. Cancer Res. 2005;65(23):11118-28.

118. Hua H, Kong Q, Yin J, Zhang J, Jiang Y. Insulin-like growth factor receptor signaling in tumorigenesis and drug resistance: a challenge for cancer therapy. Journal of Hematology & Oncology. 2020;13(1):64.

119. Hanahan D, Weinberg RA. Hallmarks of cancer: the next generation. Cell. 2011;144(5):646-74.

120. Sun Y, Sun X, Shen B. Molecular imaging of IGF-1R in cancer. Molecular imaging. 2017;16:1536012117736648.

121. Yeo CD, Park KH, Park CK, Lee SH, Kim SJ, Yoon HK, et al. Expression of insulin-like growth factor 1 receptor (IGF-1R) predicts poor responses to epidermal growth factor receptor (EGFR) tyrosine kinase inhibitors in non-small cell lung cancer patients harboring activating EGFR mutations. Lung Cancer. 2015;87(3):311-7.

122. Heskamp S, Boerman OC, Molkenboer-Kuenen JD, Wauters CA, Strobbe LJ, Mandigers CM, et al. Upregulation of IGF-1R expression during neoadjuvant therapy predicts poor outcome in breast cancer patients. PloS one. 2015;10(2):e0117745.

123. Farabaugh SM, Boone DN, Lee AV. Role of IGF1R in Breast Cancer Subtypes, Stemness, and Lineage Differentiation. Frontiers in endocrinology. 2015;6:59-.

124. Chen PC, Kuo YC, Chuong CM, Huang YH. Niche Modulation of IGF-1R Signaling: Its Role in Stem Cell Pluripotency, Cancer Reprogramming, and Therapeutic Applications. Front Cell Dev Biol. 2020;8:625943.

125. Chang WW, Lin RJ, Yu J, Chang WY, Fu CH, Lai A, et al. The expression and significance of insulin-like growth factor-1 receptor and its pathway on breast cancer stem/progenitors. Breast Cancer Res. 2013;15(3):R39.

126. Dallas NA, Xia L, Fan F, Gray MJ, Gaur P, van Buren G, 2nd, et al. Chemoresistant colorectal cancer cells, the cancer stem cell phenotype, and increased sensitivity to insulin-like growth factor-I receptor inhibition. Cancer Res. 2009;69(5):1951-7.

127. Ngo MT, Jeng HY, Kuo YC, Diony Nanda J, Brahmadhi A, Ling TY, et al. The Role of IGF/IGF-1R Signaling in Hepatocellular Carcinomas: Stemness-Related Properties and Drug Resistance. Int J Mol Sci. 2021;22(4).

128. Xu C, Xie D, Yu SC, Yang XJ, He LR, Yang J, et al. β-Catenin/POU5F1/SOX2 transcription factor complex mediates IGF-I receptor signaling and predicts poor prognosis in lung adenocarcinoma. Cancer Res. 2013;73(10):3181-9.

129. Osuka S, Sampetrean O, Shimizu T, Saga I, Onishi N, Sugihara E, et al. IGF1 receptor signaling regulates adaptive radioprotection in glioma stem cells. Stem Cells. 2013;31(4):627-40.

130. Codony-Servat J, Cuatrecasas M, Asensio E, Montironi C, Martínez-Cardús A, Marín-Aguilera M, et al. Nuclear IGF-1R predicts chemotherapy and targeted therapy resistance in metastatic colorectal cancer. British journal of cancer. 2017;117(12):1777-86.

131. Bodzin AS, Wei Z, Hurtt R, Gu T, Doria C. Gefitinib resistance in HCC mahlavu cells: upregulation of CD133 expression, activation of IGF-1R signaling pathway, and enhancement of IGF-1R nuclear translocation. J Cell Physiol. 2012;227(7):2947-52.

132. Sarfstein R, Pasmanik-Chor M, Yeheskel A, Edry L, Shomron N, Warman N, et al. Insulin-like growth factor-I receptor (IGF-IR) translocates to nucleus and autoregulates IGF-IR gene expression in breast cancer cells. The Journal of biological chemistry. 2012;287(4):2766-76.

133. Warsito D, Lin Y, Gnirck A-C, Sehat B, Larsson O. Nuclearly translocated insulin-like growth factor 1 receptor phosphorylates histone H3 at tyrosine 41 and induces SNAI2 expression via Brg1 chromatin remodeling protein. Oncotarget. 2016;7(27):42288-302.

134. Jiang L, Zhu W, Streicher K, Morehouse C, Brohawn P, Ge X, et al. Increased IR-A/IR-B ratio in non-small cell lung cancers associates with lower epithelial-mesenchymal transition signature and longer survival in squamous cell lung carcinoma. BMC Cancer. 2014;14:131-.

135. Pandini G, Vigneri R, Costantino A, Frasca F, Ippolito A, Fujita-Yamaguchi Y, et al. Insulin and insulin-like growth factor-I (IGF-I) receptor overexpression in breast cancers leads to insulin/IGF-I hybrid receptor overexpression: evidence for a second mechanism of IGF-I signaling. Clinical Cancer Research. 1999;5(7):1935-44.

136. Pandini G, Vigneri R, Costantino A, Frasca F, Ippolito A, Fujita-Yamaguchi Y, et al. Insulin and insulin-like growth factor-I (IGF-I) receptor overexpression in breast cancers leads to insulin/IGF-I hybrid receptor overexpression: evidence for a second mechanism of IGF-I signaling. Clinical cancer research : an official journal of the American Association for

Cancer Research. 1999;5(7):1935-44.

137. Cox ME, Gleave ME, Zakikhani M, Bell RH, Piura E, Vickers E, et al. Insulin receptor expression by human prostate cancers. Prostate. 2009;69(1):33-40.

138. Avnet S, Sciacca L, Salerno M, Gancitano G, Cassarino MF, Longhi A, et al. Insulin receptor isoform A and insulin-like growth factor II as additional treatment targets in human osteosarcoma. Cancer Res. 2009;69(6):2443-52.

139. Haywood NJ, Slater TA, Matthews CJ, Wheatcroft SB. The insulin like growth factor and binding protein family: Novel therapeutic targets in obesity & diabetes. Molecular metabolism. 2019;19:86-96.

140. Shanmugalingam T, Bosco C, Ridley AJ, Van Hemelrijck M. Is there a role for IGF-1 in the development of second primary cancers? Cancer medicine. 2016;5(11):3353-67.

141. Wu Y, Cui K, Miyoshi K, Hennighausen L, Green JE, Setser J, et al. Reduced circulating insulin-like growth factor I levels delay the onset of chemically and genetically induced mammary tumors. Cancer Res. 2003;63(15):4384-8.

142. Majeed N, Blouin MJ, Kaplan-Lefko PJ, Barry-Shaw J, Greenberg NM, Gaudreau P, et al. A germ line mutation that delays prostate cancer progression and prolongs survival in a murine prostate cancer model. Oncogene. 2005;24(29):4736-40.

143. Schairer C, McCarty CA, Isaacs C, Sue LY, Pollak MN, Berg CD, et al. Circulating insulin-like growth factor (IGF)-I and IGF binding protein (IGFBP)-3 levels and postmenopausal breast cancer risk in the prostate, lung, colorectal, and ovarian cancer screening trial (PLCO) cohort. Horm Cancer. 2010;1(2):100-11.

144. Cao H, Wang G, Meng L, Shen H, Feng Z, Liu Q, et al. Association between circulating levels of IGF-1 and IGFBP-3 and lung cancer risk: a meta-analysis. PloS one. 2012;7(11):e49884.

145. Renehan AG, Zwahlen M, Minder C, O'Dwyer ST, Shalet SM, Egger M. Insulin-like growth factor (IGF)-I, IGF binding protein-3, and cancer risk: systematic review and meta-regression analysis. Lancet. 2004;363(9418):1346-53.

146. Martin DC, Fowlkes JL, Babic B, Khokha R. Insulin-like growth factor II signaling in neoplastic proliferation is blocked by transgenic expression of the metalloproteinase inhibitor TIMP-1. J Cell Biol. 1999;146(4):881-92.

147. Camacho-Hubner C, Busby WH, Jr., McCusker RH, Wright G, Clemmons DR. Identification of the forms of insulin-like growth factor-binding proteins produced by human fibroblasts and the mechanisms that regulate their secretion. J Biol Chem. 1992;267(17):11949-56.

148. Conover CA, Kiefer MC, Zapf J. Posttranslational regulation of insulin-like growth factor binding protein-4 in normal and transformed human fibroblasts. Insulin-like growth factor dependence and biological studies. The Journal of clinical investigation. 1993;91(3):1129-37.

149. Cohick WS, Gockerman A, Clemmons DR. Regulation of insulin-like growth factor

(IGF) binding protein-2 synthesis and degradation by platelet-derived growth factor and the IGFs is enhanced by serum deprivation in vascular smooth muscle cells. J Cell Physiol. 1995;164(1):187-96.

150. Salahifar H, Baxter RC, Martin JL. Insulin-like Growth Factor Binding Protein (IGFBP)-3 Protease Activity Secreted by MCF-7 Breast Cancer Cells: Inhibition by IGFs Does Not Require IGF-IGFBP Interaction*. Endocrinology. 1997;138(4):1683-90.

151. Cohen P, Graves HC, Peehl DM, Kamarei M, Giudice LC, Rosenfeld RG. Prostate-specific antigen (PSA) is an insulin-like growth factor binding protein-3 protease found in seminal plasma. J Clin Endocrinol Metab. 1992;75(4):1046-53.

152. Chen YM, Qi S, Perrino S, Hashimoto M, Brodt P. Targeting the IGF-Axis for Cancer Therapy: Development and Validation of an IGF-Trap as a Potential Drug. Cells. 2020;9(5):1098.

153. Samani AA, Nalbantoglu J, Brodt P. Glioma Cells With Genetically Engineered IGF-I Receptor Downregulation Can Persist in the Brain in a Dormant State. Frontiers in oncology. 2020;10:555945.

154. Dunn SE, Ehrlich M, Sharp NJ, Reiss K, Solomon G, Hawkins R, et al. A dominant negative mutant of the insulin-like growth factor-I receptor inhibits the adhesion, invasion, and metastasis of breast cancer. Cancer Res. 1998;58(15):3353-61.

155. Jiang Y, Rom WN, Yie TA, Chi CX, Tchou-Wong KM. Induction of tumor suppression and glandular differentiation of A549 lung carcinoma cells by dominant-negative IGF-I receptor. Oncogene. 1999;18(44):6071-7.

156. Burfeind P, Chernicky CL, Rininsland F, Ilan J, Ilan J. Antisense RNA to the type I insulin-like growth factor receptor suppresses tumor growth and prevents invasion by rat prostate cancer cells in vivo. Proc Natl Acad Sci U S A. 1996;93(14):7263-8.

157. Bohula EA, Playford MP, Macaulay VM. Targeting the type 1 insulin-like growth factor receptor as anti-cancer treatment. Anticancer Drugs. 2003;14(9):669-82.

158. Buck E, Gokhale PC, Koujak S, Brown E, Eyzaguirre A, Tao N, et al. Compensatory insulin receptor (IR) activation on inhibition of insulin-like growth factor-1 receptor (IGF-1R): rationale for cotargeting IGF-1R and IR in cancer. Molecular cancer therapeutics. 2010;9(10):2652-64.

159. Osher E, Macaulay VM. Therapeutic targeting of the IGF axis. Cells. 2019;8(8):895.

160. Schanzer JM, Wartha K, Moessner E, Hosse RJ, Moser S, Croasdale R, et al., editors. XGFR*, a novel affinity-matured bispecific antibody targeting IGF-1R and EGFR with combined signaling inhibition and enhanced immune activation for the treatment of pancreatic cancer. MAbs; 2016: Taylor & Francis.

161. Runcie K, Budman DR, John V, Seetharamu N. Bi-specific and tri-specific antibodies- the next big thing in solid tumor therapeutics. Mol Med. 2018;24(1):50.

162. Weroha SJ, Haluska P. IGF-1 receptor inhibitors in clinical trials--early lessons. J Mammary Gland Biol Neoplasia. 2008;13(4):471-83.

163. Tian D, Kreeger PK. Analysis of the quantitative balance between insulin-like growth factor (IGF)-1 ligand, receptor, and binding protein levels to predict cell sensitivity and therapeutic efficacy. BMC systems biology. 2014;8(1):98.

164. Bowers LW, Rossi EL, O'Flanagan CH, deGraffenried LA, Hursting SD. The Role of the Insulin/IGF System in Cancer: Lessons Learned from Clinical Trials and the Energy Balance-Cancer Link. Front Endocrinol (Lausanne). 2015;6:77.

165. de Bono JS, Piulats JM, Pandha HS, Petrylak DP, Saad F, Aparicio LM, et al. Phase II randomized study of figitumumab plus docetaxel and docetaxel alone with crossover for metastatic castration-resistant prostate cancer. Clin Cancer Res. 2014;20(7):1925-34.

166. Langer CJ, Novello S, Park K, Krzakowski M, Karp DD, Mok T, et al. Randomized, phase III trial of first-line figitumumab in combination with paclitaxel and carboplatin versus paclitaxel and carboplatin alone in patients with advanced non-small-cell lung cancer. J Clin Oncol. 2014;32(19):2059-66.

167. Fuchs CS, Azevedo S, Okusaka T, Van Laethem JL, Lipton LR, Riess H, et al. A phase 3 randomized, double-blind, placebo-controlled trial of ganitumab or placebo in combination with gemcitabine as first-line therapy for metastatic adenocarcinoma of the pancreas: the GAMMA trial. Ann Oncol. 2015;26(5):921-7.

168. Tap WD, Demetri G, Barnette P, Desai J, Kavan P, Tozer R, et al. Phase II study of ganitumab, a fully human anti-type-1 insulin-like growth factor receptor antibody, in patients with metastatic Ewing family tumors or desmoplastic small round cell tumors. J Clin Oncol. 2012;30(15):1849-56.

169. Smith TJ, Kahaly GJ, Ezra DG, Fleming JC, Dailey RA, Tang RA, et al. Teprotumumab for Thyroid-Associated Ophthalmopathy. N Engl J Med. 2017;376(18):1748-61.

170. Sclafani F, Kim TY, Cunningham D, Kim TW, Tabernero J, Schmoll HJ, et al. A Randomized Phase II/III Study of Dalotuzumab in Combination With Cetuximab and Irinotecan in Chemorefractory, KRAS Wild-Type, Metastatic Colorectal Cancer. J Natl Cancer Inst. 2015;107(12):djv258.

171. Weickhardt A, Doebele R, Oton A, Lettieri J, Maxson D, Reynolds M, et al. A phase I/II study of erlotinib in combination with the anti-insulin-like growth factor-1 receptor monoclonal antibody IMC-A12 (cixutumumab) in patients with advanced non-small cell lung cancer. J Thorac Oncol. 2012;7(2):419-26.

172. Abou-Alfa GK, Capanu M, O'Reilly EM, Ma J, Chou JF, Gansukh B, et al. A phase II study of cixutumumab (IMC-A12, NSC742460) in advanced hepatocellular carcinoma. J Hepatol. 2014;60(2):319-24.

173. Kundranda M, Gracian AC, Zafar SF, Meiri E, Bendell J, Algül H, et al. Randomized, double-blind, placebo-controlled phase II study of istiratumab (MM-141) plus nab-paclitaxel and gemcitabine versus nab-paclitaxel and gemcitabine in front-line metastatic pancreatic cancer (CARRIE). Ann Oncol. 2020;31(1):79-87.

174. Anderson PM, Bielack SS, Gorlick RG, Skubitz K, Daw NC, Herzog CE, et al. A

phase II study of clinical activity of SCH 717454 (robatumumab) in patients with relapsed osteosarcoma and Ewing sarcoma. Pediatr Blood Cancer. 2016;63(10):1761-70.

175. von Mehren M, Britten CD, Pieslor P, Saville W, Vassos A, Harris S, et al. A phase 1, open-label, dose-escalation study of BIIB022 (anti-IGF-1R monoclonal antibody) in subjects with relapsed or refractory solid tumors. Invest New Drugs. 2014;32(3):518-25.

176. Smith DC, Britten C, Clary DO, Nguyen LT, Woodard P, Hurwitz HI. A phase I study of XL228, a potent IGF1R/AURORA/SRC inhibitor, in patients with solid tumors or hematologic malignancies. Journal of Clinical Oncology. 2009;27(15_suppl):3512-.

177. Aiken R, Axelson M, Harmenberg J, Klockare M, Larsson O, Wassberg C. Phase I clinical trial of AXL1717 for treatment of relapsed malignant astrocytomas: analysis of dose and response. Oncotarget. 2017;8(46):81501-10.

178. Cortes J, Martinez Janez N, Sablin M-P, Perez-Fidalgo JA, Neven P, Hedayati E, et al. Phase 1b/2 trial of BI 836845, an insulin-like growth factor (IGF) ligand-neutralizing antibody, combined with exemestane (Ex) and everolimus (Ev) in hormone receptor-positive (HR+) locally advanced or metastatic breast cancer (BC): primary phase 1b results. Journal of Clinical Oncology. 2016;34(15_suppl):530-.

179. Haluska P, Menefee M, Plimack ER, Rosenberg J, Northfelt D, LaVallee T, et al. Phase I dose-escalation study of MEDI-573, a bispecific, antiligand monoclonal antibody against IGFI and IGFII, in patients with advanced solid tumors. Clin Cancer Res. 2014;20(18):4747-57.

180. Hoffman HM, Throne ML, Amar NJ, Sebai M, Kivitz AJ, Kavanaugh A, et al. Efficacy and safety of rilonacept (interleukin-1 Trap) in patients with cryopyrin-associated periodic syndromes: results from two sequential placebo-controlled studies. Arthritis Rheum. 2008;58(8):2443-52.

181. Holash J, Davis S, Papadopoulos N, Croll SD, Ho L, Russell M, et al. VEGF-Trap: a VEGF blocker with potent antitumor effects. Proc Natl Acad Sci U S A. 2002;99(17):11393-8.

182. Samani AA, Chevet E, Fallavollita L, Galipeau J, Brodt P. Loss of tumorigenicity and metastatic potential in carcinoma cells expressing the extracellular domain of the type 1 insulin-like growth factor receptor. Cancer Res. 2004;64(10):3380-5.

183. Wang N, Fallavollita L, Nguyen L, Burnier J, Rafei M, Galipeau J, et al. Autologous bone marrow stromal cells genetically engineered to secrete an igf-I receptor decoy prevent the growth of liver metastases. Mol Ther. 2009;17(7):1241-9.

184. Wang N, Rayes RF, Elahi SM, Lu Y, Hancock MA, Massie B, et al. The IGF-Trap: novel inhibitor of carcinoma growth and metastasis. Molecular cancer therapeutics. 2015.

185. Garcia-Fabiani MB, Comba A, Kadiyala P, Haase S, Núñez FJ, Altshuler D, et al. Isolation and characterization of immune cells from the tumor microenvironment of genetically engineered pediatric high-grade glioma models using the sleeping beauty transposon system. Methods Enzymol. 2020;632:369-88.

186. Blionas A, Giakoumettis D, Klonou A, Neromyliotis E, Karydakis P, Themistocleous MS. Paediatric gliomas: diagnosis, molecular biology and management. Ann Transl Med. 2018;6(12):251-.

187. Simpson AD, Soo YWJ, Rieunier G, Aleksic T, Ansorge O, Jones C, et al. Type 1 IGF receptor associates with adverse outcome and cellular radioresistance in paediatric high-grade glioma. British journal of cancer. 2020;122(5):624-9.

188. Metselaar DS, du Chatinier A, Stuiver I, Kaspers GJL, Hulleman E. Radiosensitization in Pediatric High-Grade Glioma: Targets, Resistance and Developments. Frontiers in oncology. 2021;11:662209.

189. Miyahara H, Yadavilli S, Natsumeda M, Rubens JA, Rodgers L, Kambhampati M, et al. The dual mTOR kinase inhibitor TAK228 inhibits tumorigenicity and enhances radiosensitization in diffuse intrinsic pontine glioma. Cancer Lett. 2017;400:110-6.

190. Flannery PC, DeSisto JA, Amani V, Venkataraman S, Lemma RT, Prince EW, et al. Preclinical analysis of MTOR complex 1/2 inhibition in diffuse intrinsic pontine glioma. Oncol Rep. 2018;39(2):455-64.

191. Bielen A, Perryman L, Box GM, Valenti M, de Haven Brandon A, Martins V, et al. Enhanced efficacy of IGF1R inhibition in pediatric glioblastoma by combinatorial targeting of PDGFRalpha/beta. Mol Cancer Ther. 2011;10(8):1407-18.

192. Hsieh A, Ellsworth R, Hsieh D. Hedgehog/GLI1 regulates IGF dependent malignant behaviors in glioma stem cells. J Cell Physiol. 2011;226(4):1118-27.

193. Tsui J, Qi S, Perrino S, Leibovitch M, Brodt P. Identification of a Resistance Mechanism to IGF-IR Targeting in Human Triple Negative MDA-MB-231 Breast Cancer Cells. Biomolecules. 2021;11(4):527.

194. Egbivwie N, Cockle JV, Humphries M, Ismail A, Esteves F, Taylor C, et al. FGFR1 Expression and Role in Migration in Low and High Grade Pediatric Gliomas. Frontiers in oncology. 2019;9:103-.

195. Dong X. Current Strategies for Brain Drug Delivery. Theranostics. 2018;8(6):1481-93.

196. Pardridge WM. Drug transport across the blood-brain barrier. J Cereb Blood Flow Metab. 2012;32(11):1959-72.

197. Mulvihill JJ, Cunnane EM, Ross AM, Duskey JT, Tosi G, Grabrucker AM. Drug delivery across the blood-brain barrier: recent advances in the use of nanocarriers. Nanomedicine (Lond). 2020;15(2):205-14.

198. Rizvi S, Khan AM. Use of Transcranial Magnetic Stimulation for Depression. Cureus. 2019;11(5):e4736-e.

199. Vazana U, Veksler R, Pell GS, Prager O, Fassler M, Chassidim Y, et al. Glutamate-mediated blood–brain barrier opening: implications for neuroprotection and drug delivery. Journal of Neuroscience. 2016;36(29):7727-39.

200. Sontheimer H. A role for glutamate in growth and invasion of primary brain tumors. J Neurochem. 2008;105(2):287-95.

201. Provenzale JM, Mukundan S, Dewhirst M. The role of blood-brain barrier permeability in brain tumor imaging and therapeutics. AJR Am J Roentgenol. 2005;185(3):763-7.